

---

---

# Neutron Dosimetry at Commercial Nuclear Plants

Final Report of Subtask C:  $^3\text{He}$  Neutron Spectrometer

---

---

Prepared by L. W. Brackenbush, W. D. Reece, J. E. Tanner

**Pacific Northwest Laboratory**  
Operated by  
Battelle Memorial Institute

Prepared for  
U.S. Nuclear Regulatory  
Commission

8410120008 840930  
PDR NUREG  
CR-3610 R PDR

## NOTICE

This report was prepared as an account of work sponsored by an agency of the United States Government. Neither the United States Government nor any agency thereof, or any of their employees, makes any warranty, expressed or implied, or assumes any legal liability of responsibility for any third party's use, or the results of such use, of any information, apparatus, product or process disclosed in this report, or represents that its use by such third party would not infringe privately owned rights.

## NOTICE

### Availability of Reference Materials Cited in NRC Publications

Most documents cited in NRC publications will be available from one of the following sources:

1. The NRC Public Document Room, 1717 H Street, N.W.  
Washington, DC 20555
2. The NRC/GPO Sales Program, U.S. Nuclear Regulatory Commission,  
Washington, DC 20555
3. The National Technical Information Service, Springfield, VA 22161

Although the listing that follows represents the majority of documents cited in NRC publications, it is not intended to be exhaustive.

Referenced documents available for inspection and copying for a fee from the NRC Public Document Room include NRC correspondence and internal NRC memoranda; NRC Office of Inspection and Enforcement bulletins, circulars, information notices, inspection and investigation notices; Licensee Event Reports; vendor reports and correspondence; Commission papers; and applicant and licensee documents and correspondence.

The following documents in the NUREG series are available for purchase from the NRC/GPO Sales Program: formal NRC staff and contractor reports, NRC-sponsored conference proceedings, and NRC booklets and brochures. Also available are Regulatory Guides, NRC regulations in the *Code of Federal Regulations*, and *Nuclear Regulatory Commission Issuances*.

Documents available from the National Technical Information Service include NUREG series reports and technical reports prepared by other federal agencies and reports prepared by the Atomic Energy Commission, foreign agency to the Nuclear Regulatory Commission.

Documents available from public and special technical libraries include all open literature items, such as books, journal and periodical articles, and transactions. *Federal Register* notices, federal and state legislation, and congressional reports can usually be obtained from these libraries.

Documents such as theses, dissertations, foreign reports and translations, and non-NRC conference proceedings are available for purchase from the organization sponsoring the publication cited.

Single copies of NRC draft reports are available free, to the extent of supply, upon written request to the Division of Technical Information and Document Control, U.S. Nuclear Regulatory Commission, Washington, DC 20555.

Copies of industry codes and standards used in a substantive manner in the NRC regulatory process are maintained at the NRC Library, 7920 Norfolk Avenue, Bethesda, Maryland, and are available there for reference use by the public. Codes and standards are usually copyrighted and may be purchased from the originating organization or, if they are American National Standards, from the American National Standards Institute, 1430 Broadway, New York, NY 10018.

# Neutron Dosimetry at Commercial Nuclear Plants

Final Report of Subtask C:  $^3\text{He}$  Neutron Spectrometer

---

Manuscript Completed: July 1984  
Date Published: September 1984

Prepared by  
L. W. Brackenbush, W. D. Reece, J. E. Tanner

Pacific Northwest Laboratory  
Richland, WA 99352

Prepared for  
Division of Radiation Programs and Earth Sciences  
Office of Nuclear Regulatory Research  
U.S. Nuclear Regulatory Commission  
Washington, D.C. 20555  
NRC FIN B2282

## ABSTRACT

In commercial nuclear power plants, personnel routinely enter containment for maintenance and inspections while the reactor is operating and can be exposed to intense neutron fields. The low-energy neutron fields found in reactor containment cause problems in proper interpretation of TLD-albedo dosimeters and survey instrument readings. This report describes a technique that can aid plant health physicists to improve the accuracy of personnel neutron dosimetry programs.

A  $^3\text{He}$  neutron spectrometer can be used to measure neutron energy spectra and determine dose equivalent rates at work locations inside containment. Energy correction factors for TLD-albedo dosimeters can be determined from the measured spectra if the dosimeter energy response is known, or from direct measurements with dosimeters placed on phantoms at locations where the dose equivalent rate has been measured. This report describes how to assemble a spectrometer system using only commercially available components, how to use it for reactor energy spectrum measurements, and how to analyze the data and interpret the results. Both  $^3\text{He}$  and multisphere spectrometers were used to measure neutron energy spectra and dose equivalent at three PWRs and one BWR. In general, the  $^3\text{He}$  spectrometer measures higher dose equivalent rates than the multisphere spectrometer. In the energy range from 10 keV to 1 MeV, the dose equivalents measured by the  $^3\text{He}$  spectrometer and multisphere spectrometer agree within about 35% for the spectra measured.

## SUMMARY

The thermoluminescent-albedo dosimeter (referred to as TLD-albedo dosimeter) has been demonstrated to be the best dosimeter type currently available for use in commercial nuclear power plants (NUREG/CR-2956). Unfortunately, the TLD-albedo dosimeter is highly energy-dependent, and a correction must be made for this energy dependence for dosimeters used inside containment of nuclear power plants. The Pacific Northwest Laboratory has devised one method of obtaining energy correction factors using a  $^3\text{He}$  neutron energy spectrometer to measure the neutron flux density and dose equivalent. Personnel neutron dosimeters can be directly calibrated by exposing them on phantoms where the dose equivalent has been measured by the  $^3\text{He}$  spectrometer or other spectrometers.

This report describes a relatively simple method for plant health physicists to improve the accuracy of their TLD-albedo dosimeters. The report describes all the equipment used, how to assemble and calibrate it, and how to analyze the data. Examples of  $^3\text{He}$  spectrometer use to measure approximate neutron energy spectra in commercial nuclear power plants are presented. Additional information is included on limitations of the  $^3\text{He}$  spectrometer system.

Because the response of the TLD-albedo dosimeter is almost constant over limited energy regions, it is not necessary to determine the exact differential neutron energy flux density over all energy ranges. Instead, the differential neutron energy spectrum as a function of energy needs to be measured only for energies above about 10 keV, where the dosimeter response per unit of dose equivalent decreases rapidly with increasing neutron energy. At lower energies it is necessary only to determine the total flux density integrated over two energy ranges.

Previous measurements in NUREG/CR-1769 have shown that very few neutrons with energies above 1 MeV are found inside reactor containment. Although no "ideal" spectrometer exists, four types appear to be useful for reactor spectra measurements:

- multisphere or Bonner sphere
- activation foils
- proton recoil proportional counters
- $^3\text{He}$  proportional counters.

All suffer from some deficiencies and do not cover the entire energy range of thermal to 1 MeV with great accuracy. Some are complex, difficult to use and often require complex unfolding codes. The  $^3\text{He}$  spectrometer is a compromise between accuracy and ease of use. The  $^3\text{He}$  spectrometer has three primary advantages:

- reasonable accuracy in the energy range of 50 keV to 1 MeV
- an operating energy range extendable to thermal energies using neutron absorbing filters to determine approximate neutron spectra

- demonstrated effectiveness in environmental chambers and the harsh environments of operating nuclear power plants.

The  $^3\text{He}$  neutron energy spectrometer has three primary disadvantages:

- It is not an "off-the-shelf" instrument--care must be taken in setting up a spectrometer system from commercially available components.
- The  $^3\text{He}$  detector is very sensitive to low-energy neutrons--neutron absorbing filters and other techniques must be used to prevent pulse pile-up from giving erroneous data in the 20-keV to 700-keV range of energies.
- Only a crude estimate of the total flux density can be obtained in the energy range of 1 eV to 10 keV using a single cadmium filter.

The  $^3\text{He}$  spectrometer demonstrated good performance in the laboratory to measure monoenergetic neutrons from a Van de Graaff generator and the filtered beam facility at the National Bureau of Standards. The low-energy spectra found inside containment of nuclear power plants are much more difficult to measure because of the pile-up problems caused by the sensitivity of the  $^3\text{He}$  detector to low-energy neutrons. However, pile-up can be reduced by using cadmium, samarium, and/or boron carbide filters to remove low-energy neutrons. A technique using a precision pulser to estimate pulse pile-up is described.

Measurements were made at three pressurized water reactors and the drywell of one boiling water reactor during startup. Data from the  $^3\text{He}$  neutron energy spectrometer indicate that more low-energy neutrons are present than are indicated by the multisphere spectrometer used at the same locations on the operating decks of the nuclear power plants. This difference has not been resolved, and it is recommended that perhaps additional measurements be made with activation foils or additional absorption filters over the  $^3\text{He}$  detector to increase the accuracy of spectrum measurements in the 1-eV to 10-keV energy range. The dose equivalent rates measured with the  $^3\text{He}$  spectrometer, a multisphere spectrometer, survey instruments such as the Snoopy cylindrical remmeter, and the tissue equivalent proportional counter for the reactor sites measured differed by a factor of two.

## CONTENTS

ABSTRACT . . . . .	iii
SUMMARY . . . . .	v
ACKNOWLEDGMENTS . . . . .	xiii
1.0 INTRODUCTION . . . . .	1
2.0 SPECTROMETER EVALUATION . . . . .	2
2.1 MULTISPHERE SPECTROMETERS . . . . .	2
2.2 ACTIVATION FOILS . . . . .	4
2.3 PROTON-RECOIL PROPORTIONAL COUNTERS . . . . .	4
2.4 <sup>3</sup> He SPECTROMETER . . . . .	5
3.0 THEORY OF <sup>3</sup> He SPECTROMETER OPERATION . . . . .	6
3.1 NUCLEAR THEORY . . . . .	6
3.1.1 Pulse Pile-Up . . . . .	9
3.2 DATA ANALYSIS TECHNIQUES . . . . .	16
3.2.1 Energy Region 1 - Thermal to 1 eV . . . . .	16
3.2.2 Energy Region 2 - 1 eV to 10 keV . . . . .	18
3.2.3 Energy Region 3 - Energies Above 10 keV . . . . .	23
4.0 EQUIPMENT REQUIRED FOR THE <sup>3</sup> He SPECTROMETER . . . . .	25
4.1 <sup>3</sup> He SPECTROMETER COMPONENTS . . . . .	25
4.1.1 Proportional Counter Tube . . . . .	25
4.1.2 Electronic Equipment . . . . .	25
4.2 TEST EQUIPMENT . . . . .	26
4.3 NEUTRON SOURCE . . . . .	26
5.0 ASSEMBLING THE <sup>3</sup> He SPECTROMETER . . . . .	28
5.1 PROPORTIONAL COUNTER TUBE EVALUATION . . . . .	28
5.1.1 Test Apparatus . . . . .	28
5.1.2 Test Procedures . . . . .	30
5.2 SPECTROMETER ELECTRONICS ASSEMBLY . . . . .	32
5.2.1 <sup>3</sup> He Spectrometer Using a Pulser Technique to Estimate Pulse Pile-Up . . . . .	32
5.2.2 <sup>3</sup> He Spectrometer Using Pulse Shape Analysis . . . . .	37

5.3	MULTICHANNEL ANALYSER LINEARITY CHECK	44
5.4	TROUBLESHOOTING	45
6.0	TESTING OF THE <sup>3</sup> He SPECTROMETER SYSTEM	47
6.1	ENVIRONMENTAL CHAMBER TESTING	47
6.2	EXPERIMENTAL VERIFICATION OF THE UNFOLDING CODE	48
7.0	REACTOR SPECTRUM MEASUREMENTS	52
7.1	EQUIPMENT AND METHODOLOGY	52
7.2	MEASUREMENT RESULTS	53
7.2.1	Reactor Site 5	54
7.2.2	Reactor Site 6	60
7.2.3	Reactor Site 4	63
7.3	REACTOR MEASUREMENT SUMMARY	69
7.4	DISCUSSION	72
8.0	RECOMMENDATIONS	73
	REFERENCES	76
	APPENDIX A - ENERGY SENSITIVITY OF THE TLD-ALBEDO NEUTRON DOSIMETER	79
	APPENDIX B - MULTISPHERE SPECTROMETER	82
	APPENDIX C - RESPONSE FUNCTIONS USED IN HESTRIP	85
	APPENDIX D - HESTRIP, A COMPUTER CODE FOR UNFOLDING SPECTRA FROM <sup>3</sup> He PROPORTIONAL COUNTER DATA	93



## FIGURES

3.1	Pulse Height Distribution for a $^3\text{He}$ Proportional Counter Exposed to Thermal Neutrons . . . . .	7
3.2	Response of an Unshielded $^3\text{He}$ Proportional Counter Exposed to Monoenergetic Neutrons . . . . .	8
3.3	Cross Sections for Neutron Interactions in $^3\text{He}$ Proportional Counters . . . . .	10
3.4	Pulse Pile-Up Resulting When Two Pulses Occur Within the Resolving Time of the Spectrometer System . . . . .	11
3.5	Absorption Cross Sections for Three Shielding Materials . . . . .	13
3.6	"Rise Time" Spectra From Ortec 458 Pulse Shape Analyzer Obtained with a Bare $^3\text{He}$ Proportional Counter Exposed to Thermal Neutrons . . . . .	15
3.7	Pulse Shape Analyzer Used to Reduce Pulse Pile-Up at High Count Rates . . . . .	15
3.8	Apparatus Used to Estimate Pulse Pile-Up Using A Pulse Generator . . . . .	16
3.9	Method of Estimating Pulse Pile-Up Using a Reference Pulser Operated at the Same Pulse Rate as the Neutron Counts . . . . .	17
3.10	Differential Neutron Flux Density Multiplied by the Neutron Energy (or Flux per Unit Lethargy) for Neutrons from a Fission Source Penetrating a Concrete Shield . . . . .	21
5.1	Example of a $^3\text{He}$ Proportional Counter with Nonuniform Gain Along the Anode . . . . .	29
5.2	Apparatus Used to Determine the Best Operating Parameters for a $^3\text{He}$ Proportional Counter . . . . .	29
5.3	Determination of Best Operation Parameters for a 1-Inch Diameter $^3\text{He}$ Proportional Counter . . . . .	30
5.4	Pulse Height Distribution Obtained From a $^3\text{He}$ Proportional Counter with Uniform Gain . . . . .	31
5.5	$^3\text{He}$ Spectrometer Electronics Using a Pulser Technique to Estimate Pulse Pile-Up . . . . .	33
5.6	Pulse Pile-Up Distribution Obtained by Operating Pulser at Different Count Rates . . . . .	35
5.7	Results of Using Pulser Technique for Estimating Gamma Pulse Pile-Up . . . . .	37
5.8	Cable Connections and Sample Settings for $^3\text{He}$ Spectrometer System Electronics Using Pulse Shape Analysis . . . . .	38
5.9	Unipolar Output Pulses of Ortec 572 Amplifier for Pole Zero Adjustment . . . . .	40

5.10	"Rise Time" Spectra From Linear Output of Ortec 458 Pulse Shape Analyzer With and Without Coincidence Gate Signal From "Window" of Pulse Shape Analyzer . . . . .	43
5.11	Plot of Channel Number of Pulser Peak Versus Pulser Setting to Determine if the ADC is Linear Through Zero . . . . .	45
6.1	Relative Humidity and Temperature for $^3\text{He}$ Spectrometer Test in PNL Environmental Chamber . . . . .	48
6.2	Comparison of Neutron Energy Spectra Measured by a Photon Recoil Spectrometer and the $^3\text{He}$ Spectrometer at the 144 keV Neutron Beam at the U.S. National Bureau of Standards . . . . .	49
7.1	Differential Neutron Energy Spectrum Calculated From Multisphere Spectrometer Measurements at Reactor Site 5 . . . . .	55
7.2	Fractional Dose Equivalent Distribution Calculated From Multisphere Spectrometer Measurements at Reactor Site 5 . . . . .	56
7.3	Pulse Height Distribution from $^3\text{He}$ Spectrometer Measurement at Reactor Site 5 . . . . .	57
7.4	Pulse Pile-Up Distribtuion for the $^3\text{He}$ Spectrometer Exposed to a Thermal Neutron Source for Reactor 5 . . . . .	57
7.5	Fluence Per Unit Lethargy Measured by the $^3\text{He}$ Spectrometer and Multisphere Spectrometer at Reactor Site 5 . . . . .	60
7.6	Differential Neutron Flux Density Calculated from the Multisphere Spectrometer Measured at Reactor Site 6 . . . . .	62
7.7	Fractional Dose Equivalent Rate Calculated from the Multisphere Spectrometer Measured at Reactor Site 6 . . . . .	63
7.8	Flux Per Unit Lethargy as a Function of Neutron Energy for the $^3\text{He}$ Spectrometer Measurements at Reactor Site 6 . . . . .	65
7.9	Differential Neutron Flux Density Calculated from the Multisphere Spectrometer Measurement at Reactor Site 4 . . . . .	68
7.10	Fractional Dose Equivalent Calculated from the Multisphere Spectrometer Measurement at Reactor Site 4 . . . . .	69
7.11	Flux per Unit Lethargy as a Function of Neutron Energy for the $^3\text{He}$ Spectrometer Measurement at Reactor Site 4 . . . . .	71
A.1	Flux Density Per Unit Lethargy for Bare $^{252}\text{Cf}$ Source, and for a Typical Nuclear Power Plant and Albedo Dosimeter Response Function as a Function of Neutron Energy . . . . .	79
A.2	Flux Density Per Unit Lethargy for $^{252}\text{Cf}$ Source Moderated by 15-cm Radius $\text{D}_2\text{O}$ . . . . .	80
A.3	Response of TLD-Albedo Neutron Dosimeter Per Unit of Dose Equivalent . . . . .	81
C.1	A Simplified Flow Chart for the Monte Carlo Computer Code WALL Used to Calculate a Response Function Matrix for Cylindrical $^3\text{He}$ Proportional Counters . . . . .	86

## TABLES

2.1	Candidate Neutron Energy Spectrometers . . . . .	3
3.1	Chance Coincidence Rate, Which Produces Pulse Pile-Up, Calculated for a 2 Microsecond Resolving Time . . . . .	12
4.1	<sup>3</sup> He Spectrometer Components and Costs . . . . .	27
5.1	Settings for <sup>3</sup> He Spectrometer Electronics Using a Pulser Technique to Estimate Pulse Pile-Up . . . . .	34
5.2	Settings for <sup>3</sup> He Spectrometer Electronics Using Pulse Shape Analysis . . . . .	39
6.1	Neutron Dose Equivalents Determined from <sup>3</sup> He Spectrometer Measurements of Nearly Monoenergetic Neutrons Produced by a Van de Graaff Accelerator . . . . .	50
7.1	Results of Multisphere Spectrometer Measurements at Reactor Site 5 . . . . .	54
7.2	Results of <sup>3</sup> He Spectrometer Measurements at Reactor Site 5 Analyzed by the Computer Code HESTRIP . . . . .	59
7.3	Results of Multisphere Spectrometer Measurements at Reactor Site 6 Analyzed by the Computer Code SPUNIT . . . . .	61
7.4	Results of the <sup>3</sup> He Spectrometer Measurements at Reactor Site 6 . . . . .	64
7.5	Results of Multisphere Spectrometer Measurements at Reactor Site 4 Analyzed by the Computer Code SPUNIT . . . . .	66
7.6	Results of Multisphere Spectrometer Measurements at Reactor Site 4 Analyzed by the Computer Code YOGI . . . . .	67
7.7	Summary of Dose Equivalent Rate Measurements Inside Containment of Commercial Nuclear Power Plants . . . . .	70
C.1	Gas Fillings for 1-Inch Diameter <sup>3</sup> He Proportional Counters Used at PNL . . . . .	87
C.2	Wall Effect Response Function for Tube #1 . . . . .	88
C.3	Wall Effect Response Function for Tube #2 . . . . .	89
C.4	Wall Effect Response Function for Tube #3 . . . . .	90
C.5	Wall Effect Response Function for Tube #4 . . . . .	91
C.6	Wall Effect Response Function for Tube #5 . . . . .	92
D.1	Sample Input for Computer Code HESTRIP . . . . .	94
D.2	Listing of Counts Per Channel From the Multichannel Analyzer for a <sup>3</sup> He Proportional Counter Exposed to the 144 keV Neutron Beam at the National Bureau of Standards . . . . .	95
D.3	Sample Output From the Computer Code HESTRIP Used to Analyze Data From a <sup>3</sup> He Proportional Counter Exposed to the 144 keV Neutron Beam at the National Bureau of Standards . . . . .	97
D.4	Listing of HESTRIP Code . . . . .	101

## ACKNOWLEDGMENTS

The authors are indebted to R. B. Schwartz of the National Bureau of Standards, who provided the proton recoil spectrometer and  $^3\text{He}$  spectrometer measurements at the filtered beam facility at the National Bureau of Standards reactor. We would also like to thank Andrea Currie, who edited the document, and Marianna Cross, who typed numerous revisions.

NEUTRON DOSIMETRY AT COMMERCIAL NUCLEAR PLANTS  
FINAL REPORT OF SUBTASK C:  $^3\text{He}$  NEUTRON SPECTROMETER

1.0 INTRODUCTION

The thermoluminescent-albedo dosimeter (TLD-albedo dosimeter) has been shown to be adequate for personnel dosimetry at commercial nuclear power plants (NUREG/CR-2956). However, the TLD-albedo dosimeter, like many other commercially available neutron dosimeters evaluated, also exhibits an energy dependence problem: the dosimeter response per unit of dose equivalent is not constant, but varies with energy. Unless precautions are taken, the neutron dose equivalent may be overestimated by as much as a factor of 20 because of the differences between the unique, low-energy spectra typically found inside reactor containment and the higher-energy spectra of the sources used to calibrate the neutron dosimeter (NUREG/CR-2956).

At the request of the U.S. Nuclear Regulatory Commission (NRC), Pacific Northwest Laboratory (PNL) has evaluated a technique which may be used to more accurately interpret the response of TLD-albedo dosimeters used in commercial nuclear power plants. The approach taken involved developing and validating a method for accurately measuring neutron energy spectra and neutron dose equivalent rates. When implemented, the method would not only verify actual neutron spectra inside reactor containment, but also provide energy correction factors to enable more accurate interpretation of TLD-albedo dosimeter measurements.

This report describes how a  $^3\text{He}$  spectrometer can be used to improve the accuracy of personnel neutron dosimetry at commercial nuclear power plants. The detailed information report is intended to enable a person unfamiliar with neutron spectrometry techniques to assemble and operate a  $^3\text{He}$  spectrometer using only commercially available equipment. Some knowledge of nuclear counting equipment is assumed. A complete set of instructions for using the  $^3\text{He}$  spectrometer to measure spectra inside reactor containment is included.

Section 2.0 documents the considerations evaluated in selecting the particular spectrometer on which to base the method. Section 3.0 discusses the theory underlying  $^3\text{He}$  spectrometer operation. Section 4.0 gives a complete description of the equipment required for the apparatus. Detailed instructions for assembling the spectrometer, including troubleshooting hints, are contained in Section 5.0. Section 6.0 documents how the assembled spectrometer was tested in the environmental chamber, as well as how the unfolding codes were verified. Section 7.0 describes the methodology used and results obtained when  $^3\text{He}$  spectrometer measurements were made at three PWRs and one BWR. These results are then compared with multisphere spectrometer measurements made at the same locations. Section 8.0 presents PNL's recommendations based on the overall effort. The appendixes include a listing of the computer code HESTRIP used to analyze the  $^3\text{He}$  spectrometer data and sample input/output.

## 2.0 SPECTROMETER EVALUATION

In personnel dosimetry, the measurement of ultimate interest is the dose equivalent. Alsmiller and Barish (1974) have used Monte Carlo computer codes to calculate the response of typical TLD-albedo dosimeters per unit dose equivalent as a function of neutron energy. Their work, summarized in Appendix A, suggests that the neutron energy spectrum measurements necessary to the calculation can be simplified by considering the neutron flux density (neutrons/cm<sup>2</sup>-sec) or the dose equivalent rate (mrem/hr) in three energy regions:

- Region 1 - <1 eV
- Region 2 - 1 eV to 10 keV
- Region 3 - >10 keV.

Previous neutron energy spectrum measurements in reactor containment indicated the presence of very few neutrons with energies above 1 MeV (NUREG/CR-1769). Threshold detectors such as polycarbonate plastic track etch detectors and NTA film showed little or no response to reactor spectra. Measurements made with NE-213 liquid scintillator and multisphere spectrometers show virtually no neutrons with energies above 1 MeV. Thus, only spectrometers that operate at energies below about 1 MeV were considered as candidates for the PNL method.

Four spectrometer types were evaluated in this study:

- multisphere spectrometers
- activation foils
- proton-recoil gas proportional counters
- <sup>3</sup>He proportional counters.

All four types appeared suitable for measuring neutron energy spectra within the nuclear power plant containment. However, as indicated by the comments in Table 2.1, none offers the ideal combination of high accuracy, ease of use, and simplicity of data analysis. Further, no single type can accurately span the entire range of energies found inside containment. Thus, the spectrometer chosen as the basis for the PNL method would necessarily represent a compromise. Each type has some operational difficulties which may prevent its use in some reactor containment measurements.

### 2.1 MULTISPHERE SPECTROMETERS

Multisphere or Bonner sphere spectrometers (Bramblett, Ewing and Bonner 1960) have a very useful wide energy range, extending from thermal to 20 MeV; they also determine both approximate neutron flux density and dose equivalent. This is the spectrometer most often used by health physicists. The authors used a multisphere spectrometer concurrently with a <sup>3</sup>He spectrometer to check the latter's measurement accuracy.

TABLE 2.1. Candidate Neutron Energy Spectrometers

Spectrometer Type	Comments
Multisphere or Bonner Sphere	<p>Advantages: - Useful over wide energy range (thermal to 20 MeV)</p> <p>- Relatively simple equipment required, but heavy spheres</p> <p>Disadvantages: - Poor resolution, especially for fast neutrons greater than 1 MeV</p> <p>- Most unfolding codes quite complex</p> <p>- Time consuming measurements with different sphere sizes</p> <p>- gain shifts with temperature</p>
Activation Foils	<p>Advantages: - Accurate for thermal and intermediate neutron energies</p> <p>- Less accurate for high energy fast neutrons</p> <p>Disadvantages: - Need elaborate gamma ray counting equipment</p> <p>- Some foils must be counted soon after irradiation</p> <p>- Usually requires higher flux levels or more complex counting equipment for lower activities</p>
Proton-Recoil Gas Proportional Counters	<p>Advantages: - Responds to wide range of neutron energies (keV to 1 MeV)</p> <p>Disadvantages: - Complex equipment for pulse risetime analysis</p> <p>- Difficult to discriminate between gamma rays and neutrons below about 10 keV</p> <p>- sensitive to temperature and vibration</p>
<sup>3</sup> He Proportional Counters	<p>Advantages: - Responds to thermal neutrons and to neutrons with energies between 30 keV to 5 MeV</p> <p>Disadvantages: - Difficult to measure intermediate energy neutrons (1 eV to 10 keV)</p> <p>- Large thermal fluxes interfere with fast neutron analysis</p>

The specific multisphere spectrometer used by the authors consisted of a set of five polyethylene spheres, a <sup>6</sup>LiI scintillation detector and associated electronics (high voltage power supply, preamplifier, shaping amplifier, and multichannel analyzer for data collection).<sup>(a)</sup> The <sup>6</sup>LiI detector fits into a hole drilled to the center of each sphere and measures the slow neutron flux at the center of the sphere. Spectral measurements are made by placing the different spheres over the <sup>6</sup>LiI neutron detector and recording the count rate; each sphere-detector combination has a different response to neutrons of different energies. The count rate from each sphere-detector combination is input to a computer code, which "unfolds" the approximate neutron energy spectrum. In the past the computer codes were quite complex, requiring a large computer for execution. Recently, however, simpler algorithms and computer codes (Johnson and Gorbics 1981; Brackenbush and Scherpelz 1983) have been developed that can be run on microprocessors and personal computers available at many commercial nuclear power plants.

(a) A complete description of the multisphere spectrometer system can be found in Appendix B.

The primary advantages of the multisphere spectrometer are the wide range of energies covered and the relatively simple equipment required. With the recently developed computer codes, data analysis has been simplified. An even more simple analysis method for determining dose equivalent from only four multisphere measurements has been developed (NUREG/CR-3400, p. 9).

The main disadvantages of the multisphere spectrometer are the time required (typically more than 20 minutes) to make five to seven different measurements in high dose rate areas and the physical effort required to carry the set of spheres; a complete set of spheres, the associated equipment, and carrying case weighs about 100 pounds. The multisphere spectrometer also has poor resolution, especially at higher neutron energies. The differential spectra may not be very accurate, but the integral flux and dose equivalents are usually reasonably accurate. Measurements made under ideal conditions in a low-scatter room at PNL indicate that, for a  $^{252}\text{Cf}$  source moderated by 15 cm of  $\text{D}_2\text{O}$ , the multisphere spectrometer measured the dose equivalent rate within 18% of the value calculated from the source intensity and flux to dose equivalent conversion factors supplied by the National Bureau of Standards. The reader should be cautioned that the spheres used by PNL were custom-made; the commercially available multispheres are of slightly different sizes, so the response functions used may not match. Also, there is no unique solution to the multisphere unfolding problem; different codes give different fluxes. Only approximate differential spectra can be obtained, as explained in Appendix B.

## 2.2 ACTIVATION FOILS

The activation foil technique consists of exposing a set of foils of various elements to neutrons for a known time period. The induced radioactivity is then measured by gamma ray spectrometers. Knowing the activation cross section as a function of energy makes it possible to calculate the neutron flux using rather complex computer codes. The solution technique involves numerically solving a coupled set of Fredholm integral equations.

The chief advantage of the activation foil technique is that it is accurate at low neutron energies, where there are a number of absorption resonances found in various elements. This technique is less accurate at higher neutron energies above about 10 keV, where there are few resonances and the activation cross sections are generally much lower.

Several problems are inherent in the activation foil technique. Counting the activity induced in the foils by relatively low neutron fluxes is tedious and time-consuming. The computer codes used to unfold the data are complex and require a large computer. However, the germanium diode gamma ray spectrometers used at many nuclear power plants for counting environmental and low level radioactive samples are suitable for foil counting, and this technique may be useful for spectrum determinations.

## 2.3 PROTON-RECOIL PROPORTIONAL COUNTERS

The proton-recoil proportional counter spectrometer consists of a set of two or more proportional counters filled with hydrogen or methane, a complex



set of electronics with pulse shape analysis capability to separate neutron- and photon-induced pulses, and a multichannel analyzer or microcomputer to record the data. The proton-recoil data are analyzed by a complex computer code to determine the differential neutron flux density as a function of energy. A variety of detectors with different gas fillings and pressures is required to cover the energy range from a few keV to 1 MeV.

The greatest advantage of the proton recoil spectrometer is its high accuracy when set up properly. It has even been used to verify neutron transport computer codes.

The disadvantage of the proton-recoil spectrometer is its complexity. It requires complex, fast electronics to separate neutron- and photon-induced events, especially for neutron energies less than about 10 keV. The delicate electronics may not be suitable for the harsh environments found inside some reactor containments. A complex unfolding computer code is needed to calculate and match the spectra measured by the different detectors over different energy ranges. High temperatures and vibration in some reactors may preclude using the proton recoil spectrometer, which is more suited to laboratory environments.

The proton-recoil spectrometer may be the most difficult to operate, but it gives the most accurate spectra over a wide range of energies. An excellent description of the proton-recoil proportional counter spectrometer, including a description of the custom electronics and the computer code used to analyze the data, is provided by Bennett and Yule (1971).

#### 2.4 $^3\text{He}$ SPECTROMETER

The  $^3\text{He}$  spectrometer consists of a  $^3\text{He}$  proportional counter, a set of neutron absorbers such as cadmium, samarium, and boron, and associated electronics. This spectrometer has less complex electronics and does not use the complicated unfolding codes required by the proton-recoil spectrometers. It has better energy resolution than the multisphere spectrometer at higher neutron energies, especially between 50 keV and 1 MeV.

The  $^3\text{He}$  spectrometer does have several problems, however. It is highly sensitive to slow neutrons; neutron absorbers such as cadmium and samarium are required to filter out slow (thermal and intermediate energy) neutrons to prevent pulse pile-up, which can interfere with the analysis of higher-energy neutrons. The  $^3\text{He}$  spectrometer cannot resolve neutrons with energies below about 20 keV because of the 2 to 3% resolution of commercial proportional counters. Approximate spectra below about 10 to 20 keV can be determined by using various neutron absorbers, as described later in this report. Above 1 MeV the  $^3\text{He}$  recoils can interfere with the data analysis, unless special precautions are taken.

Despite these disadvantages, the  $^3\text{He}$  spectrometer was found to be the best compromise between the level of operational difficulty and the accuracy of the measured spectra. For this reasons, it was selected as the basis of the PNL system.

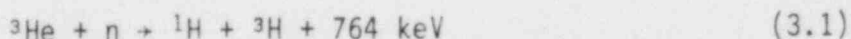
### 3.0 THEORY OF $^3\text{He}$ SPECTROMETER OPERATION

A description based on nuclear theory of how the  $^3\text{He}$  spectrometer works is presented in this section, followed by a discussion of techniques used to analyze data obtained with the device.

A number of terms are introduced which may need explanation. For this report, the term "fast neutrons" is used to designate neutrons with energies roughly above 10 keV, and the term "slow neutrons" is used to designate neutrons with energies well below 10 keV. Thus, slow neutrons include thermal and intermediate energy neutrons. Since  $^3\text{He}$  has an absorption cross section which is inversely proportional to the velocity of the neutron, a  $^3\text{He}$  proportional counter will easily detect both thermal and intermediate (or slow) energy neutrons.

#### 3.1 NUCLEAR THEORY

The isotope  $^3\text{He}$  is useful for neutron spectrometry because it undergoes the following nuclear reaction:



Neutrons interact with  $^3\text{He}$  to form two charged particles, a proton and a triton, and 764 keV of energy is also released. By convention this is represented as a  $^3\text{He}(n,p)\text{T}$  reaction. If the  $^3\text{He}$  gas is used as the fill gas in a proportional counter, the charged particles are easily detected. If the triton and proton deposit all their energy within the proportional counter gas, the pulse produced by the proportional counter tube will be equal to the initial energy of the neutron plus the 764 keV (the Q-value of the nuclear reaction). Note that some of the gamma rays will interact in the walls of the counter to produce electrons, which will also produce pulses. However, because of the large Q-value of the nuclear reaction (764 keV), the gamma pulses will be much smaller and easily discriminated from the neutron-induced pulses.

In an ideal detector monoenergetic neutrons would produce a single peak with an energy equal to the incident neutron energy plus 764 keV. Unfortunately, proportional counters are not ideal detectors. Counters having the best resolutions are usually small, so that some of the protons and tritons are not stopped in the counter gas, but strike the walls or the insensitive regions at the ends of the counter. These "wall effects" produce a continuum of smaller pulses. Figure 3.1 shows the results obtained by exposing a  $^3\text{He}$  proportional counter to thermal neutrons. If both the triton and proton are stopped in the counter gas, a full energy peak of 764 keV is produced. If the proton strikes the wall, all of the triton energy (191 keV) plus a fraction of the proton energy is deposited in the gas, depending on how far away from the wall the interaction occurred. This produces the sharp edge at 191 keV and the continuum of events at higher energies. A similar edge (at 573 keV) and continuum of pulses at higher energies occurs if the triton strikes the wall. The full energy peak at 764 keV has a width of 2.4% or 18 keV at half the maximum height due to the finite resolution of the proportional counter. This

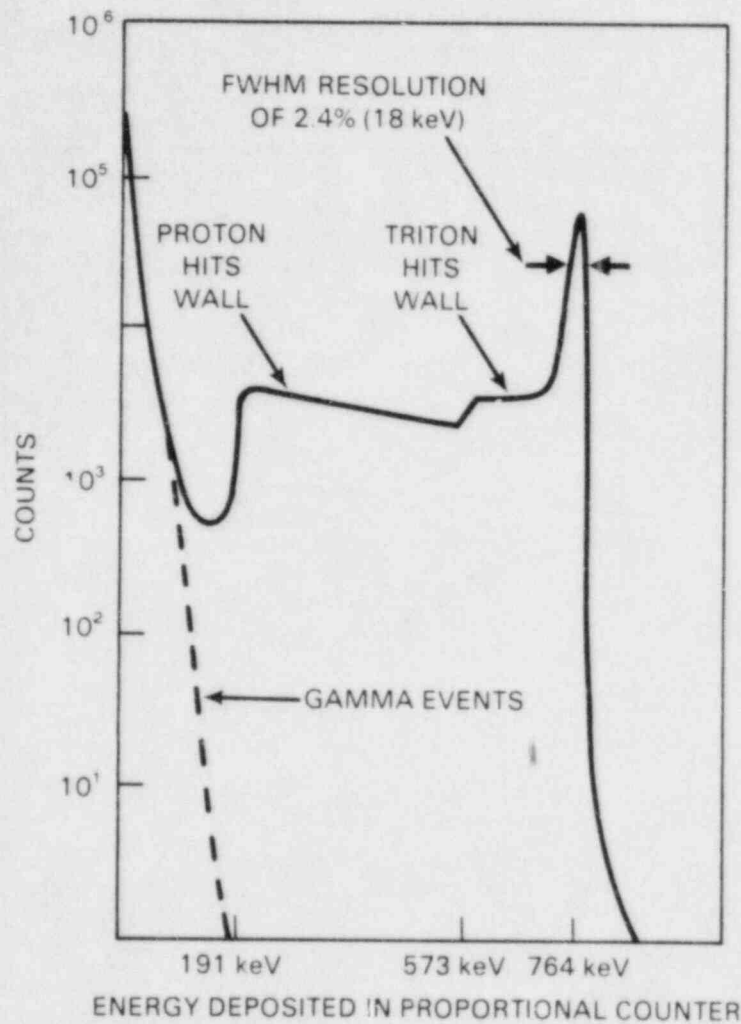


FIGURE 3.1. Pulse Height Distribution for a  $^3\text{He}$  Proportional Counter Exposed to Thermal Neutrons

is referred to as a resolution of 18 keV full width half maximum (18 keV FWHM resolution). Neutrons with energies below the full width half maximum produce a "shoulder" on the peak and cannot be fully resolved. Thus, only neutrons with energies greater than the full width half maximum can be analyzed with the  $^3\text{He}$  proportional counter.

If the  $^3\text{He}$  proportional counter is completely surrounded by a 40-mil (0.10-cm) layer of cadmium, no thermal neutrons can reach the counter, and the gamma ray events, shown as the dashed line in Figure 3.1, are measured. These gamma ray events deposit much less energy in the proportional counter and can be easily distinguished from neutron events on the basis of pulse size.

Figure 3.2 shows the response of an unshielded  $^3\text{He}$  proportional counter exposed to nearly monoenergetic neutrons with an average energy of 660 keV produced by a Van de Graaff accelerator at PNL. Because of neutrons scattered and slowed down by the concrete floor and walls, there is a thermal neutron

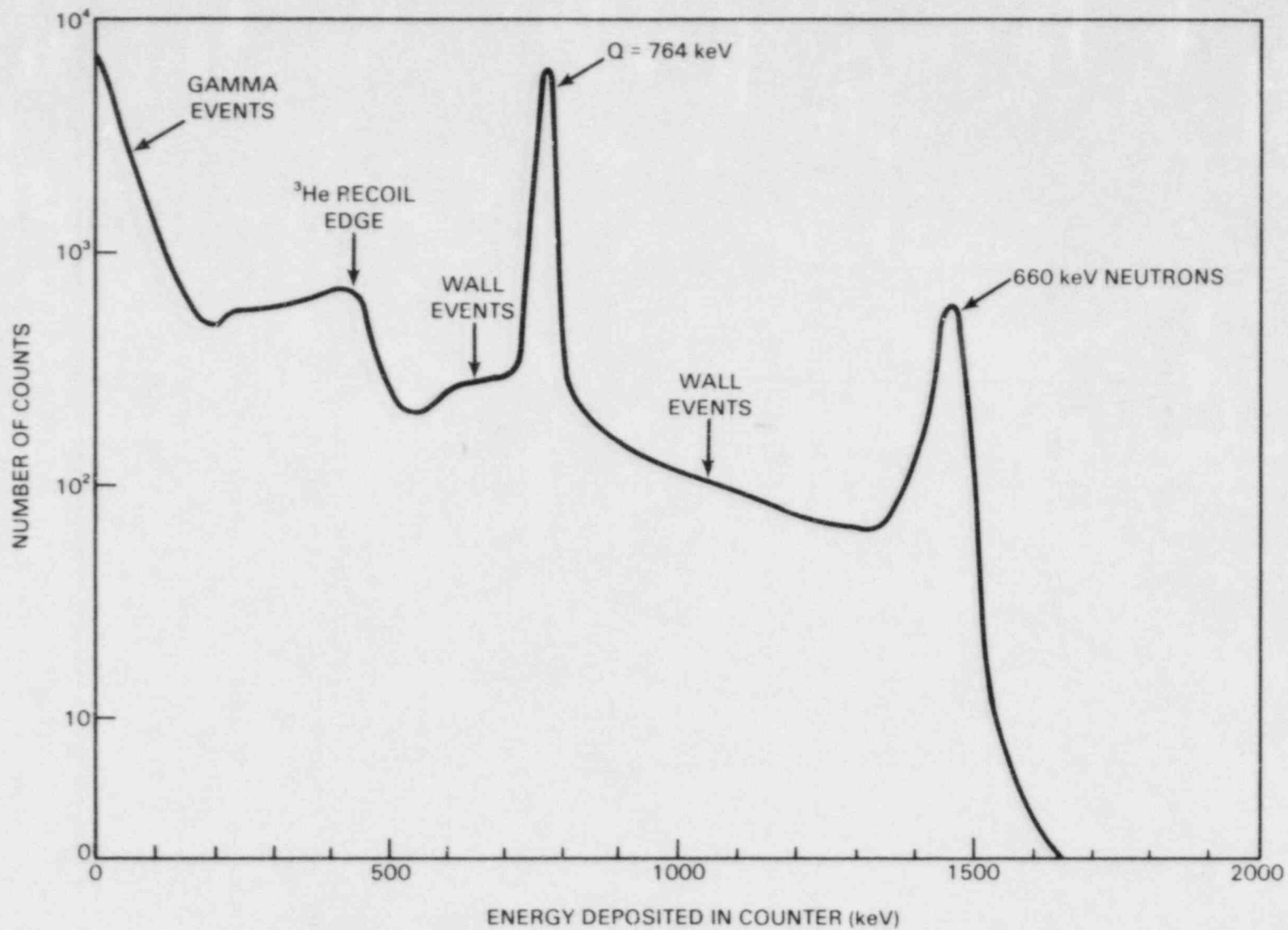


FIGURE 3.2. Response of an Unshielded  $^3\text{He}$  Proportional Counter Exposed to Monoenergetic Neutrons

peak produced at 764 keV, which can be used for energy calibration. Figure 3.2 shows some features that were not evident in Figure 3.1. An edge at about 450 keV is produced by the elastic scatter of neutrons from the  $^3\text{He}$  nucleus. From the Laws of Conservation of Energy and Momentum, it can be shown that the energy of the recoil nucleus is related to the energy of the incident neutron by the relationship

$$E_R = \frac{4A}{(1+A)^2} (\cos^2 \theta) E_n \quad (3.2)$$

where

$E_R$  is the energy of the recoil  $^3\text{He}$  nucleus

$E_n$  is the energy of the incident neutron

$A$  is the atomic weight of the target  $^3\text{He}$  nucleus

$\theta$  is the scattering angle in the laboratory coordinate system.

For  $^3\text{He}$  nuclei,  $A = 3$ , and Equation (3.2) reduces to  $E_R = 3/4 E_n \cos^2\theta$ . Thus,  $^3\text{He}$  recoils can produce pulses that vary in energy from zero energy (for a glancing collision where the recoil is emitted at  $90^\circ$  to the incoming neutron) to three-fourths of the energy of the incident neutron (for a head-on collision at  $\theta = 0^\circ$ ). Because the desired  $^3\text{He}(n,p)\text{T}$  reaction has a Q-value of 764 keV, only neutrons with energies greater than 1 MeV can produce recoils with enough energy to be confused with the  $^3\text{He}(n,p)\text{T}$  reaction. Fortunately, as noted in Section 2.0, few neutrons in containment have energies above 1 MeV, so it is not necessary to account for  $^3\text{He}(n,n')^3\text{He}$  reactions producing recoil events above the slow neutron peak.

The  $^3\text{He}(n,p)\text{T}$  cross section is shown in Figure 3.3. Helium-3 has a cross section proportional to the inverse of the velocity of the neutron (or the inverse of the square root of the neutron energy) over a wide range of energies. The  $^3\text{He}(n,p)\text{T}$  cross section is 5,327 barns at 0.0253 keV or 2200 m/sec and can be represented by

$$\sigma = \frac{847.3}{\sqrt{E}} \quad (3.3)$$

from thermal energies to 1.7 keV. The cross section,  $\sigma$ , has units of barns and the energy,  $E$ , has units of electron volts (Stewart 1974, p. 151). The  $^3\text{He}$  detectors are very sensitive to low-energy neutrons. Using the cross section at 50 keV as a reference, the  $^3\text{He}$  detector is 1600 times more sensitive to thermal neutrons, 287 times more sensitive to neutrons with energies of 1 eV, and 2.5 times more sensitive to neutrons with energies of 10 keV.

### 3.1.1 Pulse Pile-Up

If two events occur nearly simultaneously in the proportional counter, the pulses can be summed together to produce a larger pulse, which can be mistaken for an event produced by a higher energy neutron. Figure 3.4 shows how two neutron interactions, labeled A and B, can produce a pulse larger than a single event, labeled C. In Figure 3.4 the resolving time,  $t$ , is defined as

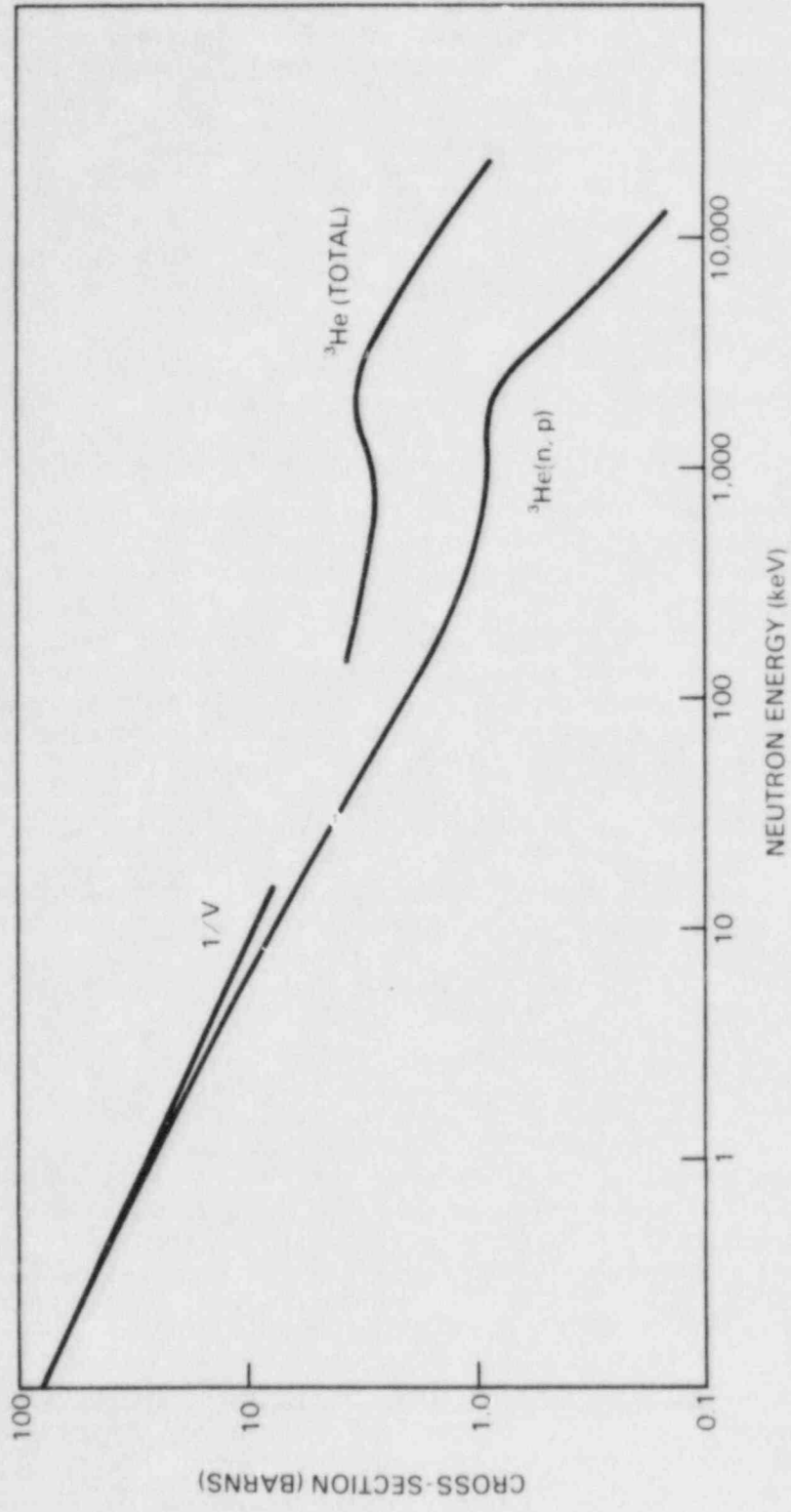


FIGURE 3.3. Cross Sections for Neutron Interactions in  $^3\text{He}$  Proportional Counters

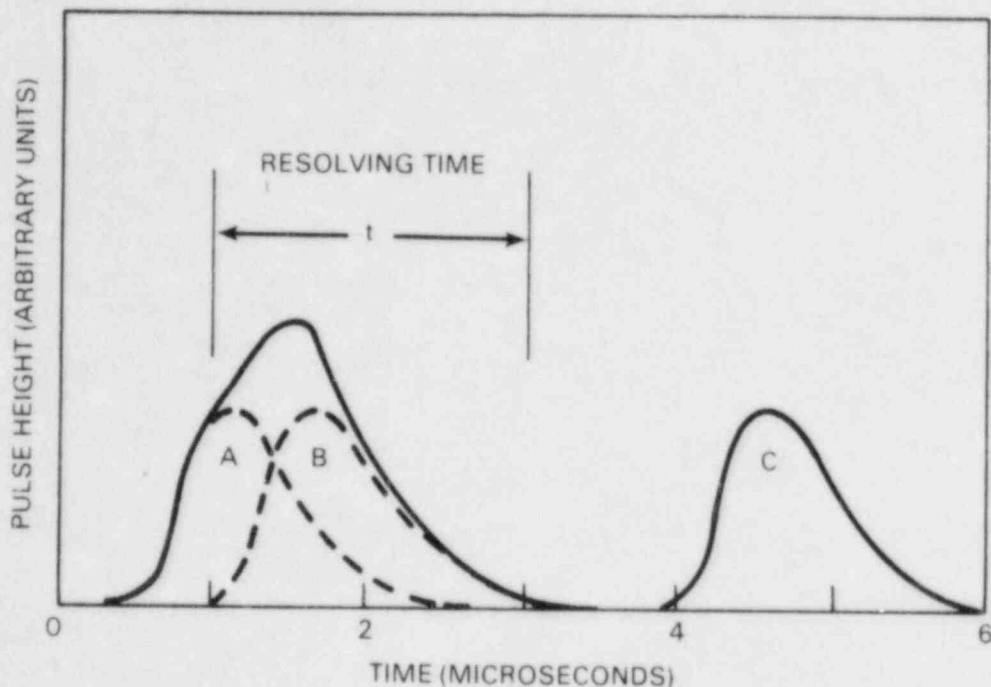


FIGURE 3.4. Pulse Pile-Up Resulting When Two Pulses Occur Within the Resolving Time of the Spectrometer System

the minimum time interval in which two separate events can be defined without overlap. The resolving time is usually determined by the time constants of the shaping amplifier, which is often dictated by the minimum pulse width that can be accepted by the multichannel analyzer used to record data. Typically, the shaping amplifier time constants are 1 to 2 microseconds.

The chance coincidence and pile-up rate can be estimated mathematically. Let  $r$  be the random count rate of interactions in a  $^3\text{He}$  proportional counter, and assume that the count rate is low so that the product of the count rate multiplied by the resolving time ( $rt$ ) is much less than unity ( $rt \ll 1$ ). The rate of chance coincidence,  $r_{\text{coinc}}$ , is the fraction of the time within the resolving time of the preceding pulse ( $rt$ ) multiplied by the rate of pulse arrival ( $r_s$ ):

$$r_{\text{coinc}} = (rt) r_s \quad (3.4)$$

The second pulse could be produced by a pulser, as will be explained later; however, if the second pulse is another random pulse produced within the proportional counter,  $r$  and  $r_s$  are identical, so the chance coincidence rate,  $r_{\text{coinc}}$ , becomes

$$r_{\text{coinc}} = r^2 t \quad (3.5)$$

TABLE 3.1. Chance Coincidence Rate, Which Produces Pulse Pile-Up, Calculated for a 2-Microsecond Resolving Time

Count Rate from Proportional Counter		Chance Coincidence Rate, $r_{\text{coinc}}$	Fraction of Pile-Up Events
Counts/min	Counts/sec	Counts/sec	
60	1	$2.0 \times 10^{-6}$	$2.0 \times 10^{-6}$
600	10	$2.0 \times 10^{-4}$	$2.0 \times 10^{-5}$
1,500	25	0.0013	$5.2 \times 10^{-5}$
3,000	50	0.005	$1.0 \times 10^{-4}$
3,600	60	0.0072	$1.2 \times 10^{-4}$
6,000	100	0.020	$2.0 \times 10^{-4}$
10,000	167	0.056	$3.4 \times 10^{-4}$
60,000	1,000	2.0	$2.0 \times 10^{-3}$

### 3.1.1.1 Pulse Pile-Up Mitigation Techniques

For the typical counting system the resolving time is about 2 microseconds. Using Equation (3.5), the chance coincidence rate at various count rates was calculated. The results, given in Table 3.1, suggest that the count rate must be kept low enough that the pile-up of neutron events is a small fraction of the higher-energy neutron events recorded by the multichannel analyzer. This can be accomplished by a combination of methods:

- make measurements in low dose equivalent rate fields
- use proportional counters with a small amount of  $^3\text{He}$
- cover the  $^3\text{He}$  proportional counter with a neutron absorber
- use electronic pulse shape analysis to reduce pile-up.

Each of these methods is discussed in the following paragraphs.

Spectrum measurements are made typically at locations inside containment where the dose equivalent rate is 10 to 100 mrem/hr. A 2.54-cm (1-in.) diameter  $^3\text{He}$  proportional counter, 30.5 cm (12 in.) long, gave satisfactory results if filled with  $^3\text{He}$  at partial pressures of 2 psia to 4 psia mixed with argon. In a 50-mrem/hr neutron field the count rate was 25 counts/sec inside a boron covering; this is sufficiently low that pulse pile-up was not significant. It may be necessary to purchase several tubes with partial pressures ranging from 1 psia to 15 psia to cover the range of neutron dose equivalent rates (from 1 mrem/hr to 500 mrem/hr) found in nuclear power plants.

Another method for reducing the pulse pile-up problem is to surround the  $^3\text{He}$  proportional counter with materials that will absorb the low-energy neutrons. The ideal absorber would be transparent to neutrons with energies above about 20 keV (the limit of resolution of the proportional counter) and would completely absorb lower-energy neutrons. The absorption cross sections for three candidate materials (cadmium, boron, and samarium) are shown in Figure 3.5.



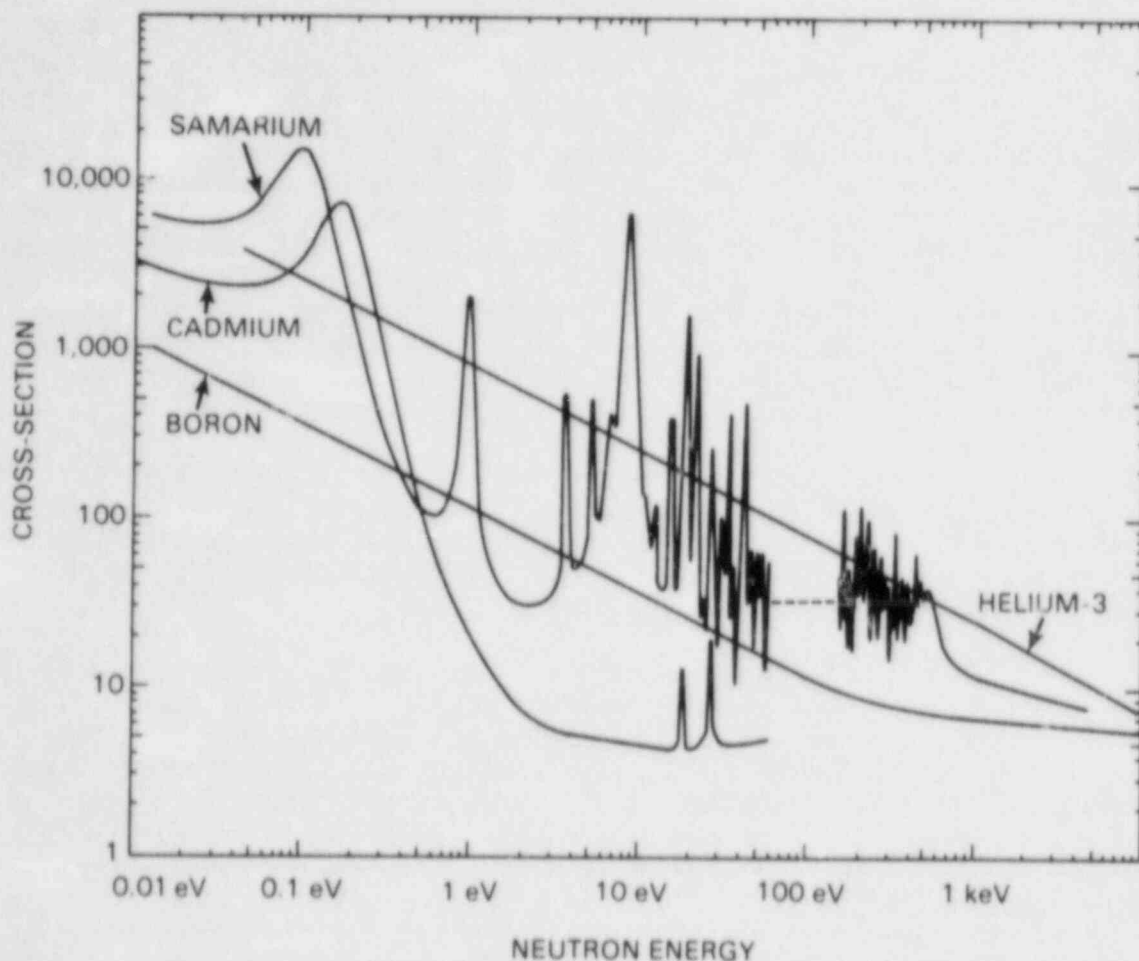


FIGURE 3.5. Absorption Cross Sections for Three Shielding Materials

Samarium has a great number of large resonances between thermal energies and 100 eV and has the largest average or effective cross section for energies below 100 eV. Unfortunately samarium metal foil is very expensive; enough material to cover a single proportional counter could cost \$5000. Impure samarium oxide is much less expensive; 1 kg costs about \$100. Oxygen has an absorption resonance at 450 keV, but this should not interfere with spectral measurements. The authors have constructed a shield containing 3 kg of samarium oxide powder between two concentric aluminum tubes 7.6 cm (3 in.) and 2.5 cm (1 in.) in diameter about 51-cm (20-in.) long.

Boron has a high absorption cross section that is inversely proportional to the velocity of the neutron and is a good neutron shield at low energies. Boron metal is expensive, but boron carbide and nitride are common industrial abrasives and are inexpensive and easy to obtain. Because boron has a low atomic number, high-energy neutrons can scatter to lower energies, and the fast neutron spectrum is distorted. Using relatively thin boron carbide shields (1 cm or less), a fast neutron will undergo a single scatter. The ratio of the minimum possible neutron energy to the original neutron energy is given by (Glasstone and Sesonske 1963, p. 151):

$$\frac{E_{\min}}{E_0} = \left( \frac{A-1}{A+1} \right)^2 \quad (3.6)$$

where  $A$  is the atomic weight of the target nucleus. For boron,  $A = 10.8$  and  $E_{\min}/E_0 = 0.69$ . For a single collision the energy can be lowered by only 31% at most. The fast neutron spectrum will be distorted, but it will be possible to detect the presence of fast neutrons and determine their relative number.

Cadmium is an excellent absorber for thermal neutrons and effectively stops all neutrons with energies below 1 eV. It also has resonances around 100 keV, but these are much smaller. Cadmium metal foil is inexpensive, readily obtained, and easy to bend and cut.

Obviously, the best material to shield the  $^3\text{He}$  proportional counter from low-energy neutrons below 10 keV is samarium. An alternative material would be boron, but this is not as satisfactory because fast neutrons can elastically scatter and transfer energy to boron. Cadmium is most effective in stopping neutrons with energies below 1 eV.

The fourth technique, pulse shape analysis, can be used to reduce pulse pile-up. Figure 3.4 showed two events that occur almost simultaneously, producing a single, larger pulse. This pulse has a much longer rise time, so that it is easy to discriminate against it. Electronics to perform the pulse shape analysis are available commercially from several sources. Figure 3.6 shows the rise time spectra obtained using this pulse shape analyzer with a bare  $^3\text{He}$  proportional counter exposed to thermal neutrons. Curve A shows the rise time spectrum obtained at very low count rates with virtually no pulse pile-up; Curve B shows the rise time spectrum obtained at a high count rate with significant pulse pile-up. Curve C shows the rise time window from the Ortec 458 pulse shape analyzer. This window can be set to exclude the longer rise time events and reduce pulse pile-up. The effect of using pulse shape analysis to reduce pile-up is obvious from Figure 3.7, which shows the pulse height distribution with and without the pulse shape analyzer.

The disadvantage of the pulse shape analysis technique is that the equipment is expensive and difficult to set up. The pulser technique described in the next section eliminates most of the complex electronics and allows one to subtract pile-up events from the  $^3\text{He}$  spectrometer data.

#### 3.1.1.2 Pulse-Pile-Up Estimation Technique

A precision pulse generator technique can be used to estimate the amount of pulse pile-up present in the data from a  $^3\text{He}$  proportional counter. This technique requires only very simple electronics as shown in Figure 3.8. The technique also enables an estimation of the amount of gamma pile-up, which may distort the spectra in the 20-keV to 60-keV energy range. It is absolutely essential that the pulser remain stable during the measurement; this may be a problem in the high-temperature environment found in nuclear reactor containment.

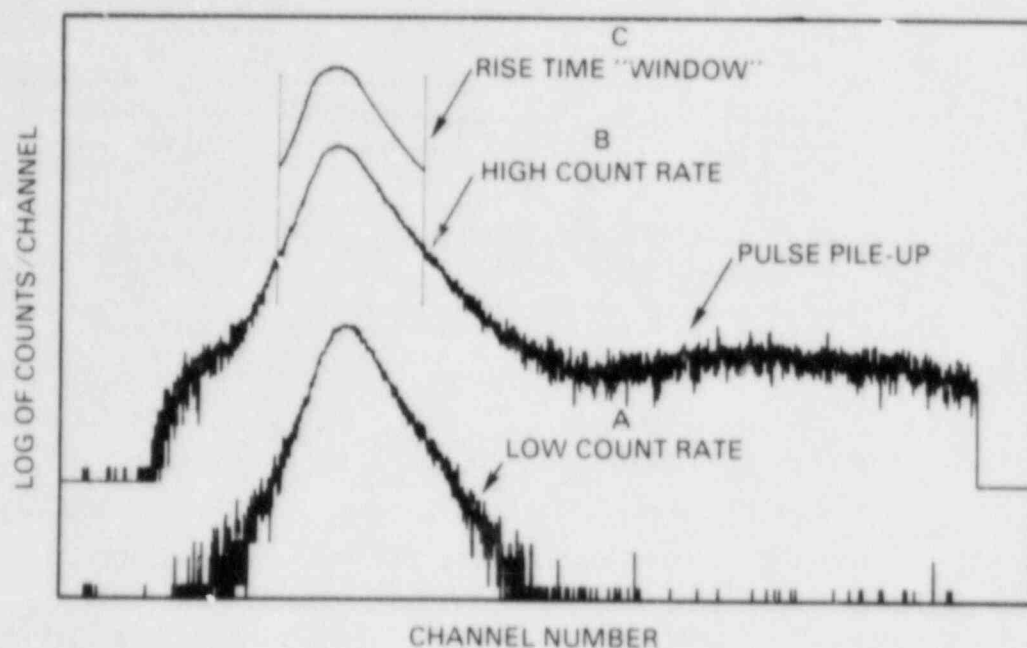


FIGURE 3.6. Rise Time Spectra From Ortec 458 Pulse Shape Analyzer Obtained with a Bare  $^3\text{He}$  Proportional Counter Exposed to Thermal Neutrons

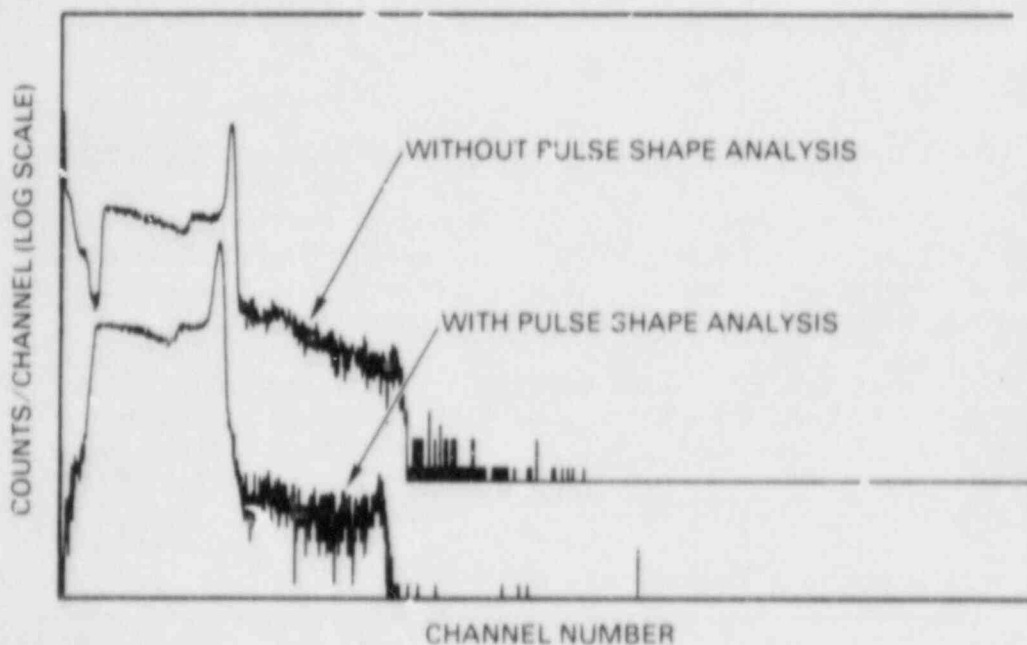


FIGURE 3.7. Pulse Shape Analyzer Used to Reduce Pulse Pile-Up at High Count Rates

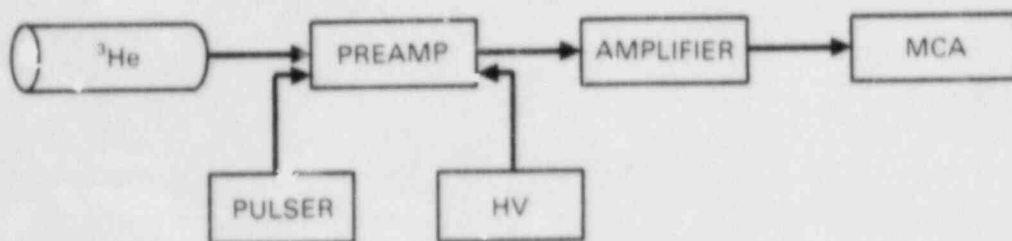


FIGURE 3.8. Apparatus for Estimating Pulse Pile-Up Using A Pulse Generator

Previously the chance coincidence rate for pulse pile-up,  $r_{\text{coinc}}$ , was shown to be  $r_{\text{coinc}} = (rt)r_s$ , where  $t$  is the resolving time,  $r$  is the count rate from random events occurring in the proportional counter, and  $r_s$  is the count rate from a second pulse occurring within the resolving time. The second pulse could be from another interaction in the proportional counter (in which case  $r_s = r$ ) or from a pulse injected into the electronic system by a precision pulse generator. If the pulse generator is adjusted so that its pulse rate is the same as the pulse rate from the proportional counter, then the random coincidence rates producing pulse pile-up will be identical, as shown in Figure 3.9. This is easy to accomplish by setting a region of interest (ROI) covering all the neutron data in the multichannel analyzer and determining the integral counts.

### 3.2 DATA ANALYSIS TECHNIQUES

The techniques described in this section may be used to analyze the data from a  $^3\text{He}$  spectrometer to obtain approximate neutron energy spectra from which to calculate dose equivalent. The methods are simple and ignore any effects other than absorption of neutron in absorbers placed around the  $^3\text{He}$  proportional counter. The techniques are presented in terms of the three energy regions noted in Section 2.0 and detailed in Appendix A.

The differential neutron flux density need not be measured over the entire range of energies from thermal to 1 MeV; the TLD-albedo dosimeter response per unit of dose equivalent is almost constant below about 10 keV. Instead, only the fraction of dose equivalent or the total flux density integrated over energy regions 1 and 2 must be measured.

#### 3.2.1 Energy Region 1 - Thermal to 1 eV

As shown in Figure 3.5, cadmium is a very efficient absorber of thermal neutrons. At 0.17 eV the cross section is 7800 barns but rapidly drops to 2.2 barns at 1 eV. Thermoluminescent-albedo dosimeters vary with respect to the extent of cadmium covering the TL material (Hankins 1972). Hence, it is necessary to measure the thermal neutron component of dose equivalent or flux density in Region 1.

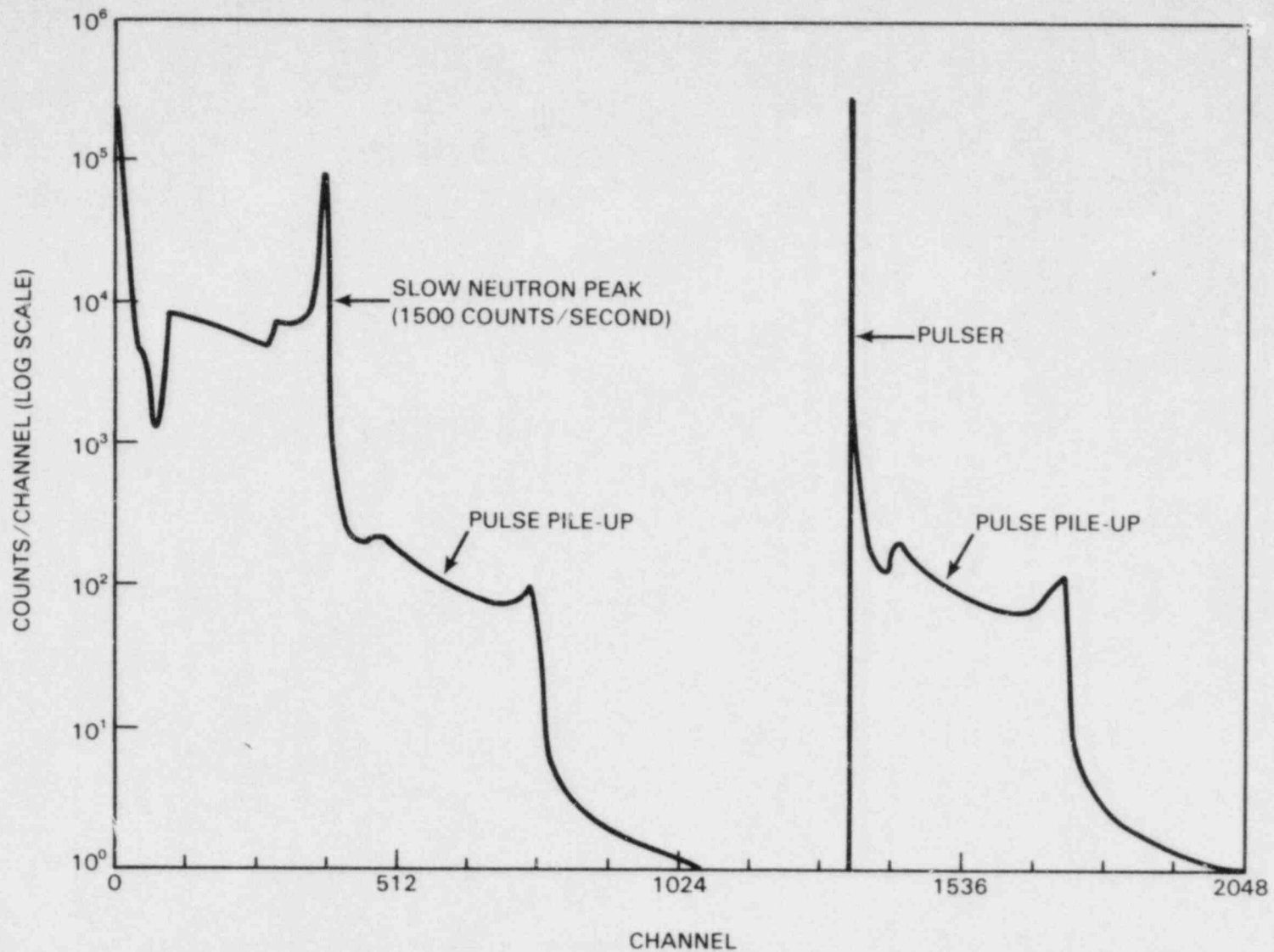


FIGURE 3.9. Method of Estimating Pulse Pile-Up Using a Reference Pulser Operated at the Same Pulse Rate as the Neutron Counts

It is possible to stop virtually all thermal neutrons from reaching the  $^3\text{He}$  in the counter by covering the entire counter with a 40-mil (0.10-cm) layer of cadmium metal. The reaction rate in the proportional counter from thermal neutrons can be measured by the difference in the areas of the slow neutron peaks at 764 keV with and without a cadmium cover:

$$R_{th} = A_{bare} - A_{Cd} \quad (3.8)$$

where  $A_{bare}$  is the integral counts in the slow neutron peak plus wall events from a bare  $^3\text{He}$  proportional counter and  $A_{Cd}$  is the integral counts in the slow neutron peak plus wall events with a cadmium cover. These integral counts can easily be measured by setting a region of interest (ROI) on the multichannel analyzer extending from the minimum separating gamma and neutron events to all higher energies (see Figure 3.1).

Ignoring any self shielding, the reaction rate is the product of the average macroscopic cross section multiplied by the integrated flux density over the energy region. For a  $1/v$  absorber such as  $^3\text{He}$ , the average cross section for a Maxwellian neutron energy distribution is the 2200 m/sec or 0.0253-eV cross section of 5327 barns divided by 1.128 (Glasstone and Sesonske 1963, p. 76). The total neutron flux density for the thermal neutron region is then given by:

$$\phi_{th} = \frac{R_{th}}{\bar{\Sigma}} = \frac{1.128 R_{th}}{5.327 \times 10^{-21} N} \quad (\text{neutrons/cm}^2\text{-sec}) \quad (3.9)$$

where  $\phi_{th}$  is the thermal neutron flux density,  $N$  is the number of  $^3\text{He}$  atoms in the sensitive volume of the proportional counter, and  $\bar{\Sigma}$  is the average macroscopic cross section. This equation is valid only if self shielding is negligible. For the  $^3\text{He}$  fillings in the proportional counters used in this study, the mean free path is tens of centimeters, so the equation is valid.

The dose equivalent contribution from thermal neutrons can be determined by multiplying the thermal flux,  $\phi_{th}$ , by the flux to dose equivalent factor of  $3.67 \times 10^{-3}$  mrem/hour per neutron/cm<sup>2</sup>-sec (ANSI/ANS-6.1.1-1977):

$$H_{th} = (3.67 \times 10^{-3}) \phi_{th} \quad (\text{millirem/hour}) \quad (3.10)$$

where the thermal dose equivalent rate,  $H_{th}$ , has units of millirem/hour and the thermal neutron flux,  $\phi_{th}$ , has units of neutrons/cm<sup>2</sup>-sec.

### 3.2.2 Energy Region 2 - 1 eV to 10 keV

As shown in Figure 3.5, for energies below 1 eV the absorption cross section for cadmium increases over 3 orders of magnitude, so a cadmium foil covering the  $^3\text{He}$  proportional counter will absorb all thermal neutrons. A small number of thermal neutrons will "leak" through the back of the counter if uncovered, so it is necessary to build an "elbow" to prevent their reaching

the proportional counter. With the cadmium cover a large number of events still occur in the 764-keV peak. These are primarily due to neutrons with energies above 1 eV but below 10 keV, which cannot be resolved because of the 2 to 3% (15 to 33 keV) FWHM resolution of the proportional counters. With only a cadmium sleeve it is not possible to determine the exact total neutron flux density in this region, but it is possible to define the possible limits. The upper limit of neutron flux density between 1 eV and 10 keV, considering all neutrons to be at 10 keV, is:

$$\phi_{hi} = \frac{R}{\sigma (10 \text{ keV}) N} = 1.2 \times 10^{23} \frac{R}{N} \text{ (neutrons/cm}^2\text{-sec)} \quad (3.11)$$

where R is the reaction rate, which is the integral counts in the slow neutron peak plus wall events with a cadmium cover divided by the time in seconds, N is the number of  $^3\text{He}$  atoms in the sensitive volume of the tube, and  $\sigma (10 \text{ keV})$  is the  $^3\text{He}(n,p)\text{T}$  cross section at 10 keV, which has a value of 8.47 barns or  $8.47 \times 10^{-24} \text{ cm}^2$  (Stewart 1974, p. 151).

The lower limit of neutron flux density, considering all of the neutrons to have an energy of 1 eV, is given by:

$$\phi_{lo} = \frac{R}{\sigma (1 \text{ keV}) N} = 1.2 \times 10^{21} \frac{R}{N} \text{ (neutrons/cm}^2\text{-sec)} \quad (3.12)$$

where the cross section at 1 eV has a value of 847 barns (Stewart 1974, p. 151).

It is often assumed that, in a moderating medium, the intermediate energy neutron flux density has an energy dependence inversely proportional to the neutron energy, especially for neutron energies close to thermal energies. It can be demonstrated that this is equivalent to a constant value for the flux per unit lethargy. The number of neutrons in a differential region is the same if represented in terms of lethargy or energy:

$$\phi(u) du = - \phi(E) dE \quad (3.13)$$

$$\phi(u) = \frac{-\phi(E)}{du/dE} \quad (3.14)$$

The lethargy, u, is defined as the natural logarithm of the ratio of the neutron energy at some reference value,  $E_0$ , which is a constant, to the energy, E, at another location:

$$u \equiv \ln E_0/E \quad (3.15)$$

Differentiation gives

$$du/dE = - 1/E \quad (3.16)$$

Substituting the value of  $du/dE$  into Equation (3.13) gives

$$\phi(u) = E \phi(E) \quad (3.17)$$

Assuming the intermediate neutron flux has a  $1/E$  dependence [ $\phi(E) = k/E$ ] gives

$$\phi(u) = E \phi(E) = k. \quad (3.18)$$

Thus, for a  $1/E$  dependence, the flux per unit lethargy is constant.

Neutron spectra from multisphere spectrometer measurements (NUREG/CR-1769) suggest that the differential neutron flux density follows a  $1/E$  dependence (which is equivalent to the differential flux per unit lethargy being almost constant on a plot of the flux per unit lethargy versus the log of energy). Figure 3.10 shows a plot of  $E \phi(E)$  (which is equivalent to the flux per unit lethargy) as a function of neutron energy for neutrons from a fission source penetrating concrete shields (Ing and Makra 1978). The differential flux is reasonably constant for thick concrete shields. Inside containment most of the neutrons are probably not from direct penetration through concrete shields, but may originate from streaming through pipes and penetrations and are albedo neutrons scattered off concrete. This would explain the lack of fission energy neutrons, which were not observed in previous measurements (NUREG/CR-1769).

These data suggest that the assumption that the differential neutron flux density has a  $1/E$  dependence for intermediate neutron energies may indeed be valid. The reaction rate for intermediate energies above cadmium cut-off (1 eV) is

$$R = \int_{E_1}^{E_2} N \sigma_{\text{He}}(E) \phi(E) dE \quad (3.19)$$

where all of the quantities have been defined previously. Assuming that the differential neutron flux has a  $1/E$  dependence [ $\phi(E) = k/E$ ] and  ${}^3\text{He}$  is a  $1/v$  neutron absorber [ $\sigma(E) = b/\sqrt{E}$ ] gives

$$R = N k b \int_{E_1}^{E_2} E^{-3/2} dE, \quad (3.20)$$

which can be integrated to give

$$R = 2 N k b \left( \frac{1}{\sqrt{E_1}} - \frac{1}{\sqrt{E_2}} \right). \quad (3.21)$$

The total number flux density integrated from  $E_1$  to  $E_2$  is

$$\phi_i = \int_{E_1}^{E_2} \phi(E) dE = \int_{E_1}^{E_2} \frac{k}{E} dE = k(\ln E_2 - \ln E_1). \quad (3.22)$$



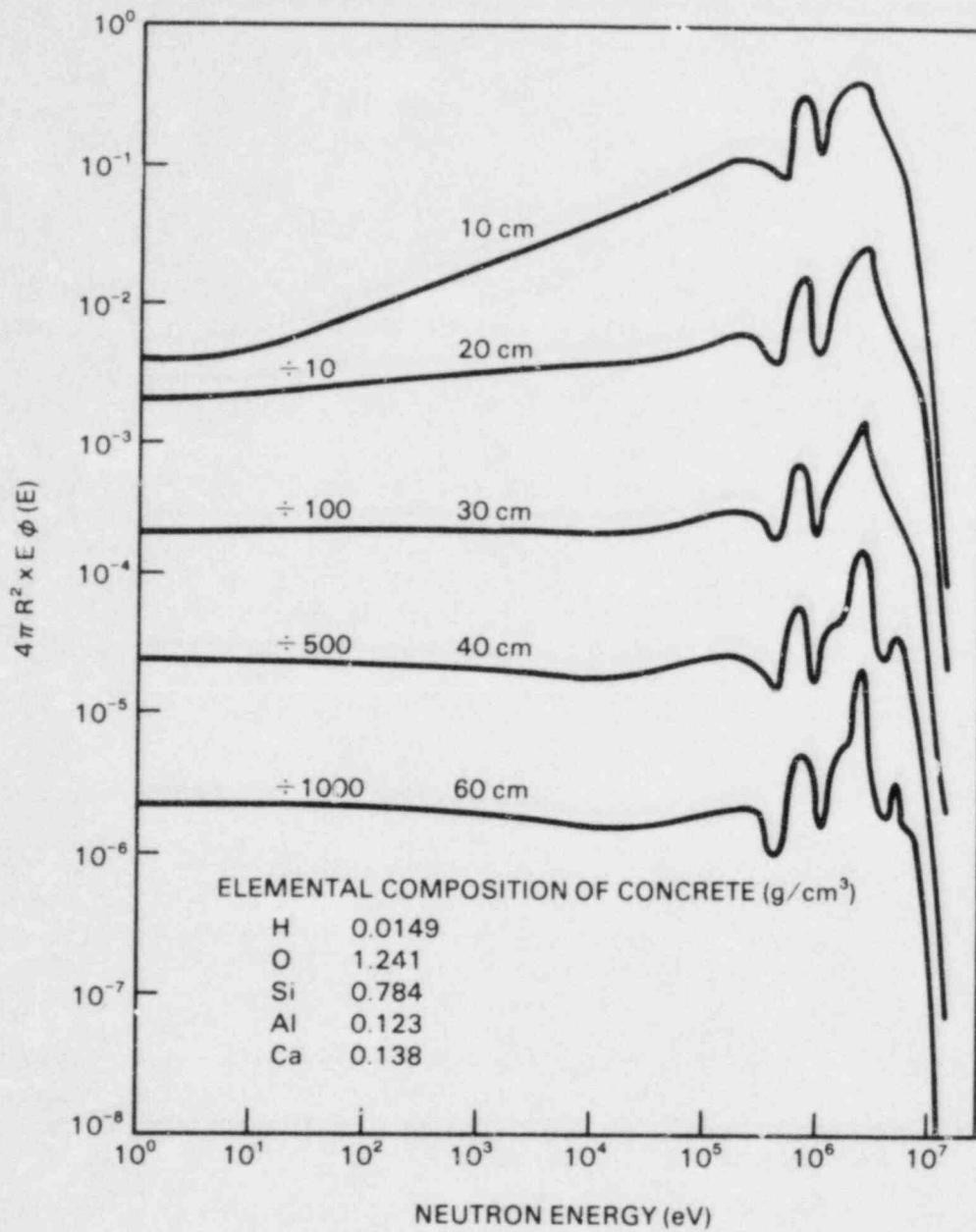


**FIGURE 3.10.** Differential Neutron Flux Density Multiplied by the Neutron Energy (or Flux per Unit lethargy) for Neutrons from a Fission Source Penetrating a Concrete Shield (Ing and Makra 1978)

Solving for  $k$  in the previous equation gives

$$\phi_i = \frac{R}{2Nb} \cdot \frac{\ln E_2 - \ln E_1}{\left(\frac{1}{\sqrt{E_2}} - \frac{1}{\sqrt{E_1}}\right)} \quad (3.23)$$

From Section 3.1 the value of  $b$  is  $847.3 \text{ barn eV}^{\frac{1}{2}}$ , so that the total neutron flux density for intermediate-energy (1 eV to 10 keV) neutrons,  $\phi_i$ , becomes

$$\phi_i = 5.5 \times 10^{21} \frac{R}{N} \text{ (neutrons/cm}^2\text{-sec)} \quad (3.24)$$

where  $R$  is the reaction rate (reactions/sec), and  $N$  is the number of  $^3\text{He}$  atoms in the sensitive volume of the  $^3\text{He}$  proportional counter. This equation assumes that the differential neutron flux has  $1/E$  dependence from  $E_1 = 1 \text{ eV}$  to  $E_2 = 10 \text{ keV}$ . The differential flux could deviate from  $1/E$  dependence a great deal at higher energies without changing the reaction rate  $R$ , because the cross section of  $^3\text{He}$  is much smaller at higher energies (1 to 10 keV).

The contribution to dose equivalent for intermediate or epi-cadmium neutron energies, assuming the flux varies as  $1/E$ , is given by

$$H_i \cong (4 \times 10^{-3}) \phi_i \text{ (mrem/hr)}. \quad (3.25)$$

These equations impose limits on the number of neutrons in the energy range above cadmium cut-off and below energies where the neutrons can be resolved from the slow neutron peak. However, with only a cadmium filter, little can be inferred about how the differential neutron flux density varies with energy.

Another possibility is to cover the  $^3\text{He}$  counter with resonance absorption materials to unfold the spectrum using the same mathematical techniques used for analyzing activation foils or multispheres. Using this technique, a set of Fredholm integral equations is solved:

$$R_i = \int \phi(E) \sigma_i(E) dE \quad (3.26)$$

where  $R_i$  is the response (i.e., the reaction rate calculated from the slow neutron peak) for the  $i$ th neutron absorber covering the proportional counter and  $\sigma_i(E)$  is the response function for the  $i$ th  $^3\text{He}$  proportional counter/neutron absorber combination. A simple iterative algorithm to solve this problem has already been proposed (Doroshenko et al. 1977). This technique has been applied to unfolding crude neutron energy spectra from a combination neutron dosimeter/spectrometer currently being developed (Brackenbush 1983). Determination of the response functions was outside the scope of this report, but is simple in principle.

### 3.2.3 Energy Region 3 - Energies Above 10 keV

All neutrons with energies below about 10 keV cannot be resolved from the "slow" (thermal plus intermediate energy) neutron peak at 764 keV because of the finite resolution of the proportional counter. Also, the  $^3\text{He}$  detector is 1600 times more sensitive to thermal neutrons than to 50-keV neutrons because of the  $1/v$  cross section. To accurately determine fast neutron spectra it is necessary to suppress the number of slow neutrons reaching the proportional counter; otherwise pulse pile-up can occur, which can obscure the actual fast neutron induced events. As discussed in Section 3.1.1.1, this can be accomplished by covering the proportional counter with absorbers such as samarium, which has a very high absorption cross sections for slow neutron energies but is "transparent" for fast neutron energies. It is also important to limit pile-up by covering the counter with 1/8-in. lead to reduce gamma pile-up and make measurements in relatively low dose equivalent rates (tens of millirem/hour or  $10^{-4}$  sieverts/hour).

The authors have somewhat arbitrarily established the criterion that the  $^3\text{He}$  proportional counter can resolve only fast neutrons with energies greater than the full width half maximum of the slow neutron peak, which is about 20 keV. The energy of a fast neutron can be found by subtracting 764 keV [the Q value of the  $^3\text{He}(n,p)\text{T}$  reaction] from the total energy deposited in the  $^3\text{He}$  proportional counter. As pointed out in Section 3.1, some neutron interactions occur near the walls of the counter and the full energy of the neutron is not measured. Some method must be devised to account for these "wall effects." It is possible to experimentally determine the wall event distribution by measurements with monoenergetic neutrons; however, this strategy is difficult, time-consuming, and expensive. Some work has been done on deriving complex analytical functions to estimate wall effects, but there is a simpler method. The authors have written a Monte Carlo computer code called WALL which calculates the number of wall effects and the distribution of energy deposition in the sensitive volume of a proportional counter as a function of incident neutron energy. As explained in Appendix C, the WALL code determines a "response function" matrix--the fraction of neutron events as a function of energy deposited in the proportional counter for different neutron energies.

Various unfolding techniques, such as matrix inversion or convolution theorems for Fourier transforms, can be used to determine the neutron flux density from the  $^3\text{He}$  spectrometer data. However, a very simple "stripping" technique can be programmed into microcomputers to correct for wall effects. The only disadvantage of this technique is that statistical uncertainty errors are propagated to the lower energy portion of the neutron energy spectrum.

Consider that the events in the highest energy bin are due to the desired  $^3\text{He}(n,p)\text{T}$  reaction. Using the response function data given in Appendix C, all the lower energy bins can be corrected for wall effects. The next lower energy bin has all of the undesirable events removed, so we can again assume all of the counts remaining are the desired  $^3\text{He}(n,p)\text{T}$  reactions for the next lower neutron energy. We can then use the response function for the next lower neutron energy to subtract wall effects. This process can be repeated until the entire spectrum is "stripped," so that only the desired  $^3\text{He}(n,p)\text{T}$

events are left. It can be demonstrated (Evans 1981) that this is mathematically equivalent to:

$$C'(j) = C(j) - \sum_{i=j+1}^{j_{\max}} C'(i) W(E_{ji}) \quad (3.27)$$

where

$C'(j)$  is the counts in bin  $j$  corrected for wall effects,  
 $C(j)$  is the uncorrected counts in bin  $j$  (the raw data), and  
 $W(E_{ji})$  is the response function for neutron energy  $E_j$  at energy bin,  $i$ .

This algorithm has been written into a spectrum unfolding code called HESTRIP. After the "stripping" process is complete, only those events that deposit all their energy in the proportional counter are left. The code then divides by the counter efficiency and the macroscopic cross section to determine the neutron flux density as a function of energy:

$$\phi(E) = \frac{C'(E)}{N \sigma(E) e(E)} \quad (3.28)$$

where

$\phi(E)$  is the neutron fluence ( $n/cm^2$ ) at a given energy bin ( $\Delta\phi/\Delta E$ )  
 $C'(E)$  is the corrected counts at a given energy bin  
 $E$  is the average energy of the bin  
 $N$  is the total number of  $^3\text{He}$  atoms in the sensitive volume of the proportional counter  
 $\sigma(E)$  is the  $^3\text{He}(n,p)\text{T}$  cross section at energy  $E$   
 $e(E)$  is the detector efficiency, the fraction of events that deposit all their energy in the sensitive volume per interaction in the proportional counter (see Appendix C).

The code calculates  $\Delta\phi/\Delta E$  as a function of energy, i.e., the number of neutrons/cm<sup>2</sup> in an energy bin of width  $\Delta E$ . Because most  $^3\text{He}$  proportional counters have a resolution of 20 keV, this was chosen as the energy bin width. Once the differential fluence is known, the code calculates the fractional dose equivalent for each energy bin. These differential values are summed to give total neutron fluence and dose equivalent. The HESTRIP code also calculates an energy correction factor for a "generic" TLD-albedo dosimeter calibrated with a bare or unmoderated  $^{252}\text{Cf}$  source. A listing and sample input/output for the HESTRIP code can be found in Appendix D. Once the energy spectrum and dose equivalent have been measured with the  $^3\text{He}$  spectrometer, the TLD-albedo dosimeter can be exposed at the same location on a water phantom to obtain a direct energy calibration.

## 4.0 EQUIPMENT REQUIRED FOR THE $^3\text{He}$ SPECTROMETER

The equipment necessary for the  $^3\text{He}$  spectrometer apparatus includes the proportional counter tube and various electronic components. In addition, a neutron source is needed for calibration, as is other electronic gear for evaluating system operation.

Two spectrometer configurations were developed during this project. The first employed the pulse shape analysis technique to suppress pulse pile-up. The second used a pulse generator technique to actually determine pulse pile-up. The components and costs specific to each are described in this section.

Specific mention of manufacturer and model is made only for documentation and replicability purposes; no endorsement is expressed or implied. All equipment purchased for this project was obtained from the lowest bidder per federal purchasing practices.

### 4.1 $^3\text{He}$ SPECTROMETER COMPONENTS

The spectrometer apparatus consists of a  $^3\text{He}$  proportional counter tube and associated electronic equipment for data collection and analysis.

#### 4.1.1 Proportional Counter Tube

Cylindrical proportional counter tubes available from two different manufacturers were found to offer the adequate resolution (2% to 3% FWHM) and the ruggedness necessary to withstand the field measurement environment. The tubes, typically 2.54 cm (1 in.) in diameter by 30.5 cm (12 in.) long, are pressurized to 1 to 4 atmospheres with mixtures of  $^3\text{He}$  and argon with about 0.5% carbon dioxide. The actual ratio of  $^3\text{He}$  to argon depends upon the neutron dose rates in the environment in which the tubes are to be used. In a 50-mrem/hr field inside reactor containment, a tube containing 0.27 atmosphere (4 psia) of  $^3\text{He}$  and 1.87 atmospheres (18 psia) of argon works well.

The cost for these proportional counter tubes ranges between \$400 and \$800 each, depending upon the manufacturer and the amount of  $^3\text{He}$  they contain. Because these tubes tend to develop slow leaks over several years, two or more tubes are necessary. The tubes can be compared periodically to determine if they are leaking.

#### 4.1.2 Electronic Equipment

The electronic components for both  $^3\text{He}$  spectrometer system configurations are identical, with a few exceptions noted below. Both systems required a preamplifier and a pulse-shaping amplifier. The latter featured variable gain, variable time constants (0.5 and 2.0 microseconds), and a switch-selectable 2-microsecond delay, as well as unipolar output with baseline restoration. A high-voltage power supply (+0 to +2000 volts) was also used, as was NIMbin and power supply equipment. A multichannel analyzer (MCA) and cassette tape recorder were also required for each system, as were neutron

absorbing shields. An array of cables and connectors provided the necessary links between and among the components within each system.

One  $^3\text{He}$  spectrometer system option used a pulse shape analyzer to help suppress pulse pile-up. The analyzer differentiates pulses with rise times varying between 0.1 and 10 microseconds; its adjustable window permitted selection of pulses in desired rise-time ranges. The pulse shape analysis technique also required a linear gate, which features switch-selectable pulse enable and pulse inhibit gates. The linear output width was adjustable to match the input requirements of the multichannel analyzer.

The other spectrometer option used a pulser to determine pulse pile-up. The precision pulses must meet the criteria of stability at temperatures up to 140°F, variable pulse rate, and variable pulse shape.

The major  $^3\text{He}$  spectrometer components and their associated costs are displayed in Table 4.1.

#### 4.2 TEST EQUIPMENT

Equipment used to test the  $^3\text{He}$  spectrometer systems included an oscilloscope and a signal pulse generator.

A Tektronic 485 dual trace oscilloscope was used for determining pulse polarity, signal tracing and setting up timing for the  $^3\text{He}$  spectrometer. The dual trace feature with external trigger was required to adjust the gates on the pulse shape analyzer.

A signal pulse generator was used to produce small negative, fast rise time pulses to simulate pulses from the  $^3\text{He}$  counter. The generator also aided in troubleshooting and signal tracing.

Miscellaneous equipment included jeweler's screwdrivers to adjust electronics and extra signal cables.

#### 4.3 NEUTRON SOURCE

The most convenient source of neutrons is a 1- to 20-microgram  $^{252}\text{Cf}$  neutron calibration source. The authors used a nominal 10-microgram source inside a paraffin-filled storage container. The  $^3\text{He}$  proportional counter is placed in a second container, so that it is completely surrounded by moderator. About 56 cm (22 in.) of paraffin moderator separate the source from the  $^3\text{He}$  counter. The separation distance between the two containers can be varied to change the count rate.

Similar containers could be constructed from metal drums filled with water. In this case, the  $^3\text{He}$  tube must be surrounded by about 30.5 cm (1 ft) of moderator to help eliminate fast neutrons that would interfere with thermal neutron measurements used to select the  $^3\text{He}$  proportional counters. If an isotopic neutron source is not available, reasonably intense neutron fields are often found near the entrance hatch to reactor containment or near pipe penetrations.

TABLE 4.1.  $^3\text{He}$  Spectrometer Components and Costs<sup>(a)</sup>

Quantity	Component	Manufacturer-Model	Cost of Component
<u>Common to Both Systems</u>			
2	$^3\text{He}$ Proportional Counter Tube: suggest 1-inch diameter, 4 psig $^3\text{He}$ , 29 psig Ar	Reuter Stokes <sup>(b)</sup> Harshaw Chemical Company <sup>(d)</sup>	\$300-\$800 <sup>(c)</sup>
1	Preamplifier	EG&G Ortec Model 142 PC <sup>(e)</sup>	\$650
1	High Voltage Power Supply	EG&G Ortec Model 456	\$780
1	NIMbin and Power Supply	EG&G Ortec Model 400VC/4002A EG&G Ortec Model 4001M	\$870
1	Multichannel Analyzer With Cassette Recorder	Canberra Industries Series 40 <sup>(f)</sup>	\$10,000-\$20,000
2	Neutron Absorbing Shields - Samarium oxide, boron carbide Cadmium metal foil (0.040 inch) Aluminum tubing and fittings	Noah Chemical <sup>(g)</sup> Local hardware/plumbing store	\$300-\$400 \$15
<u>Long Cables - 93 ohm 6.1 to 100 meters (156 to 100 feet)</u>			
1	Preamp Power Cable	Canberra Industries	\$300-\$500
1	High Voltage Cable - SNV connectors each end		
2	Signal Cables - BNC connectors each end (1 for signal from preamp; 1 for pulser signal)		
<u>Short Cables</u>			
1	61 cm long - SHV connector on one end; connector to match $^3\text{He}$ tube on other Assorted BNC signal cables to connect NIM electronics		
<u>Pulse Shape Analysis Option</u>			
2	Amplifiers	EG&G Ortec Model 572	\$1180 (x2)
1	Linear Gate	EG&G Ortec Model 476	\$375
1	Pulse Shape Analyzer	EG&G Ortec Model 458	\$1915
			Total \$8365 <sup>(h)</sup>
<u>Pulser Option</u>			
1	Amplifier	EG&G Ortec Model 572	\$1180
1	Precision Pulse Generator	EG&G Model 448	\$2490
			Total \$7185 <sup>(h)</sup>

(a) Mention of a specific product does not constitute endorsement by PNL or the Nuclear Regulatory Commission.

(b) Reuter Stokes, 18530 South Miles Parkway, Cleveland, OH 44128 (216)581-9400.

(c) Cost depends upon manufacturer and  $^3\text{He}$  filling.

(d) Harshaw Chemical Company, 68-1 Cochran Road, Solon, OH 44139 (216)248-7400.

(e) EG&G Ortec, 100 Midland Road, Oak Ridge, TN 37830 (615)482-4411.

(f) Canberra Industries Inc., 45 Gracey Ave., Meriden, CT 06450 (203)230-2351.

(g) Noah Chemical, 87 Gazza Blvd., Farmingdale, NY 11735.

(h) Price excluding multichannel analyzer.

## 5.0 ASSEMBLING THE $^3\text{He}$ SPECTROMETER

This section presents detailed guidelines for incorporating the separate pieces of equipment into the  $^3\text{He}$  spectrometer apparatus configurations. As such, the assembly steps followed by PNL are documented. However, where appropriate, suggested deviations from PNL's approach are also noted.

Because the success of the overall spectrometer system depends largely on the  $^3\text{He}$  proportional counter tube, recommended procedures for testing the tubes are presented first. Next, the steps necessary to assemble the electronics for both spectrometer options (pulser technique and pulse shape analysis technique) are listed. Third, the procedure for verifying multichannel analyzer linearity is described. The final subsection presents helpful hints for troubleshooting the assembled spectrometers.

### 5.1 PROPORTIONAL COUNTER TUBE EVALUATION

The success or failure of the  $^3\text{He}$  spectrometer depends upon selection of the proper  $^3\text{He}$  proportional counter. The resolution quoted by manufacturers is only a guide to selecting an acceptable tube. It is imperative that the  $^3\text{He}$  tube have a uniform gain along the anode. When the tube is exposed to high fluxes of slow neutrons, nonuniform gains can produce events that can easily be mistaken for higher-energy neutron events. This is shown in Figure 5.1, which presents the pulse height distribution from a 2.54-cm (1-in.) diameter cylindrical  $^3\text{He}$  proportional counter exposed to thermal neutrons using the neutron source described in Section 4.3. A very small number of pulses with higher gains can be mistaken for 140-keV neutrons.

#### 5.1.1 Test Apparatus

A block diagram of the apparatus used to test for resolution and uniformity of gain along the anode is shown in Figure 5.2 using the equipment described in Section 4.1. Typically, an operating voltage of +700 to +1800 volts is required for the proportional counter; start with the voltage recommended by the manufacturer. Using an oscilloscope, the signals from the output of the preamplifier can be traced to make certain it is operating properly. Attach a 93-ohm signal cable from the preamp output (labeled "ENERGY") to the input of the amplifier. With the oscilloscope observe the positive pulses at the unipolar output of the amplifier. The polarity switch on the amplifier may have to be changed to obtain positive output pulses. Connect the unipolar output from the amplifier to the ADC input of a multichannel analyzer using a 93-ohm cable with a "tee" to provide a signal to the oscilloscope. Vary the distance from the  $^3\text{He}$  proportional counter to a source of thermal neutrons until a reasonable count rate is obtained--something in excess of 1000 counts/minute, but low enough so there is no pulse pile-up problem. Use a pure thermal neutron source, such as that described in Section 4.3. The count rate from a bare  $^3\text{He}$  proportional counter should be at least 20 times that from the  $^3\text{He}$  counter covered with a 1-millimeter (0.040-inch) cadmium cover.



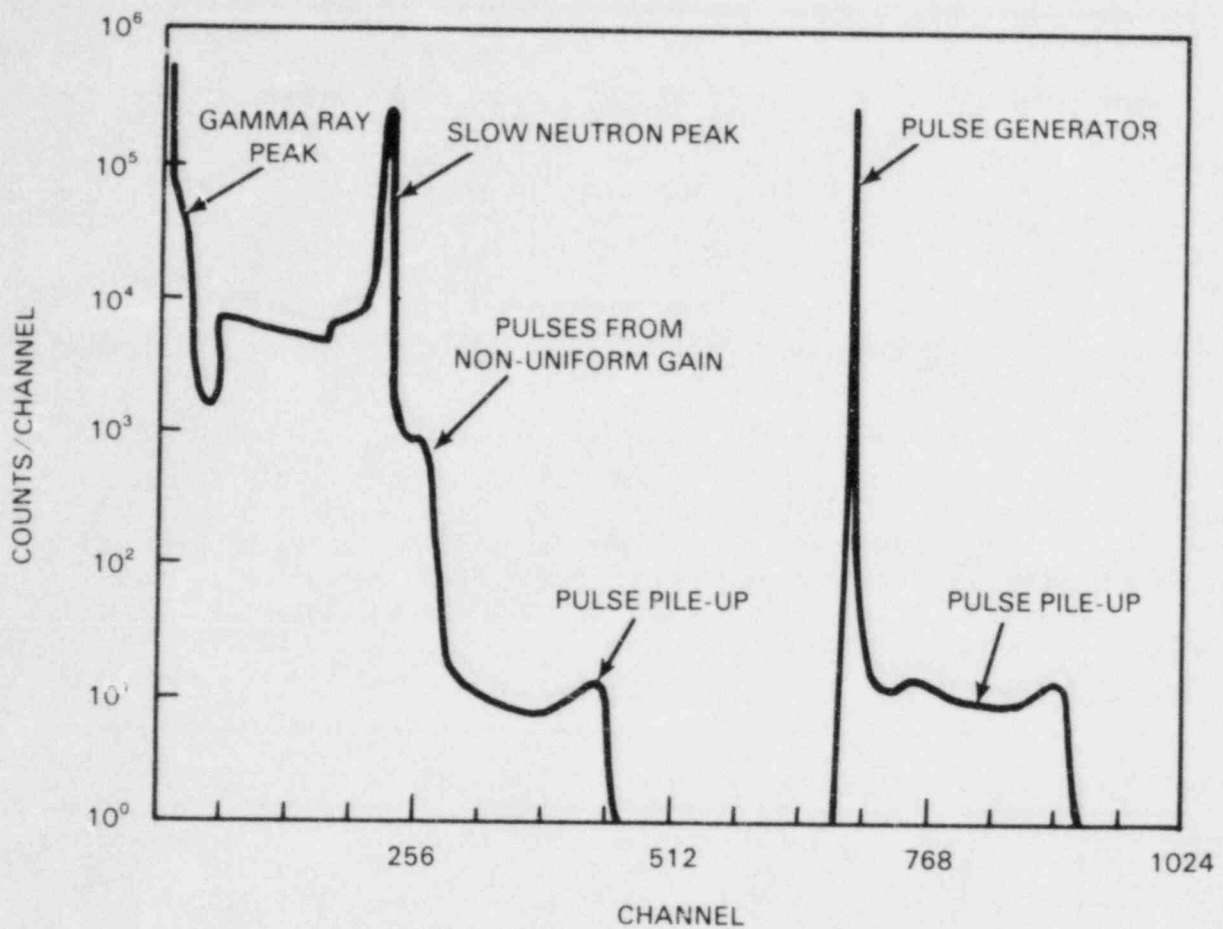


FIGURE 5.1. Example of a  $^3\text{He}$  Proportional Counter with Nonuniform Gain Along The Anode

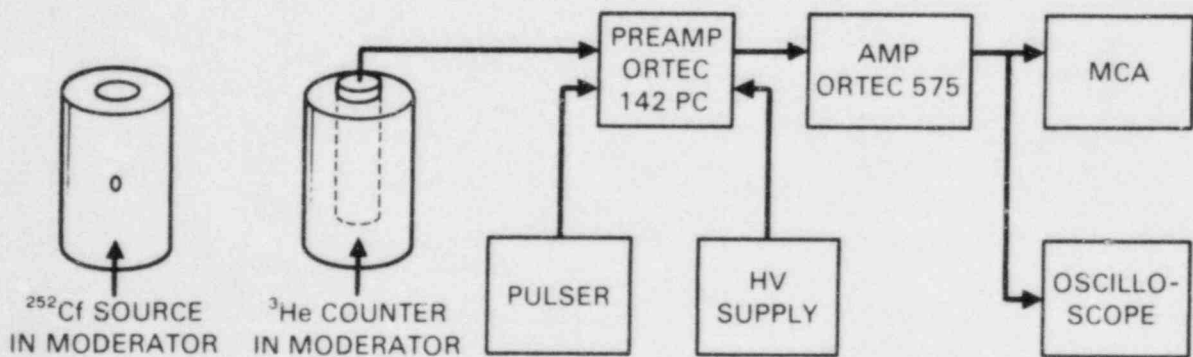


FIGURE 5.2. Apparatus Used to Determine the Best Operating Parameters for a  $^3\text{He}$  Proportional Counter

### 5.1.2 Test Procedures

Adjust the gain of the amplifier until a convenient pulse height is obtained--about 5 to 10 volts. Count for a few minutes until thousands of counts are collected in the peak channel. Determine the number of counts in the peak channel and divide by 2 to obtain the half height. Determine the width of the peak at half the peak height,  $\Delta p$ , and use the following formula to obtain the full width half maximum (FWHM) resolution in percent:

$$\% \text{ FWHM} = \Delta p/p \times 100 \quad (5.1)$$

where  $p$  is the channel number of the peak and  $\Delta p$  is the number of channels at half the peak height.

The user will find that the best resolution is obtained with long time constants set on the amplifier. Very long time constants lead to pulse pile-up problems; it is usually best to compromise and operate with a 1- to 2-microsecond time constant on the shaping amplifier. Vary the high voltage supplied to the tube and determine the percent FWHM resolution at each voltage. A plot of the results reveals the optimal settings for the best resolution as shown in Figure 5.3.

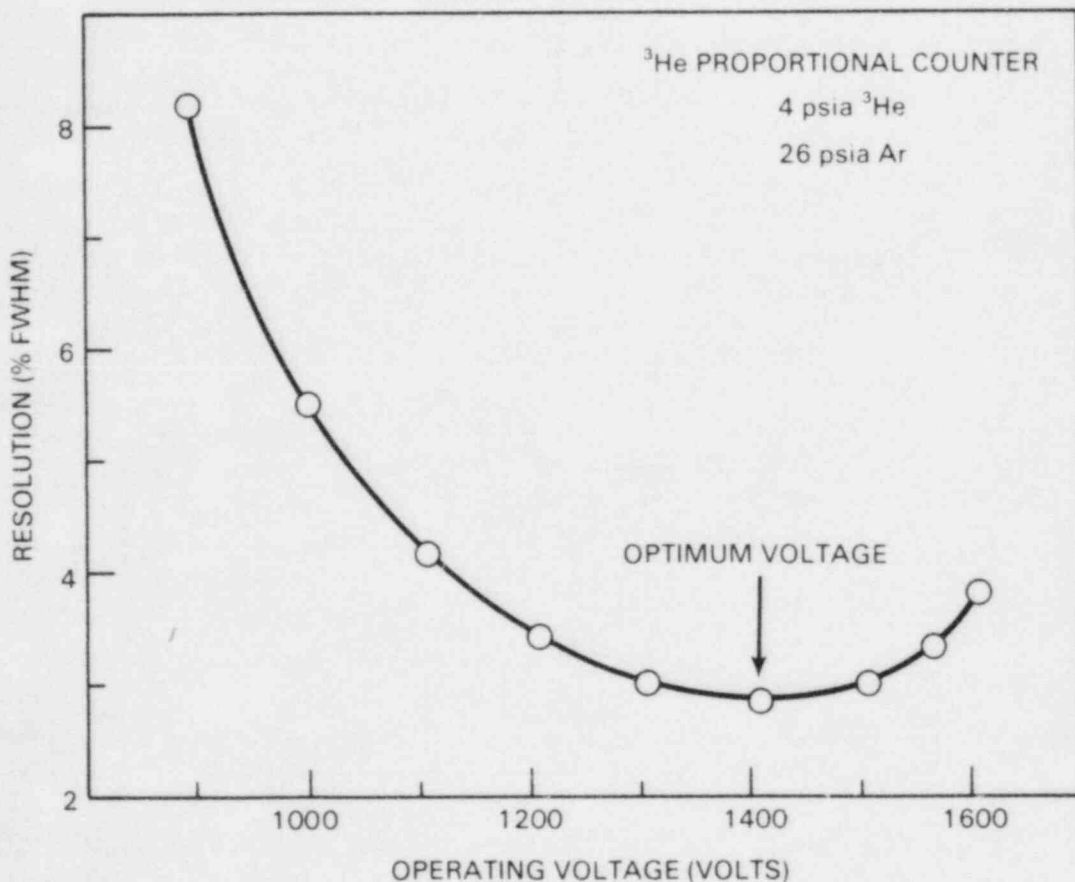


FIGURE 5.3. Determination of Best Operation Parameters for a 1-Inch Diameter <sup>3</sup>He Proportional Counter

The FWHM resolution is not the only parameter used to judge a good proportional counter tube. If it is to be used to measure fast neutrons in the 20- to 1000-keV range, the tube must have uniform gain along the anode wire. If the gain is higher at some point, slow neutrons will produce a small peak or "shoulder," which could be mistaken for higher energy neutrons. When the anode wire is welded to the "feed-throughs" at the ends of the proportional counter, surface tension can cause the diameter of the wire to shrink, and the gain to increase. Also, if too much tension is applied to the anode wire, its diameter will shrink at the point where it starts to yield.

Connect a precision pulse generator, such as a Berkeley Nucleonics Corp. Model PB-3 or GL-3, to the test input of the amplifier. Use negative polarity pulses, and adjust the amplitude of the pulser to provide pulses larger than those produced by thermal neutrons. Set up a region of interest on the multi-channel analyzer to encompass all the thermal neutron events, including wall effects. Set the lower level at the minimum between gamma and neutron induced events, as shown in Figure 5.4. Then adjust the pulse rate from the pulse generator to match the neutron count rate (the integral number of counts in the region of interest divided by the time). After collecting data for an hour or more, the user should obtain a spectrum like that shown in Figure 5.4. This pulse height distribution indicates the tube has uniform gas gain; compare it to the pulse height distribution in Figure 5.1. By adjusting the pulser rate to match the neutron count rate, the pulse pile-up rate for the pulser is the same as that for random neutron pulse pile-up. This allows a determination of whether events above the thermal neutron peak at 764 keV are produced by pulse pile-up (as in Figure 5.4) or are produced by nonuniform gains (as in Figure 5.1). This will be explained in detail in Section 5.2.1.

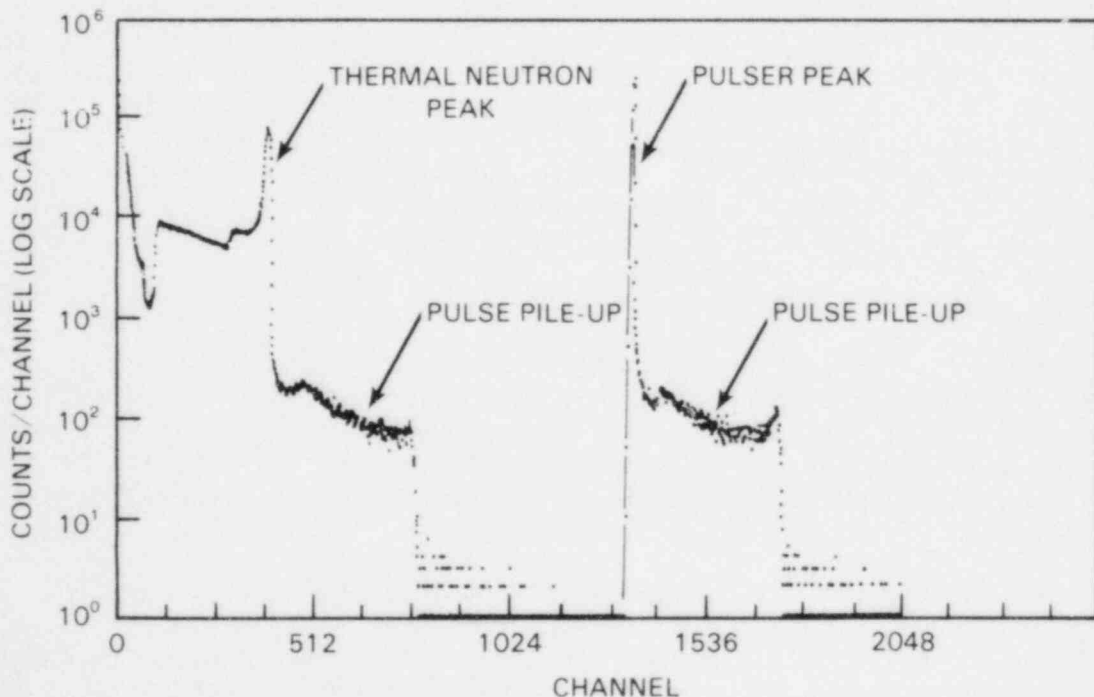


FIGURE 5.4. Pulse Height Distribution Obtained with a <sup>3</sup>He Proportional Counter with Uniform Gain

## 5.2 SPECTROMETER ELECTRONICS ASSEMBLY

At the beginning of this project the authors used a pulse shape analysis technique to reduce pulse pile-up. The procedures used to set up this equipment are described in Section 5.2.2. The equipment and procedures are complex and may be difficult to use, although this was the method used by the authors to make the spectral measurements described in Section 7.0. A technique using a pulser, as described in Section 5.2.1, may be much simpler to use.

### 5.2.1 <sup>3</sup>He Spectrometer Using A Pulser Technique to Estimate Pulse Pile-Up

The individual components comprising the pulser technique spectrometer were described in Section 4.1. The testing apparatus is the same as already described in Section 5.1.1, except that the oscilloscope is not used for field measurements.

If the pulser remains stable during a measurement, it is possible to use a pulser technique to measure the pulse pile-up. In Section 3.0 the chance coincidence rate was found to be

$$r_{\text{coinc}} = (rt) r_s \quad (5.2)$$

where

$r_{\text{coinc}}$  is the chance or random coincidence rate

$r$  is the pulse rate from the proportional counter

$t$  is the resolving time of the proportional counter

$r_s$  is rate of arrival of a second pulse.

If the second pulse is another random pulse from the proportional counter, the random coincidence rate is  $r^2t$ . However, the second pulse could be from a pulser, which has the same pulse rate as the <sup>3</sup>He counter. In this case the pile-up occurs at the same rate as pile-up from random coincidences in the proportional counter. The pile-up associated with the nonrandom pulser pulses has almost the same distribution as random coincidences in the proportional counter, except the pulser has better resolution. This analysis assumes that the pulses produced by the pulser have exactly the same shape as those produced by neutron interactions.

Set up the <sup>3</sup>He spectrometer electronics using the block diagram of Figure 5.5 and the cable connections and instrument settings listed in Table 5.1 as a guide. Make certain the power is turned off. Never change polarity on the high voltage power supply with the power on, or the unit will be damaged. The preamplifier could also possibly be damaged by attaching cables with the high voltage on.

Once the electronics have been set up, test the unit by exposing it to thermal neutrons using the apparatus described in Section 4.3. Turn on the NIMbin power first; then make certain the dials on the front of the high voltage power supply are correct and, finally, turn on the high voltage. Using an oscilloscope, trace the signals through the electronics using the pulse shapes shown in Figure 5.6 as a guide.

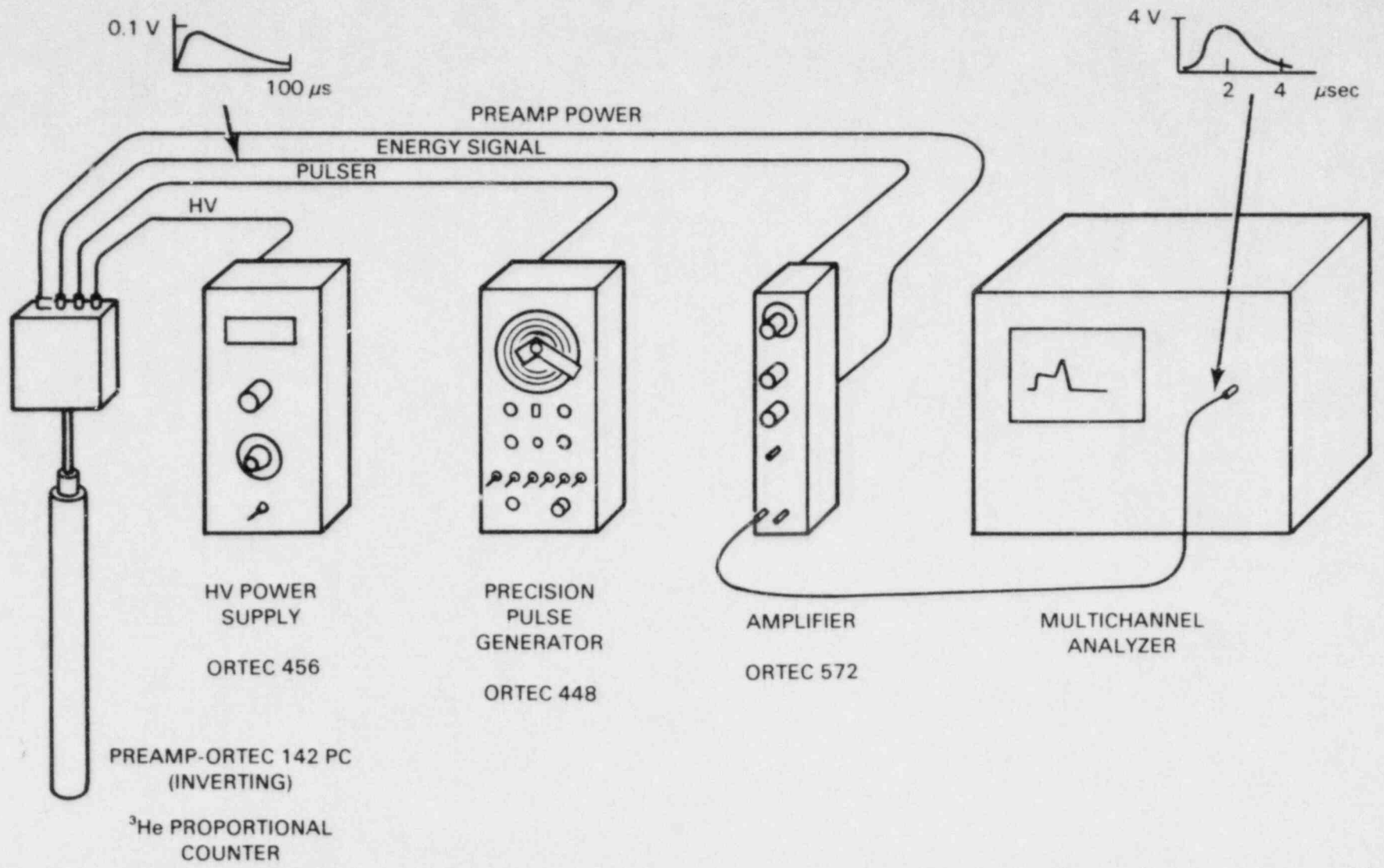


FIGURE 5.5. <sup>3</sup>He Spectrometer Electronics Using a Pulser Technique to Estimate Pulse Pile-Up

TABLE 5.1. Settings for  $^3\text{He}$  Spectrometer Electronics Using a Pulser Technique to Estimate Pulse Pile-Up

$^3\text{He}$  Proportional Counter

Make certain the high voltage and power are off!  
Connect to preamplifier with cable with SHV connectors.

Preamplifier - Ortec 142PC

INPUT connected to  $^3\text{He}$  proportional counter  
BIAS (SHV connector) to high voltage power supply with long cable with SHV connectors  
ENERGY (BNC connector) connected to long BNC signal cable to IN (BNC connector) on amplifier  
TEST (BNC connector) connected to long BNC cable to OUTPUT of pulser. It is a good idea to label each end of cable.

High Voltage Power Supply - Ortec 456

Make certain the unit is turned off! Power switch located on front panel.  
OUTPUT (SHV connector on back of unit) connected to preamp (BIAS) with long SHV cable.  
POLARITY switch on back of unit - Make certain power is off and set switch to positive using a screwdriver.

Amplifier - Ortec 572

PREAMP POWER (21-pin connector on back of unit) connected to preamplifier with long power cable.  
IN (BNC connector on back of unit) connected to ENERGY on preamp with long BNC cable.  
UNI (BNC connector on front of unit) connected to ADC IN of multichannel analyzer  
FINE GAIN - 1.00  
COURSE GAIN - 50  
SHAPING TIME - 2 microseconds  
BLR - auto  
INPUT - positive  
DELAY - out  
OUTPUT - uni

---

It is also necessary to adjust the pole zero on the amplifier, following the instructions supplied by the manufacturer. Set the BLR AUTO toggle switch on the center of the Ortec 572 amplifier to the "PZ ADJ" position. Look at the output of the amplifier with an oscilloscope, and use a jeweler's screwdriver to adjust the PZ potentiometer until the tail of the pulse returns to the baseline without overshoot or undershoot. Return the "PZ ADJ" switch to the "BLR AUTO" position. Unless the pulser count rate is so high that the pulses overlap and change shape, the shape of the pile-up distribution from the pulser does not change with pulser rate, as shown in Figure 5.6 where the pulser is operated at the same rate and at 100 times the count rate as the count rate from the proportional counter. The amount of pulse pile-up in reactor measurements can then be estimated as follows:

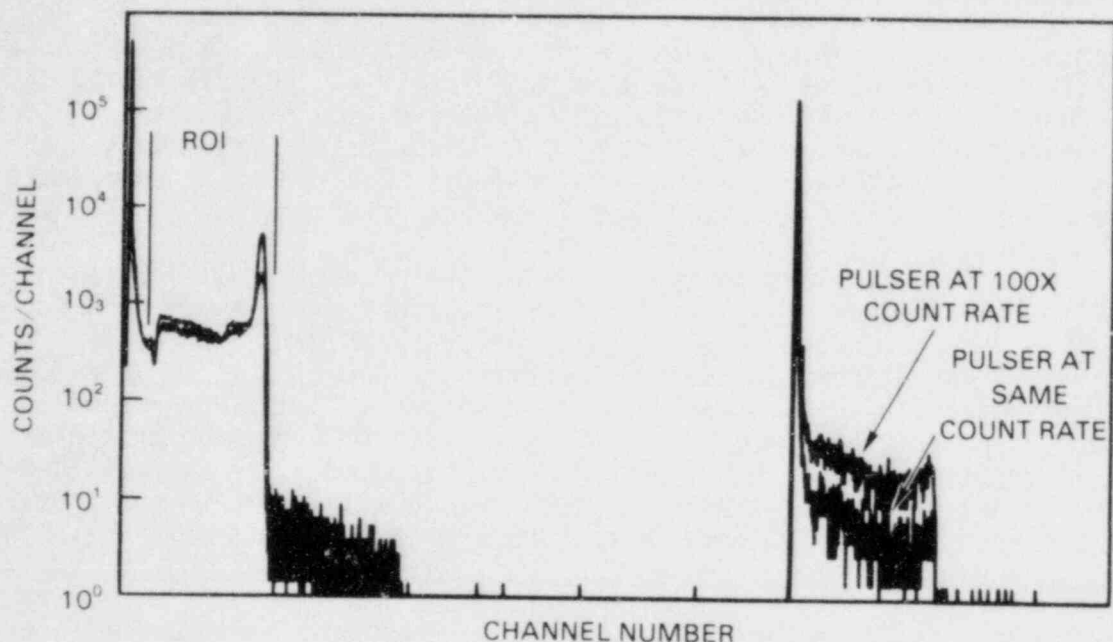


FIGURE 5.6. Pulse Pile-Up Distribution Obtained by Operating Pulser at Different Count Rates

1. First, adjust the amplitude of the pulser pulses to be at least twice as large as the slow neutron pulses from the  $^3\text{He}$  proportional counter. On some multichannel analyzers it may be possible to place the spectrum in half the memory by placing the proportional counter spectrum in the first quarter and the pulser spectrum in the second quarter of memory. Overlapping the quarters allows direct comparison of the pile-up from the pulser with the proportional counter spectrum.
2. Set up regions of interest to determine the integral number of counts from the proportional counter (slow neutron peak and wall events) and from the pulser.
3. Adjust the pulse generator to produce the same count rate as that from the neutron pulses from the proportional counter or some multiple of the count rate. If better counting statistics are preferred, set the pulse generator to produce 100 times as many pulses, and divide the spectrum by 100 to normalize it to the  $^3\text{He}$  proportional counter spectrum.
4. Collect the spectral data. If a samarium or boron slow neutron absorber is placed over the  $^3\text{He}$  proportional counter, comparing the pulser pile-up spectrum to the reactor spectrum from the  $^3\text{He}$  proportional counter may indicate that the pile-up is insignificant.

5. If the pulser pile-up is a significant fraction of the spectrum from the neutron data, the pile-up can be subtracted. First, determine the integral number of counts in the neutron data and in the pulser data. Normalize the pulser pile-up data by multiplying the pulser pile-up data (counts/channel) by the ratio of the integral counts of the neutron data divided by the integral counts of the pulser data. This gives a "background" pile-up spectrum that can be input to the computer code used to analyze the data to remove the pile-up background.

This technique allows one to determine the amount of pulse pile-up; if excessive, pile-up may be subtracted from the spectrum measurement data. It also allows one to determine gamma pulse pile-up. However, the pulser has much better resolution than the  $^3\text{He}$  proportional counter, so it is not possible to subtract a pulse pile-up "background" on a channel-by-channel basis. An energy bin structure based upon the full width half maximum criterion allows the pulser pile-up background to be subtracted. The main disadvantage of this technique is that the pulser must remain stable; many laboratory pulsers may not be able to operate at high temperatures without a gain shift.

The usefulness of this technique for estimating gamma pulse pile-up is shown in Figure 5.7. A bare  $^3\text{He}$  proportional counter was exposed to a thermal neutron source, and a pulser signal was introduced at 1000 times the count rate of the neutron pulses. This gives much better counting statistics. Curve A of Figure 5.7 shows the results obtained with only the neutron source; Curve B shows the results obtained with a 40-mrem/hr gamma ray field from a  $^{137}\text{Cs}$  source. The gamma ray pile-up can be seen in the pulser pile-up distribution.

While pulse pile-up can be estimated by this method, the results produced by nonlinear gains in the proportional counter cannot. It is necessary to compare the pile-up corrected spectrum with the spectrum obtained with a thermal neutron source to make certain that the spectrum observed in the reactor measurement is not produced by nonlinear gain from slow neutron events.

This technique assumes that the pulses produced by the pulser have the same shape as those produced by neutron interactions in the  $^3\text{He}$  proportional counter. This may not always be true, especially if very long 30-m (100-ft) cables are used between the preamplifier and main amplifier. For this case, there may not be an exact correspondence between the number of pile-up pulses produced by the pulser and by the  $^3\text{He}$  proportional counter. It is still possible to estimate pulse pile-up by exposing the  $^3\text{He}$  counter to a source of thermal neutrons as described in Sections 4.3 and 5.1.1. Carefully adjust the count rate from the thermal neutron source to match that of the reactor measurement, and be certain the gamma fields are also similar. If the irradiation conditions are similar, the pile-up from the thermal neutron source will be almost the same as that from the reactor measurement. The results of this technique are shown in Figure 7.4 and described in Section 7.2.1.



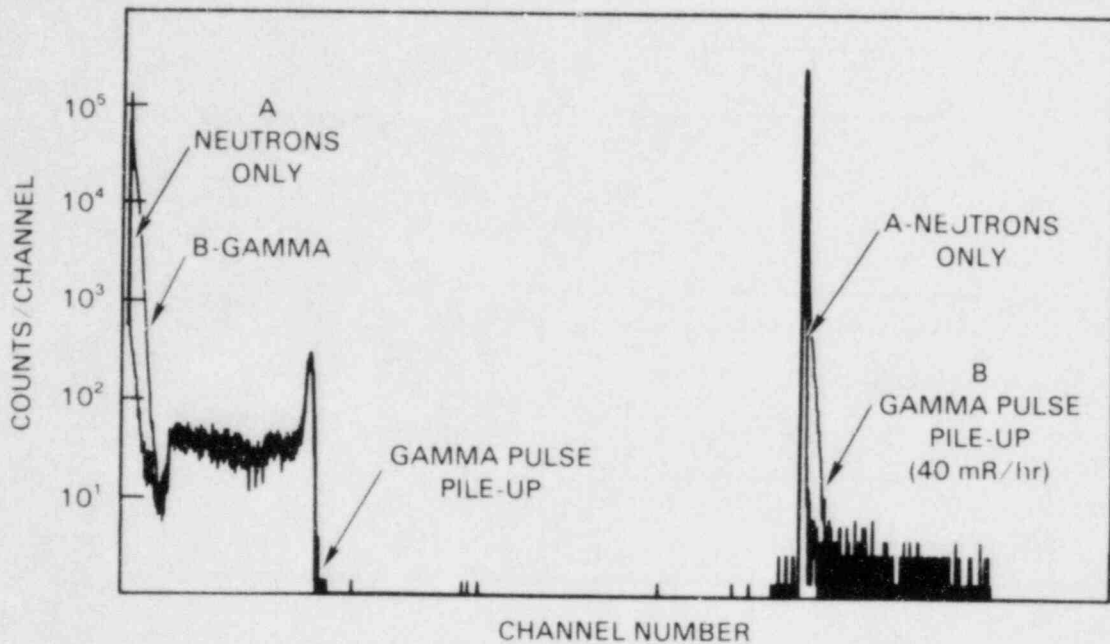


FIGURE 5.7. Results of Using Pulser Technique for Estimating Gamma Pulse Pile-Up

## 5.2.2 <sup>3</sup>He Spectrometer Using Pulse Shape Analysis

### 5.2.2.1 Laboratory Adjustments

The equipment used for the spectral measurements reported in Section 7.0 used a pulse shape analysis technique with the equipment described in Section 5.1.1. Assemble the equipment in a NIMbin using Figure 5.8 as a guide. Table 5.2 can also be used as a guide for the positions of the switches and cable routings. Make certain the power is off to the high voltage power supply and to the NIMbin. Potentially lethal voltages can be produced by the Ortec 456 power supply, and connecting cables with high voltage on could damage the preamplifier, even though it has a built-in protection circuit for the FET input. Make certain the Ortec 456 power supply is off before changing the polarity!

First, attach the <sup>3</sup>He proportional counter to the preamp using a short (2-foot) cable with a SHV connector on one end and a connector that mates to the proportional counter on the other. Make certain the preamp power cable is connected to the back of the amplifier and the 93-ohm signal cable is attached to the BNC connector labeled IN on the back of the amplifier. Make certain the Ortec 456 power supply is off and the polarity switch is in the positive polarity position. Attach the high voltage cable with SHV connectors on both ends. All three of these cables should be 6.1 to 30.5 meters (20 to 100 feet) long so that spectral measurements can be made with the detector far removed from the electronics. Place the <sup>3</sup>He tube in a thermal neutron field with the cover removed.

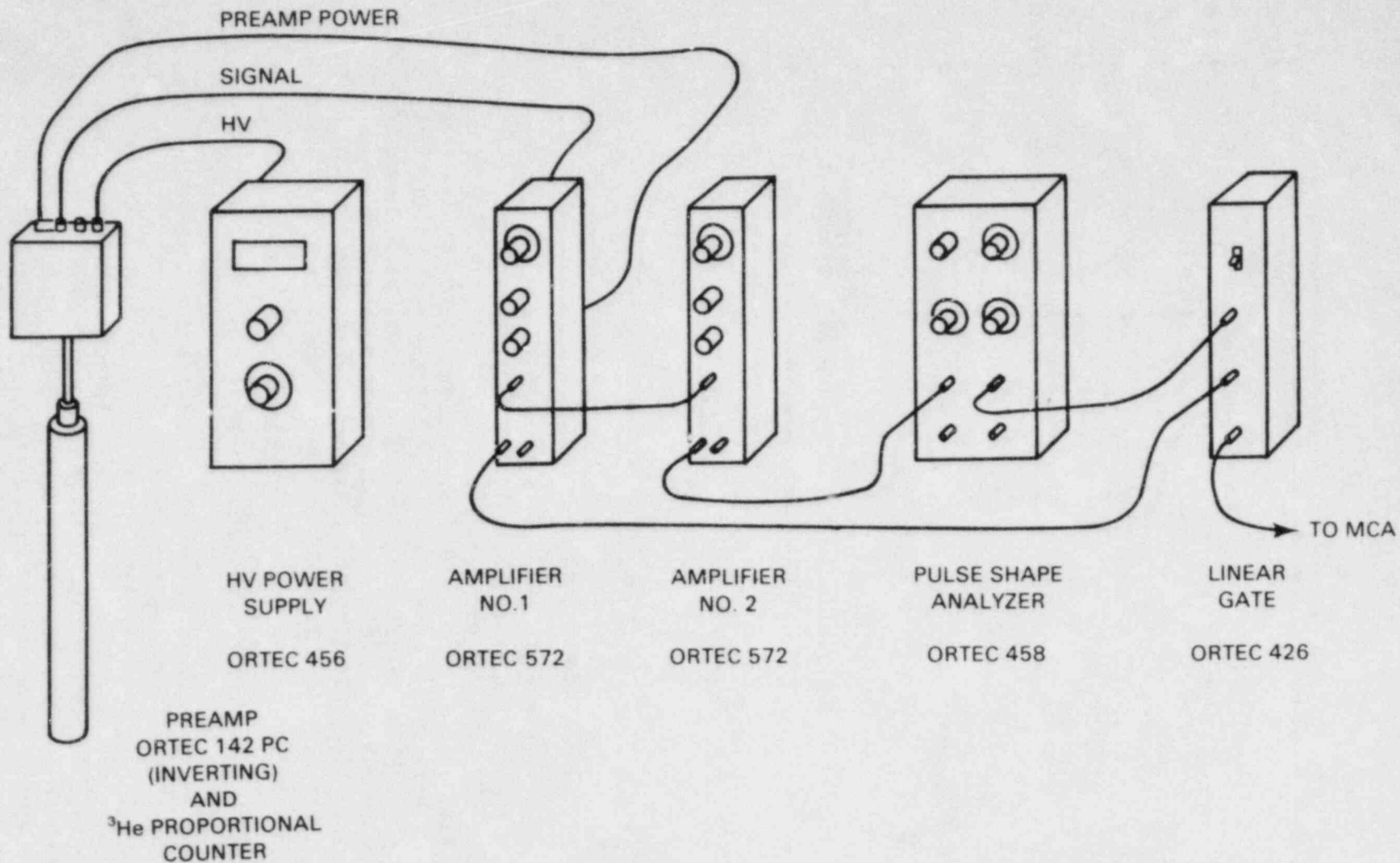


FIGURE 5.8. Cable Connections for  $^3\text{He}$  Spectrometer System Electronics Using Pulse Shape Analysis

TABLE 5.2. Settings for  $^3\text{He}$  Spectrometer Electronics  
Using Pulse Shape Analysis

Preamplifier - Ortec 142PC

Cable connections

INPUT connected to  $^3\text{He}$  proportional counter  
BIAS connected to high voltage power supply with long SHV cable  
ENERGY connected to IN of amplifier with long BNC cable  
POWER cable connected to back of amplifier for preamp power

High Voltage Power Supply - Ortec 456

Make certain unit is turned off!

Cable connection

OUTPUT connected to preamp with SHV cable  
POLARITY switch on back of unit - positive

Amplifier 1 - Ortec 572

Cable connections

PREAMP POWER on back of unit connected to preamplifier  
IN (BNC connector on back of unit) connected to preamplifier  
UNI (BNC connector on front) connected to ENABLE of linear gate  
INPUT on front connected to input of amplifier 2

FINE GAIN - 1.00

COARSE GAIN - 50

SHAPING TIME - 2 microseconds

BLR - auto

INPUT - positive

DELAY - in

OUTPUT - uni

Amplifier 2 - Ortec 572

Cable connections

INPUT on front connected to input of amplifier 1  
UNI on front connected to input of pulse shape analyzer

FINE GAIN - 1.00

COARSE GAIN - 20

SHAPING TIME - 0.5 microseconds

BLR - auto

INPUT - positive

DELAY - out

OUTPUT - uni

Pulse Shape Analyzer - Ortec 458

Time  $0.8 \times 10$

Disc  $060 \times 10$

PSA window upper 250, lower 195

Connections

INPUT connected to UNI of amplifier 2  
WINDOW connected to ENABLE of linear gate

Linear Gate - Ortec 426

NORM - normal mode

Connections

ENABLE connected to WINDOW of pulse shape analyzer  
INPUT connected to UNI of amplifier 1  
OUT connected to ADC INPUT of multichannel analyzer

Set the voltage on the Ortec 456 HV power supply to the voltage that gives the best resolution, as determined in Section 5.1. Turn on the NIMbin power, then turn on the high voltage power supply. With an oscilloscope observe that millivolt pulses are produced by the preamplifier and much larger positive pulses are produced on the unipolar output of both amplifiers. Amplifier 1 is used to provide linear signals to the multichannel; amplifier 2 is used as part of the pulse shape analysis electronics. Separate amplifiers are used so that if the gains are changed it is not necessary to readjust the remainder of the instruments.

### PZ Adjustment

After the system is set up, the preamp and amplifier must be made compatible by matching impedances. This can be done by using an oscilloscope and looking at the undershoot or overshoot of the pulses generated from a pulser or radiation field. Connect the signal from the UNI output of the amp to input of the oscilloscope. Switch the triggering switch on the oscilloscope to the channel you are working on so that it triggers whenever a pulse is sent from the amplifier. Set the oscilloscope timing so that the peaks are fairly narrow. Set the BLR AUTO toggle switch on the center of the amp to the "PZ adj" position. With a jeweler's screwdriver adjust the PZ until the pulses look like those in Figure 5.9. Adjust the pole zero on both amplifiers, then return the toggle switch to the BLR AUTO position.

### Pulse Shape Analyzer Adjustment

1. Amplifier 2 is used to provide a positive signal to the Ortec 458 pulse shape analyzer. Set the shaping time constant on the Ortec 572 amplifier to 0.5 microseconds and adjust the gain so that the slow neutron pulses are about 2-volt positive pulses. Attach a signal cable from the UNI output of amplifier 2 to the INPUT of the Ortec 458 pulse shape analyzer.

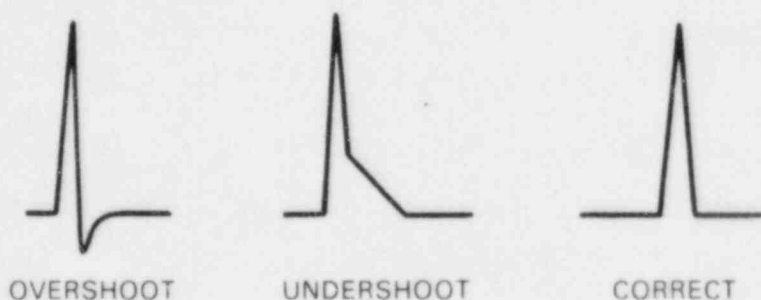


FIGURE 5.9. Unipolar Output Pulses of Ortec 572 Amplifier for Pole Zero Adjustment

2. Connect an oscilloscope to the LINEAR output of the Ortec 458 pulse shape amplifier; make certain it is producing positive output pulses from the neutron pulses. Remove the neutron source and replace it with a gamma source. Adjust the threshold discriminator so that the pulse shape analyzer does not trigger on gamma pulses, but does trigger on neutron pulses. This allows the unit to function in high count rates. It will be necessary to readjust the threshold discriminator if the  $^3\text{He}$  tube is changed.
3. Replace the gamma source with the neutron source. Check the UNI output of amplifier 1 to be certain that positive pulses about 2 to 5 volts high are produced by the neutron source. Make certain the delay is in the IN position.
4. Connect the external trigger of the oscilloscope to trigger on fast bipolar pulses of amplifier 2. Connect one channel of the oscilloscope to observe the UNI output of amplifier 1; connect the other channel to observe the WINDOW output of the pulse shape analyzer. Adjust the upper level of the PSA window to 1000 and the lower level to 000 (trigger on all neutron pulses). Set the oscilloscope to alternate between channels 1 and 2. Adjust the time constant of amplifier 1 so that the WINDOW gate pulse arrives before the peak of the linear signal from amplifier 1. Remove the oscilloscope and reconnect the cables as shown in Figure 5.8.

#### Adjustment of Linear Gate

5. The enable gate signal from the WINDOW of the pulse shape analyzer should enable the Ortec 426 linear gate just before the linear signal from amplifier 1. Attach the oscilloscope to the output of the linear gate. With a jeweler's screwdriver adjust the gate width to be about 2 to 3 microseconds wide.

The unit is now ready for use in the field. First, however, check the linearity of the multichannel analyzer using the procedures outlined in Section 5.3.

#### 5.2.2.2 Field Measurements with the $^3\text{He}$ Spectrometer

##### Instrument Assembly

The electronics assembly is normally shipped intact, except that the preamp and cables are disconnected. The following procedures are used to set up the unit for neutron energy spectrum measurements.

1. Unpack the instrument and inspect for damage. Inspect the cables carefully; the connectors can be broken in transit with little sign of damage.
2. Attach the preamp cables using Figure 5.8 as a guide. Attach the preamplifier power cable to the connector on the back of one of the Ortec 572 amplifiers. It may be necessary to loosen the amplifier in the NIMbin to fasten the cable in place. Attach the high voltage from the

preamplifier to the SHV connector on the high voltage power supply. Check to make certain that the HV power supply is turned off. Finally, attach the signal cable to the amplifier input labeled "IN" (not "INH", the inhibit BNC connector)!

3. Using a short cable, attach the  $^3\text{He}$  proportional counter to the input of the Ortec 142PC preamplifier. Note that on some tubes a special connector adapter is required.
4. Attach a BNC signal cable from the output of the linear gate to the signal input of the multichannel analyzer (MCA). Turn on the MCA and let it warm up.
5. Plug in the NIMbin and turn on the power.
6. Check the voltage rating of the  $^3\text{He}$  proportional counter (usually +900 to +1400 volts). The operating voltage can be written on the tube. Set the high voltage power supply to the correct voltage, be certain the unit is plugged in, and turn on the high voltage.
7. Remove the neutron shields and place the bare  $^3\text{He}$  proportional counter in a neutron field.
8. Turn on the multichannel analyzer to "COLLECT"; you should observe a definite peak from slow neutrons. If not, check to make certain there is power to the units and they are turned on. Then check all the connections listed in Step 2. If this does not correct the problem, review Section 5.4, TROUBLESHOOTING. This may take some time, so make certain you are in a low dose rate area to avoid unnecessary radiation exposure.

#### Calibration

9. After the unit has reached operating temperature, check the "time window" to make certain the unit has not drifted excessively. Connect the signal cable from the input of the multichannel analyzer (MCA) to the "LINEAR OUTPUT" BNC connector on the front face of the Ortec 458 pulse shape analyzer. Set the MCA to collect data in one-half or one-quarter of the memory, and collect a "risetime" spectrum.
10. Next, connect a BNC signal cable from the "WINDOW" BNC connector on the Ortec 458 pulse shape analyzer to the coincidence gate input on the multichannel analyzer. Set the MCA to collect data in another half or quarter of the memory and collect data in coincidence with the window "gate" signal. This gives the "risetime" spectrum of events selected by the pulse shape analyzer, as shown in Figure 5.10. Adjust the "UPPER LEVEL" and "LOWER LEVEL" dials to select only the desired events. Slow risetime events usually correspond to pulse pile-up and should be rejected.

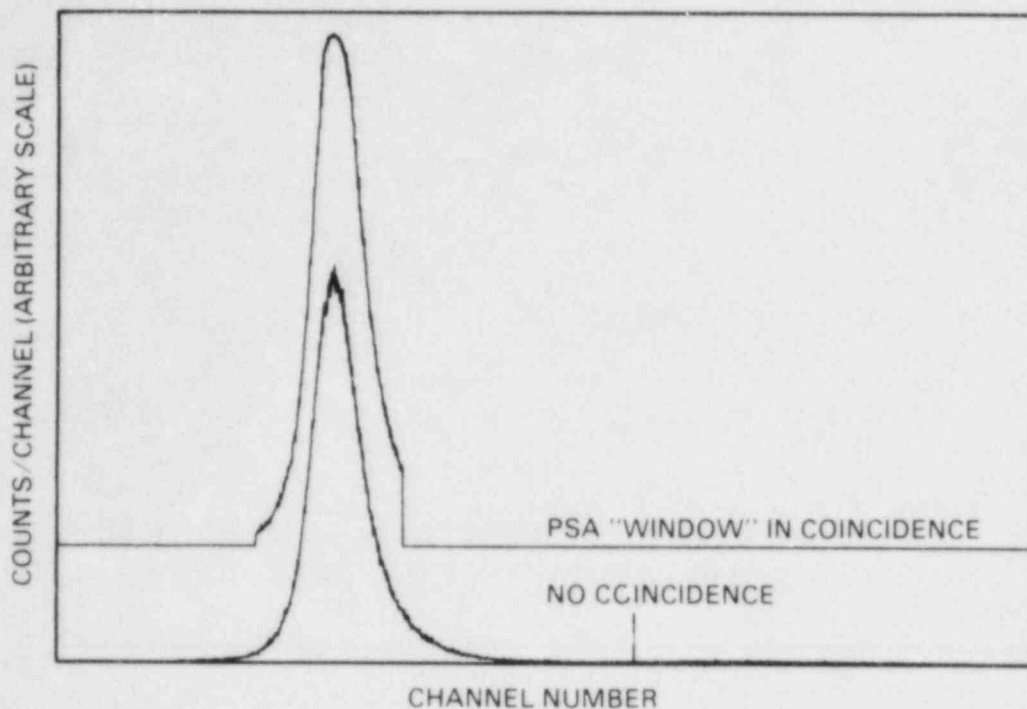


FIGURE 5.10. "Rise Time" Spectra From Linear Output of Ortec 458 Pulse Shape Analyzer With and Without Coincidence Gate Signal From "Window" of Pulse Shape Analyzer

11. Record the "risetime" spectrum with the "window" gate pulses. Remove the signal cables from the pulse shape analyzer and reconnect the short cable from the "ENABLE" of the linear gate to the "WINDOW" of the pulse shape analyzer.
12. Reconnect a signal cable from the MCA input to the output of the linear gate.
13. Using the fine gain control, adjust the gain of amplifier 1 to place the slow neutron peak in channel 382 (to give an energy calibration of 2 keV/channel).
14. Place the  $^3\text{He}$  proportional counter back in the neutron shield to suppress pulse pile-up from thermal neutrons.

#### Collecting Data

15. Set the multichannel analyzer to a preset data collection time and select the area of memory you wish to use. Erase any data in the memory you are using. Push the "COLLECT" button and start collecting spectral data.
16. Observe the data to make certain that enough data is collected to be statistically significant and that the unit is operating properly. You should obtain tens of counts per channel in the region corresponding to

100 keV neutrons. If the spectrometer has been adjusted to 2 keV/channel with the slow neutron peak at channel 382, 100 keV neutrons correspond to channel 432.

17. Check to make certain that pulse pile-up does not occur. This is evidenced by a sum peak at channel 764 if the slow neutron peak is at channel 382. At high count rates the pulse rejection circuits will be functioning and the unit will have high dead times. If there is evidence of pulse summing, the data obtained will not be indicative of the true neutron energy spectrum. Shut off the high voltage power supply and substitute a less sensitive  $^3\text{He}$  proportional counter (i.e., a tube with a lower  $^3\text{He}$  gas filling). If a new tube is used, be certain to adjust the high voltage power supply to the proper voltage (Step 6) and adjust the "risetime window" as described in Steps 9, 10, and 11. Adjust the gain as outlined in Steps 12 and 13.
18. Collect the data and read it out to a recording device. Be certain to record the identification number of the  $^3\text{He}$  proportional counter used for the measurement.

### 5.3 MULTICHANNEL ANALYZER LINEARITY CHECK

Before the  $^3\text{He}$  spectrometer is used, check to make certain the analog-to-digital converter (ADC) of the multichannel analyzer is properly set up and linear through zero channel. The MCA must be linear through zero for the  $^3\text{He}$  spectrometer to be self-calibrating using the 764-keV thermal neutron peak.

1. Connect a cable from a pulse attenuated output to the "TEST" BNC connector on the Ortec 142PC preamplifier.
2. Connect a cable from the bipolar output of the amplifier (labelled "BI") to the multichannel analyzer input.
3. Turn on the pulser and set the controls to produce positive pulses. You can observe the pulser with an oscilloscope at the output BNC of the pulser, at the output of the preamplifier, or at the bipolar output of the amplifier.
4. Turn on the multichannel analyzer to see if pulses from the pulser are being counted.
5. Set the level control of the pulser to 5.00 and adjust the attenuation and gain or normalization until the pulser peak occurs at about channel 50.
6. Erase the MCA and collect data for a short time with the pulser set at 5.00. Stop collecting data, move the pulser level control to 4.00, and collect more data. Repeat at 3.00, 2.00, and 1.00. If the MCA is linear through zero, the plot of pulser height versus pulser level setting should linearly extrapolate through the origin, as shown in Figure 5.11. If the ADC is not linear through zero, make the following adjustments. First, calculate the average number of channels between pulser peaks.



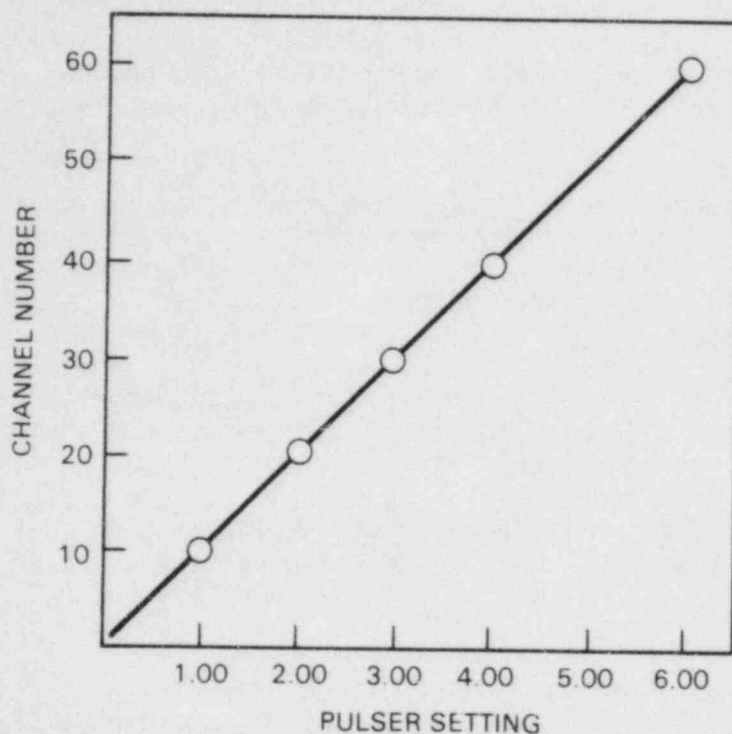


FIGURE 5.11. Plot of Channel Number of Pulser Peak Versus Pulser Setting to Determine if the ADC is Linear Through Zero

Set the pulser to 1.00 and adjust the zero level of the ADC until the pulser peak is in the channel corresponding to the number of channels between peaks. Alternately adjust the lower level discriminator and readjust the zero level to maintain the pulser peak at the correct channel number. The lower level discriminator should be as low as possible without triggering on electronic noise.

#### 5.4 TROUBLESHOOTING

The electronics used in the  $^3\text{He}$  spectrometer are quite rugged and stable and usually function even after being abused by rough handling in shipment and high operating temperatures. If no signals are collected when everything is turned on, first check the obvious. Is everything--the NIMbin power, the high voltage power supply and the multichannel analyzer--really turned on? Next, check the cables to make certain they have been connected properly. First, check the cable from the  $^3\text{He}$  proportional counter to the preamplifier. The weight of the preamp hanging on the cable is sometimes enough to pull the connections apart inside the connector. Support the preamp so that it is not pulling on the connector. Check the cables fastened to the preamp and make certain they are connected properly at the other end. A common mistake is to connect the preamp signal cable to the inhibit output BNC labeled "INH" instead of to the amplifier input BNC labeled "IN" on the back of the Ortec 572 amplifier. Another common problem is that the preamp power cable on the back of

the Ortec 572 amplifier is connected only on one side and pulls loose if the cable is pulled when moving the preamp around. Check to make certain that a cable runs from the output of the second linear gate and goes to the signal input of the ADC, and that the MCA is turned on and not in the coincidence mode.

If the above checks do not solve the problem, it may be more serious and require a careful scrutiny of the spectrometer electronics. Using Figure 5.8 as a guide, check to make certain that all the cables are connected properly and all the switches are in the correct position. It is possible that someone may have changed them.

If this does not solve the problem, you should begin tracing the signals with an oscilloscope. Start with the preamp and observe that a signal is being generated by the  $^3\text{He}$  tube. Sometimes the high voltage is not set correctly so that the signals out of the preamp are too small to be analyzed properly. Check the value listed for your tube. High voltage power supplies do fail, or it is possible that someone borrowed it and put it back with the wrong polarity. In general, you should use +900 to +1500 volts with 1-inch diameter tubes.

Next, check the signal at the other end of the preamp cable. Cable connectors can come loose in transit or could be damaged by stepping on them, or the cable could be broken by being cut, crimped, or caught in a door.

Check the signal at the unipolar output of both Ortec 572 amplifiers. Follow the energy signal from amplifier 1 through the linear gate. If the signal reaches the linear gate, but no output is observed at the output of the linear gate, there could be a logic gate problem.

If a different  $^3\text{He}$  tube is being used it is possible that the "time" window is completely out of adjustment. Check this by connecting a cable from the "LINEAR" output of the pulse shape analyzer (Ortec 458PSA) to the ADC input of the multichannel analyzer. A risetime spectrum should be observed when the MCA is turned on. Next, connect a cable from the "WINDOW" output to the coincidence gate input on the MCA. Set the MCA to enable the coincidence and collect a spectrum. Adjust the "UPPER LEVEL" and "LOWER LEVEL" to contain the peak corresponding to the desired  $^3\text{He}(n,p)\text{T}$  events. Reject the very fast or very slow risetime events with the window adjustments.

If the unit is not functioning properly, start from the beginning for the initial set-up procedure and trace the signal through in a logical step-by-step sequence as outlined in the set-up procedures. First, however, make certain that the  $^3\text{He}$  tube is functioning properly at the correct voltage.

## 6.0 TESTING THE $^3\text{He}$ SPECTROMETER SYSTEM

The  $^3\text{He}$  spectrometer system using pulse shape analysis was tested in an environmental chamber to simulate typical reactor containment conditions. The accuracy of the  $^3\text{He}$  spectrometer was checked by comparing its response with that of a proton-recoil spectrometer. These tests are described in this section.

### 6.1 ENVIRONMENTAL CHAMBER TESTING

The environment inside containment of nuclear power reactors operating at full power is typically very hostile. The authors have experienced high temperatures ranging from a cool  $90^\circ\text{F}$  ( $32^\circ\text{C}$ ) to a rather warm  $180^\circ\text{F}$  ( $82^\circ\text{C}$ ). Humidity of up to 90% was also encountered in a reactor with a number of steam leaks. These conditions may adversely affect electronic equipment comprising the  $^3\text{He}$  spectrometer apparatus.

To evaluate its operation at high temperatures, the pulse shape analysis version of the  $^3\text{He}$  spectrometer, using Ortec electronics and a Canberra Series 40 multichannel analyzer, was placed inside the PNL environmental chamber. A signal from the output of the Ortec electronics was connected to a second multichannel analyzer, a Canberra 8180, to determine if any drift that occurred was produced in the  $^3\text{He}$  spectrometer electronics or in the multichannel analyzer. A small  $^{252}\text{Cf}$  source (about 5 micrograms) was placed outside the environmental chamber to provide a source of neutrons.

The test started with the temperature at  $72^\circ\text{F}$  at 47% relative humidity. The air temperature and relative humidity profiles during the test are shown in Figure 6.1 as a function of time. The temperature and humidity were raised to  $100^\circ\text{F}$  and 90% relative humidity in about 15 to 20 minutes. Because the walls of the chamber and equipment were cooler than the air, moisture condensed on everything in the chamber. The Canberra Series 40 multichannel analyzer failed, apparently because of condensation resulting from moist air introduced inside the unit by the cooling fan. The unit was turned off and restarted; it appeared to function for a short time at a constant gain, then failed again. The unit was left alone for the remainder of the test. After the test was over the Canberra Series 40 was turned off, then restarted; the thermal neutron peak was found to be at exactly the same channel as at the beginning of the test. This behavior was never observed in the Canberra Series 40 multichannel analyzers used in previous reactor measurements. The authors believe that the unexpected failure of the analyzer during the environmental chamber tests was caused by condensation inside the analyzer. In a reactor measurement, 15 to 20 minutes are required to set up the equipment, allowing the unit to come to thermal equilibrium. When the unit is then turned on, moisture does not condense on the inside.

A second multichannel analyzer (Canberra 8180) was used to monitor any gain shifts produced by temperature or humidity effects in the  $^3\text{He}$  spectrometer electronics. As shown in Figure 6.1, the gain of the Ortec system changed to less than 0.8% during the entire test. In reactor measurements gain shifts of a few percent have been noticed; the greatest gain shift is apparently due to the multichannel analyzer.

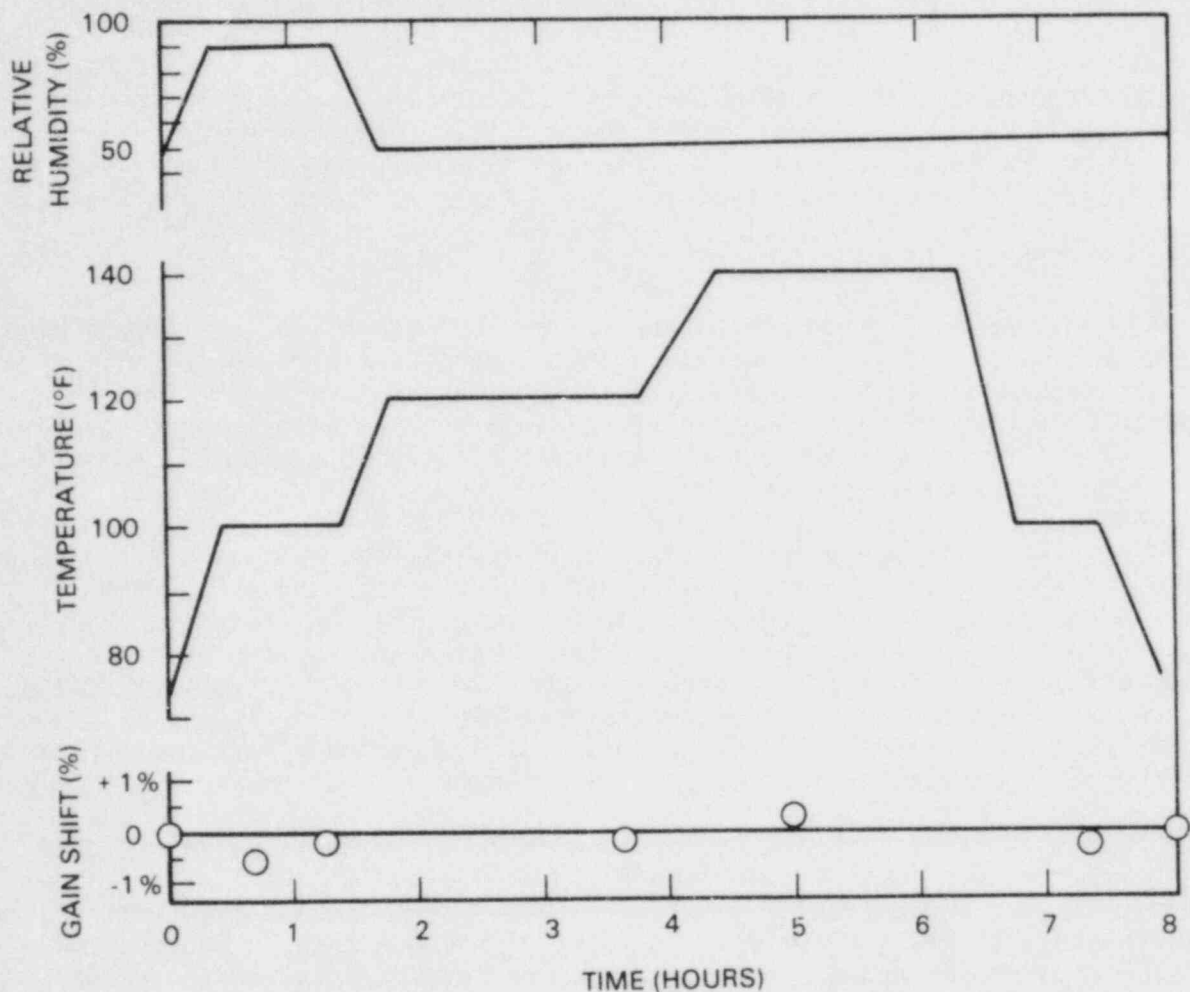


FIGURE 6.1. Relative Humidity and Temperature for  $^3\text{He}$  Spectrometer Test in PNL Environmental Chamber

The  $^3\text{He}$  spectrometer electronics appear to change gain by less than 0.8% for operating temperatures ranging from 70°F to 140°F (21°C to 60°C). The spectrometer system will also function at 90% relative humidity.

## 6.2 EXPERIMENTAL VERIFICATION OF THE UNFOLDING CODE

The theory behind the computer code HESTRIP used to "unfold" the neutron energy spectrum is explained in Section 3.2.3, and a listing of the code can be found in Appendix D. This unfolding code is derived from first principals, i.e., no experimental calibration is used in the code or in setting up the  $^3\text{He}$  spectrometer. Obviously, some sort of experimental verification of the  $^3\text{He}$  spectrometer and unfolding code are necessary. The 144-keV filtered neutron beam facility at the National Bureau of Standards was used to help verify the accuracy of the unfolding algorithm used in HESTRIP. The neutron energy spectrum of this beam was measured with a proton-recoil proportional counter spectrometer and documented (Schwartz 1977). The 144-keV and 51-keV energies are in the range of neutron energies found inside reactor containment.

Figure 6.2 shows the neutron energy spectra obtained with the  $^3\text{He}$  proportional counter spectrometer and with a proton-recoil proportional counter exposed to the 144-keV neutron beam at the National Bureau of Standards. The  $^3\text{He}$  spectrometer measurements were made with a 2.54-cm (1-in.) diameter by 30.5-cm (12-in.) long  $^3\text{He}$  proportional counter filled with a mixture of  $^3\text{He}$  and argon at partial pressures of 4 psia (0.23 atmosphere) of  $^3\text{He}$  and 26 psia (1.77 atmospheres) of argon. No pulse pile-up or pulse shape analysis electronics were used for these measurements. The proton-recoil proportional counter spectrum in Figure 6.2 obviously has much better resolution, but the  $^3\text{He}$  spectrometer spectrum is quite acceptable. The  $^3\text{He}$  spectrometer has poorer resolution, but the two measured spectra agree fairly well over almost 2 orders of magnitude. The pulse height distribution from the  $^3\text{He}$  proportional counter is not Gaussian as evidenced by the deviations at energies above about 180 keV. Below the 144-keV peak there is evidence of "tailing," which is a characteristic of the proportional counter tube used. The unfolding code uses a spectral "stripping" technique in which a response function was calculated to account for wall effects. The stripping technique appears

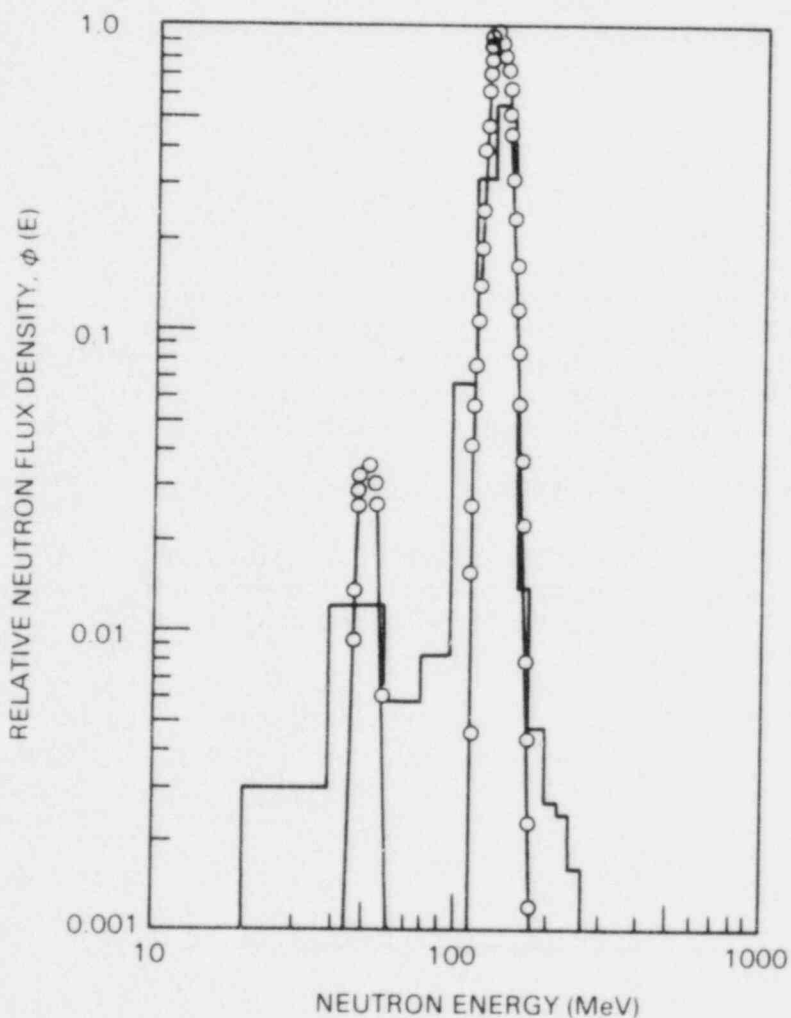


**FIGURE 6.2.** Comparison of Neutron Energy Spectra Measured by a Proton Recoil Spectrometer (circles) and the  $^3\text{He}$  Spectrometer (histogram) at the 144 keV Neutron Beam at the National Bureau of Standards

to work reasonably well, although improvements could be made. However, it would require days of computer running time to significantly improve the accuracy of the Monte Carlo calculations. The calculated flux at lower energies is less than 1% of the 144-keV peak, so there is not much point of refining the response functions to achieve better accuracy.

Additional measurements were made with the  $^3\text{He}$  spectrometer exposed to nearly monoenergetic neutrons produced by a Van de Graaff accelerator. The apparatus used has been described previously (NUREG/CR-2956, Section 2.2, p. 8). A precision long counter was used to monitor the fast neutron fluence. A 2.54-cm (1-in.) diameter  $^3\text{He}$  proportional counter filled with  $^3\text{He}$  at a partial pressure of 4 psia (0.27 atmosphere) and argon at a partial pressure of 26 psia (1.77 atmospheres) was positioned near the target with the axis of the cylinder aligned toward the target. The long counter and the  $^3\text{He}$  proportional counter were positioned at the same angle with respect to the accelerator beam line, so that both instruments were exposed to the same neutron energy and intensity. It was assumed that the fast neutron flux varied inversely with the square of the distance from the target, so that the fast neutron flux at the geometric mean of the  $^3\text{He}$  counter could be determined from the long counter measurement.

The results of the measurements are shown in Table 6.1. A very thin target was used, and the neutron energy measured by the  $^3\text{He}$  proportional counter was within 6% of that calculated by nuclear reaction kinematics (NUREG/CR-2956, Section 2.2.1.2, p. 10). The  $^3\text{He}$  proportional counter was modeled as a point detector at the geometric mean distance from the target. The dose equivalents determined by the  $^3\text{He}$  spectrometer measurements are in reasonable agreement with those calculated from fluences measured by the long counter for higher neutron energies. This is encouraging because dose equivalent is determined from the measured reaction rate and the size and  $^3\text{He}$  partial pressure in the proportional counter; no neutron calibration is necessary.

TABLE 6.1. Neutron Dose Equivalents Determined from  $^3\text{He}$  Spectrometer Measurements of Nearly Monoenergetic Neutrons Produced by a Van de Graaff Accelerator

Maximum Neutron Energy (MeV)		Dose Equivalent (mrem)		
Calculated from Reaction Kinematics	Measured by $^3\text{He}$ Proportional Counter	Calculated from Fluence Measured by Long Counter	Determined by $^3\text{He}$ Proportional Counter	Percent Difference
576 keV	609 keV	496 mrem	339 mrem	-32
352 keV	352 keV	343 mrem	285 mrem	-17

Because the response function used in the unfolding code HESTRIP does not account for  $^3\text{He}$  recoils from the elastic scatter of neutrons, it is not possible to check the accuracy of the  $^3\text{He}$  spectrometer with calibrated  $^{252}\text{Cf}$  sources. A modification must be made to the Monte Carlo computer code used to generate the response function. Also, larger tubes (2-in. diameter) at higher pressures (4 atmospheres) must be used to reduce the number of wall events from the higher energy neutrons from isotopic neutron sources.

## 7.0 REACTOR SPECTRUM MEASUREMENTS

To demonstrate its usefulness, the  $^3\text{He}$  spectrometer was used to measure containment spectra at several commercial nuclear power reactors. This section documents the equipment and methods used in the field. The results obtained at each reactor site are presented and discussed. The data for all three sites are then combined and the overall findings are summarized.

### 7.1 EQUIPMENT AND METHODOLOGY

Concurrent with the  $^3\text{He}$  spectrometer measurements, several other measurements were made to help determine  $^3\text{He}$  spectrometer accuracy. The equipment and data analysis methods have already been fully described (NUREG/CR-1769, Section 2.0, page 2.1). General information is presented here.

Approximate differential neutron flux densities and fractional dose equivalent distributions were obtained from the multisphere spectrometer (NUREG/CR-1769, Section 2.1.1, p. 2.1). The multisphere spectrometer consists of a scintillation detector placed inside polyethylene spheres with diameters of 7.6, 12.7, 20.3, 25.5, and 30.5 cm. The fast neutron response of this system increases with sphere size, because the larger spheres moderate fast neutrons to lower energies, where they are detected by the  $^6\text{LiI}$  scintillator. The computer code LOUHI (Routti and Sandberg 1978) was used originally to determine neutron energy spectra from the count rate data for each size of sphere. The authors, however, used two new codes to analyze the multisphere data: YOGI (Johnson and Gorbics 1981) and SPUNIT (Brackenbush and Scherpelz 1983). Comparisons among the codes show that all three calculate about the same value for integral quantities (total neutron flux density integrated over energy and total dose equivalent rate) but the differential values (neutron flux density per energy bin) may vary from code to code.

The tissue equivalent proportional counter (TEPC) was used to measure absorbed neutron dose and determine dose equivalent (NUREG/CR-1769, Section 2.2.2, p. 2.6). The TEPC is a hollow sphere of tissue equivalent plastic filled with tissue equivalent gas. The proportional counter measures energy deposited in a tissue-like medium; this is a direct measure of absorbed neutron dose. With the appropriate algorithms it is also possible to determine neutron quality factors and dose equivalents from the TEPC data.

Portable neutron survey instruments, such as a Snoopy cylindrical remmeter and Eberline PNR-4 spherical remmeter, were also used to monitor neutron dose equivalent rates. The Snoopy was manufactured to Hanford specifications, and prior to use it was calibrated at the PNL calibrations facility using an unmoderated  $^{252}\text{Cf}$  source with source strength and dose equivalent rate calibrations traceable to the U.S. National Bureau of Standards. The PNR-4 survey meters were provided by the utility staff, and were calibrated using unmoderated PuBe sources. However, the authors are not familiar with the calibration procedures used by the utilities.



In general, moderator-based remmeters often overestimate neutron dose equivalent when exposed to neutrons with energies below 1 MeV. This overestimation of dose equivalent has been documented in several independent studies. Measurements made with monoenergetic neutrons produced by an accelerator showed that eight different commercial neutron survey meters, including the PNR-4, overestimate dose equivalent by at least a factor of 2 when exposed to 26 keV and 110 keV neutrons (Cosack and Lesiechi 1981). A study made in a heavily shielded accelerator facility concluded that portable neutron survey instruments overestimated dose equivalent by factors of between 3 to 50 when compared to the results obtained using a multisphere spectrometer system with data unfolded using the computer code BON (Schlapper et al. 1983). Previous measurements made by PNL personnel in nuclear power plants also demonstrate that most portable neutron survey instruments overestimate dose equivalent (NUREG/CR-1769).

Measurements were made with the  $^3\text{He}$  spectrometer system described in Section 5.2.2. Pulse pile-up was reduced by surrounding the  $^3\text{He}$  proportional counter with a boron carbide sleeve to absorb slow neutrons. The 51-cm (20-in.) long sleeve was made from a 1-mm (0.040-in.) thick cadmium tube placed inside a 10-cm (4-in.) tube obtained from the local hardware store. The annular region between the cylinders was filled with boron carbide powder, so that the  $^3\text{He}$  tube was surrounded by 1.4 g/cm<sup>2</sup> of boron carbide. With this thickness of material, it is estimated that more than half of the fast neutrons at 50 keV will scatter once in passing through the shield. These neutrons may lose as much as 31% of their energy in a single scatter, so the neutron energy spectrum will be degraded to somewhat lower energies in passing through the boron carbide absorber. Measurements were also made with the  $^3\text{He}$  tube inside a 1-mm (0.040-in.) thick cadmium absorber; this allowed a crude determination of the thermal and intermediate energy flux.

## 7.2 MEASUREMENT RESULTS

Measurements were made at three pressurized water reactors (PWRs), designated Sites 4, 5, and 6. Measurements were also attempted at two boiling water reactors (BWRs). At one BWR the containment was inerted (filled with nitrogen), and operating procedures excluded the possibility of entry while the reactor was operating. An Eberline PNR-4 survey meter indicated the dose equivalent rate near the equipment hatch was below 1 mrem/hr, which was not high enough to make measurements in 1 day. The dose equivalent rates inside the equipment hatch were high enough to make measurements, but the utility corporate policy did not permit opening the outer hatch door while the reactor was operating.

Measurements were made at a second BWR at a location outside containment where there was a large pipe penetration with a steel plate welded over each side of the penetration. Neutron streaming through the penetration was sufficient to produce dose equivalent rates of several mrem/hour, and  $^3\text{He}$  spectrometer measurements were made overnight. An analysis of the data showed that the equipment had malfunctioned during the measurements. After the equipment was returned to the laboratory, it was determined that the linear gate was not functioning properly; this unit was replaced for the remaining measurements discussed in the next subsection.

### 7.2.1 Reactor Site 5

At Site 5 neutron energy spectrum and dose equivalent measurements were made 1 m above the floor on the edge of the operating deck overlooking the reactor cavity. The PNL Snoopy indicated the neutron dose equivalent rate was 55 mrem/hr at the position where spectral measurements were made with the <sup>3</sup>He spectrometer and the multisphere spectrometer. Measurements were also made with a tissue equivalent proportional counter. These data are suspect, however, because of a broken cable, which created noise in the event spectrum used to determine dose and dose equivalent.

The multisphere spectrometer results are listed in Table 7.1. The neutron flux, dose and dose equivalent distributions calculated by the SPUNIT computer code are presented. The differential neutron flux density (neutrons/cm<sup>2</sup>-sec/energy bin) is plotted as a function of neutron energy in Figure 7.1. Because the datum of interest is a determination of neutron dosimeter response per unit of dose equivalent, it may be more useful to plot the fractional dose equivalent (mrem/hr/energy bin) as a function of neutron energy. The graph in

TABLE 7.1. Results of Multisphere Spectrometer Measurements at Reactor Site 5

BIN NO	ENERGY (MEV)	FLUX N/CM <sup>2</sup> -S	* DIFFERENTIAL *		* CUMULATIVE *	
			DOSE (RAD/HR)	DOSE EQUIV (REM/HR)	DOSE DIST (RAD/HR)	DOSE EQUIV (REM/HR)
1	2.57E-07	4.35E+02	8.23E-04	1.76E-03	4.12E-03	2.64E-02
2	5.48E-07	6.70E+01	1.47E-04	3.07E-04	3.30E-03	2.46E-02
3	1.06E-06	4.76E+01	1.06E-04	2.22E-04	3.15E-03	2.43E-02
4	2.25E-06	3.94E+01	8.70E-05	1.84E-04	3.04E-03	2.41E-02
5	4.77E-06	3.05E+01	6.66E-05	1.43E-04	2.96E-03	2.39E-02
6	1.01E-05	2.58E+01	5.58E-05	1.20E-04	2.89E-03	2.38E-02
7	2.14E-05	2.14E+01	4.61E-05	9.80E-05	2.83E-03	2.36E-02
8	4.52E-05	2.31E+01	4.93E-05	1.03E-04	2.79E-03	2.35E-02
9	9.58E-05	1.57E+01	3.33E-05	6.79E-05	2.74E-03	2.34E-02
10	2.03E-04	1.41E+01	2.90E-05	5.89E-05	2.71E-03	2.34E-02
11	4.34E-04	1.35E+01	2.65E-05	5.36E-05	2.68E-03	2.33E-02
12	9.13E-04	1.36E+01	2.58E-05	5.21E-05	2.65E-03	2.33E-02
13	1.92E-03	1.46E+01	2.70E-05	5.44E-05	2.62E-03	2.32E-02
14	4.07E-03	1.68E+01	3.07E-05	6.16E-05	2.60E-03	2.32E-02
15	8.62E-03	2.06E+01	3.73E-05	7.54E-05	2.57E-03	2.31E-02
16	1.82E-02	2.71E+01	5.49E-05	1.52E-04	2.53E-03	2.30E-02
17	3.86E-02	4.09E+01	9.77E-05	4.16E-04	2.47E-03	2.29E-02
18	8.18E-02	7.55E+01	2.13E-04	1.40E-03	2.38E-03	2.24E-02
19	1.67E-01	1.65E+02	6.18E-04	5.25E-03	2.16E-03	2.10E-02
20	3.37E-01	2.31E+02	1.21E-03	1.21E-02	1.55E-03	1.58E-02
21	6.79E-01	4.15E+01	3.35E-04	3.65E-03	3.39E-04	3.69E-03
22	1.39E+00	3.05E-01	3.74E-06	3.69E-05	3.77E-06	3.71E-05
23	2.78E+00	1.55E-03	2.36E-08	1.92E-07	2.41E-08	1.88E-07
24	5.54E+00	2.43E-06	5.05E-11	3.53E-10	5.43E-10	-3.74E-09
25	1.12E+01	1.54E-08	3.68E-13	2.54E-12	4.92E-10	-4.09E-09
26	2.04E+01	1.69E-13	5.52E-18	3.82E-17	4.92E-10	-4.09E-09
TOTAL		1.38E+03	4.12E-03	2.64E-02		

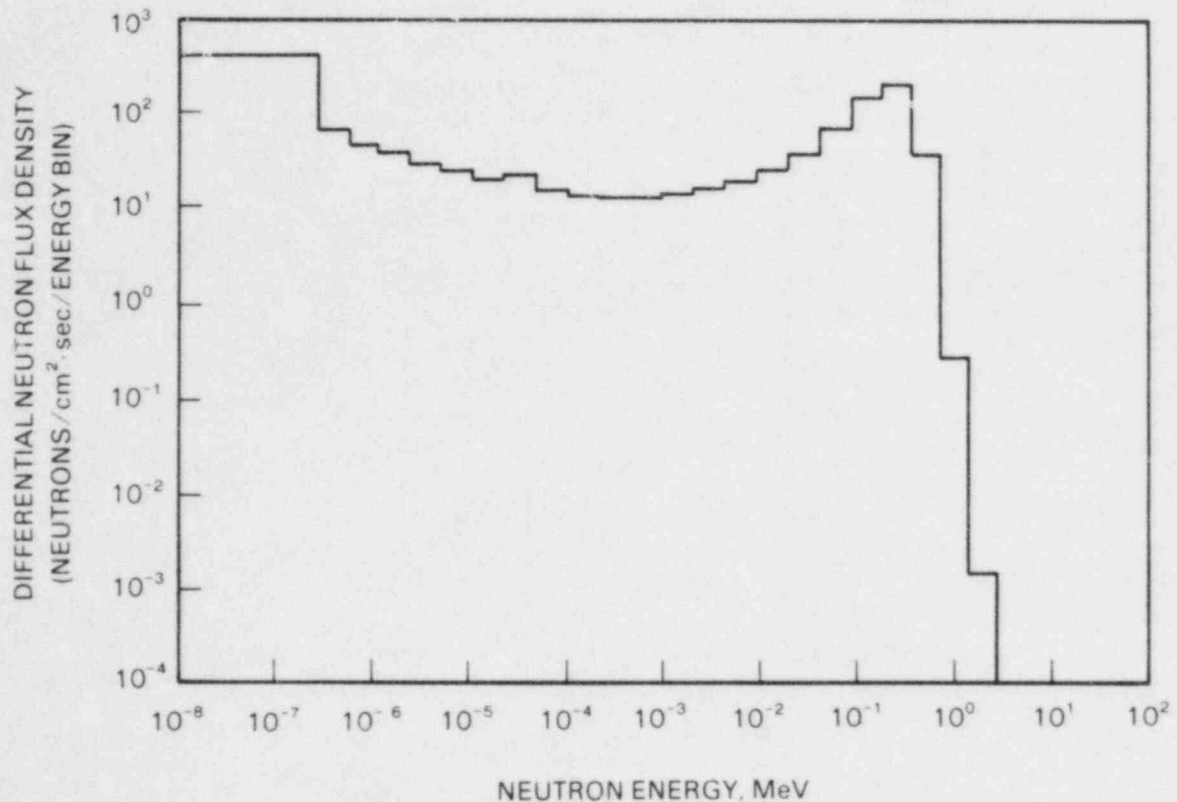


FIGURE 7.1. Differential Neutron Energy Spectrum Calculated From Multisphere Spectrometer Measurements at Reactor Site 5

Figure 7.2 has been divided into the three energy regions used to determine TLD-albedo dosimeter response, as explained in Appendix A. In Figure 7.2, about 87% of the dose equivalent is produced by neutrons with energies above about 10 keV; in this energy region the TLD-albedo dosimeter response per unit of dose equivalent decreases rapidly with increasing energy.

Measurements were also made with the  $^3\text{He}$  spectrometer counter inside the boron carbide slow neutron absorber. Data were collected for 1-1/2 hours to produce the pulse height distribution shown in Figure 7.3 using a 2.5-cm (1-in.) diameter  $^3\text{He}$  proportional counter filled at a partial pressure of 4 psia (0.27 atmosphere) of  $^3\text{He}$  and 10.7 psia (0.73 atmosphere) of argon. It is necessary to determine if the pulse distribution above the slow neutron peak at 764 keV was produced by 1) pulse pile-up in the  $^3\text{He}$  proportional counter or 2) nonlinear gains in the proportional counter. This could have been determined if a pulser had been used during the measurements, as explained in Section 5.2.1.

It is possible to determine pulse pile-up using a technique similar to that discussed in Section 5.1. As demonstrated previously, the amount of pulse pile-up is a function of the count rate. The count rate was determined to be 24 counts/second by setting up a region of interest and integrating all of the neutron events in the pulse height distribution and dividing by the

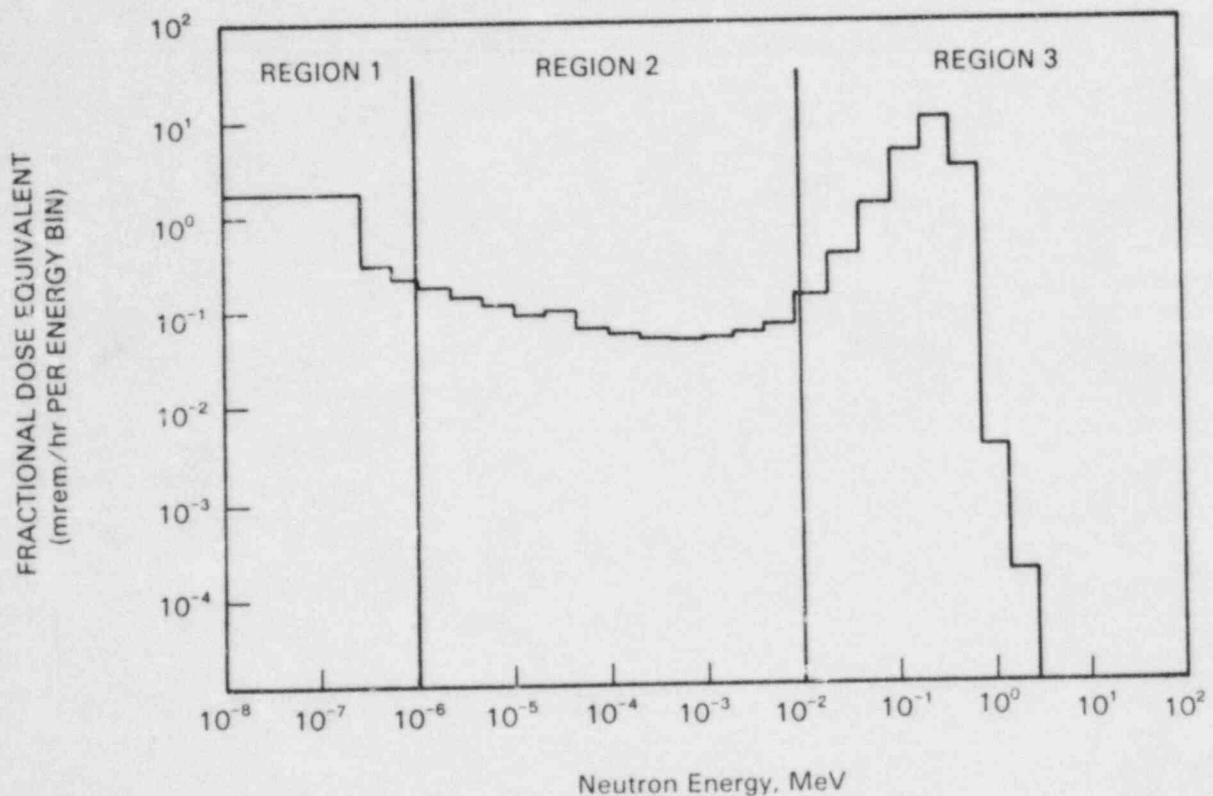


FIGURE 7.2. Fractional Dose Equivalent Distribution Calculated From Multisphere Spectrometer Measurements at Reactor Site 5

time. Using the same instrument settings for the spectrometer, the bare  $^3\text{He}$  proportional counter was exposed to the thermal neutron source described in Section 4.3. The distance between the source and detector was varied until the count rate from the thermal neutron source was the same as that from the reactor measurement for the same region of interest. A Berkeley Nucleonics Model PB-3 pulser was attached to the "TEST" input of the preamplifier, and the pulse shape was adjusted to match that produced by the  $^3\text{He}$  proportional counter. Pulses were supplied to the  $^3\text{He}$  spectrometer system at 1000 times the count rate from the  $^3\text{He}$  proportional counter. The pile-up with the pulser can be divided by 1000 to equate it with that resulting from pulses produced by random coincidence in the proportional counter. Because there was some concern that gamma rays might also introduce some pile-up problems, a  $^{137}\text{Cs}$  gamma source was positioned to produce a 40 mR/hr field at the position of the proportional counter. The resulting pulse height distribution is shown in Figure 7.4. The number of pulses in the region above the thermal neutron peak is less than 2% of the number of pulses in the same region in the reactor spectrum. This demonstrates that almost all (about 98%) of the pulses are indeed produced by fast neutrons and are not the result of pulse pile-up or nonuniform gain in the proportional counter. Even gamma pulse pile-up does not appear to be much of a problem for this particular measurement.

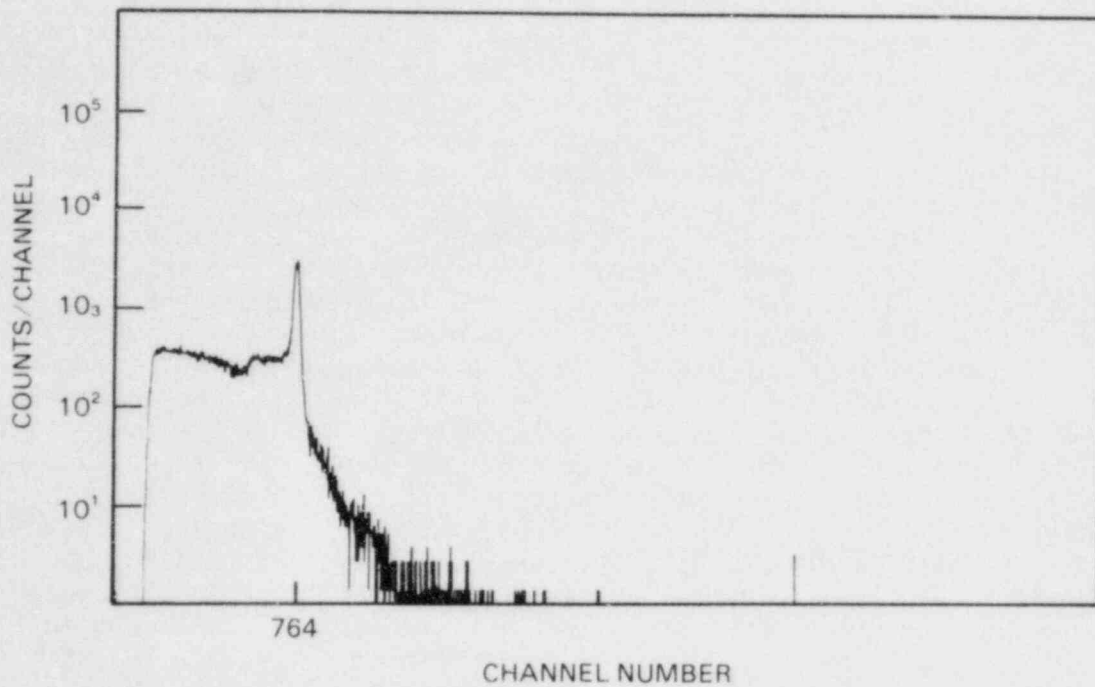


FIGURE 7.3. Pulse Height Distribution from  $^3\text{He}$  Spectrometer Measurement at Reactor Site 5

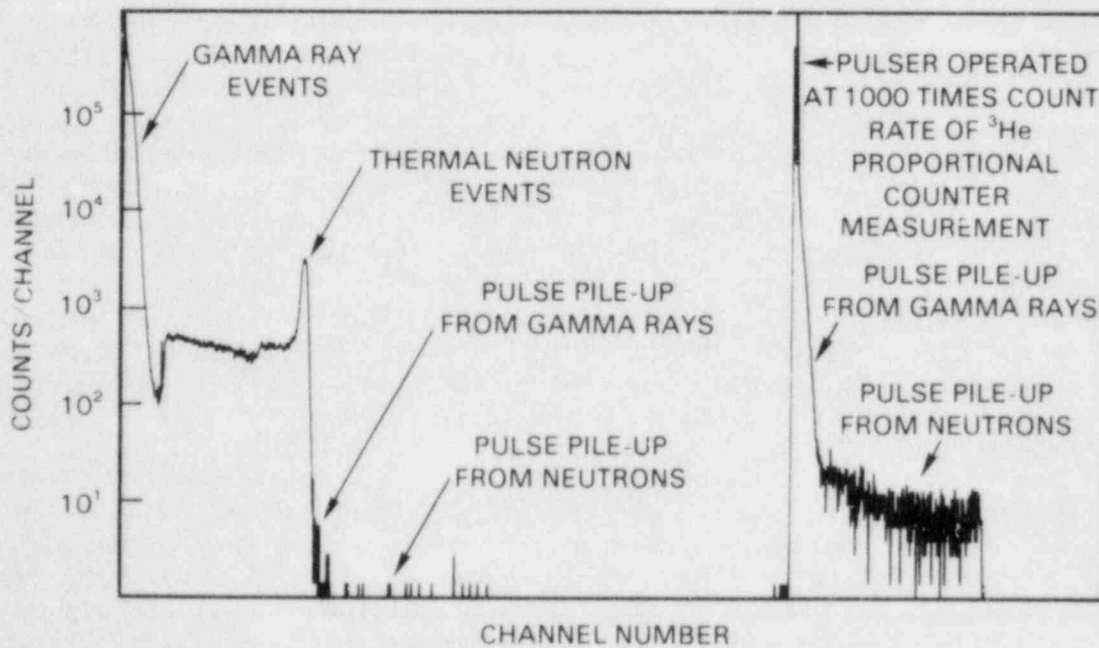


FIGURE 7.4. Pulse Pile-Up Distribution for the  $^3\text{He}$  Spectrometer Exposed to a Thermal Neutron Source for Reactor Site 5

The reactor spectrum data were analyzed by the computer code HESTRIP, and the results are presented in Table 7.2. These results must be divided by the time of the exposure (1.57 hours) before comparing them with the multisphere spectrometer results. The differential neutron fluence (neutrons/cm<sup>2</sup> per energy bin) is typical of moderated spectra and is much larger at lower energies. By convention, fluence is usually plotted per unit lethargy or logarithmic energy interval; this is preferred because the fluence plotted against energy displays a steep negative slope at lower energies. It was shown in Section 3.2.2 that the fluence per unit lethargy is the same as the energy multiplied by the fluence as a function of energy [ $\phi(u) = E\phi(E)$ ]. Figure 7.5 shows the <sup>3</sup>He spectrometer and multisphere spectrometer results plotted as  $E\phi(E)$  versus the energy on a logarithmic scale. Because only the shape of the curves is of interest, no attempt was made to normalize the multisphere spectrum to the <sup>3</sup>He spectrometer spectrum. The sharp dip in the spectrum measured by the <sup>3</sup>He spectrometer at 450 keV and 850 keV was perplexing until the spectra for fission neutrons penetrating concrete (Ing and Makra 1978, p. 89) were examined. Although these dips may be fortuitous because of poor counting statistics (there is less than 1 count/channel), the measured spectrum seems to be in agreement with the Monte Carlo calculations for neutrons penetrating concrete. Note that, for energies above 200 keV, the fluence was rebinned into 100 keV energy bins to improve counting statistics.

The differential neutron spectrum from the multisphere spectrometer bears little resemblance to that from the <sup>3</sup>He spectrometer. This is to be expected because of the poor resolution of the multisphere spectrometer, in which the flux from 26 energy bins is calculated from seven measured data points. It is interesting to note that average quantities calculated by both spectrometers are about the same; half of the dose equivalent is produced for neutrons below 350 keV for both the <sup>3</sup>He spectrometer and the multisphere spectrometer.

Measurements were also made with the <sup>3</sup>He proportional counter covered by a 1-mm (0.040-in.) thick cadmium absorber and with a bare <sup>3</sup>He proportional counter. Using the formulas given in Sections 3.2.1 and 3.2.2 and the count rates with and without the cadmium thermal neutron absorber, the dose equivalent rate from thermal neutrons with energies below 1 eV is calculated to be 2.4 mrem/hr (which compares to a value of 2.1 mrem/hr calculated by the multisphere spectrometer). Assuming a 1/E neutron energy spectrum between 1 eV and 10 keV, the dose equivalent rate measured by the <sup>3</sup>He spectrometer is 4.4 mrem/hr, which compares with 1.3 mrem/hr calculated by the multisphere spectrometer.

The HESTRIP code, used to analyze the <sup>3</sup>He spectrometer data, calculates that a "generic" TLD-albedo dosimeter (the Hanford multipurpose dosimeter) would overestimate the dose equivalent by a factor of 9.8 if it were exposed to the reactor spectrum after being calibrated with a bare <sup>252</sup>Cf source or by a factor of 1.3 if calibrated using a <sup>252</sup>Cf source moderated with 15-cm of deuterium oxide.

TABLE 7.2. Results of <sup>3</sup>He Spectrometer Measurements at Reactor Site 5 Analyzed by the Computer Code HESTRIP

ENERGY BIN	AVERAGE ENERGY KEV	UNCORRECTED COUNTS	CORRECTED COUNTS	ABSOLUTE FLUENCE N/CM2	COUNTING UNCERTAINTY N/CM2	DOSE EQUIVALENT (MREM)	QUALITY FACTOR	RUNNING SUM OF DOSE EQUIV. (MREM)
1	10	0 19186E+03	0 00000E+00	0 00000E+00	0 68511E+01	0 00000E+00	0 20000E+01	0 00000E+00
2	30	0 85331E+03	0 16028E+04	0 36511E+06	0 92302E+02	0 85751E+00	0 35400E+01	0 85751E+00
3	50	0 51677E+03	0 93676E+03	0 29079E+06	0 72913E+02	0 10196E+01	0 49400E+01	0 18771E+01
4	70	0 38695E+03	0 71094E+03	0 27822E+06	0 65740E+02	0 12701E+01	0 60900E+01	0 31472E+01
5	90	0 30900E+03	0 59059E+03	0 25273E+06	0 62110E+02	0 14051E+01	0 70100E+01	0 45523E+01
6	110	0 24963E+03	0 48156E+03	0 23457E+06	0 58172E+02	0 15430E+01	0 76200E+01	0 60958E+01
7	130	0 20806E+03	0 42403E+03	0 20677E+06	0 56703E+02	0 18108E+01	0 80600E+01	0 79066E+01
8	150	0 15383E+03	0 31358E+03	0 20511E+06	0 50710E+02	0 17844E+01	0 85000E+01	0 96910E+01
9	170	0 11853E+03	0 24415E+03	0 16201E+06	0 46610E+02	0 15776E+01	0 89400E+01	0 11269E+02
10	190	0 89957E+02	0 18216E+03	0 12265E+06	0 42007E+02	0 13201E+01	0 93800E+01	0 12589E+02
11	210	0 70250E+02	0 13619E+03	0 93420E+05	0 37959E+02	0 11003E+01	0 97200E+01	0 13689E+02
12	230	0 63261E+02	0 12924E+03	0 92101E+05	0 38610E+02	0 11773E+01	0 98900E+01	0 14866E+02
13	250	0 54727E+02	0 11415E+03	0 84639E+05	0 37953E+02	0 11663E+01	0 10060E+02	0 16033E+02
14	270	0 46842E+02	0 95235E+02	0 73594E+05	0 36329E+02	0 10869E+01	0 10230E+02	0 17119E+02
15	290	0 52486E+02	0 13220E+03	0 10668E+06	0 45001E+02	0 16799E+01	0 10400E+02	0 18799E+02
16	310	0 50360E+02	0 14484E+03	0 12169E+06	0 49635E+02	0 20351E+01	0 10540E+02	0 20834E+02
17	330	0 38350E+02	0 11126E+03	0 95224E+05	0 4541E+02	0 16848E+01	0 10610E+02	0 23519E+02
18	350	0 24513E+02	0 58546E+02	0 51061E+05	0 34635E+02	0 95257E+00	0 10680E+02	0 23472E+02
19	370	0 27817E+02	0 86804E+02	0 77175E+05	0 44382E+02	0 15136E+01	0 10750E+02	0 24985E+02
20	390	0 19066E+02	0 53461E+02	0 48472E+05	0 36717E+02	0 99682E+00	0 10820E+02	0 25982E+02
21	410	0 15006E+02	0 42719E+02	0 39675E+05	0 34717E+02	0 85349E+00	0 10870E+02	0 26836E+02
22	430	0 70393E+01	0 16872E+01	0 15863E+04	0 70862E+01	0 35620E-01	0 10900E+02	0 26871E+02
23	450	0 89177E+01	0 28667E+00	0 15201E+05	0 23315E+02	0 35559E+00	0 10930E+02	0 27237E+02
24	470	0 62539E+01	0 33475E+02	0 27633E+03	0 29250E+01	0 67223E-02	0 10960E+02	0 27234E+02
25	490	0 10735E+02	0 33475E+02	0 32681E+05	0 37527E+02	0 82543E+00	0 10990E+02	0 28059E+02
26	510	0 83261E+01	0 21705E+02	0 21418E+05	0 31976E+02	0 55644E+00	0 11000E+02	0 28616E+02
27	530	0 73895E+01	0 15820E+02	0 15747E+05	0 28570E+02	0 41715E+00	0 11000E+02	0 29033E+02
28	550	0 13236E+02	0 68064E+02	0 68283E+05	0 62245E+02	0 18432E+01	0 11000E+02	0 30876E+02
29	570	0 87131E+01	0 39487E+02	0 40000E+05	0 49892E+02	0 10995E+01	0 11000E+02	0 31975E+02
30	590	0 79131E+01	0 39105E+02	0 39967E+05	0 52378E+02	0 11179E+01	0 11000E+02	0 34099E+02
31	610	0 65519E+01	0 34391E+02	0 35347E+05	0 51977E+02	0 10056E+01	0 11020E+02	0 34099E+02
32	630	0 28000E+01	0 00000E+00	0 00000E+00	0 13757E+01	0 00000E+00	0 11010E+02	0 36010E+02
33	650	0 86198E+01	0 62994E+02	0 65036E+05	0 77274E+02	0 19107E+01	0 11000E+02	0 36529E+02
34	670	0 37000E+01	0 16820E+02	0 17405E+05	0 41983E+02	0 51925E+00	0 10990E+02	0 37471E+02
35	690	0 46000E+01	0 29992E+02	0 31104E+05	0 59130E+02	0 94191E+00	0 10980E+02	0 37471E+02
36	710	0 44487E+01	0 33075E+02	0 34380E+05	0 65680E+02	0 10563E+01	0 10950E+02	0 38527E+02
37	730	0 45900E+01	0 40827E+02	0 42534E+05	0 75944E+02	0 13254E+01	0 10930E+02	0 39852E+02
38	750	0 19000E+01	0 92975E+02	0 99507E+04	0 38236E+02	0 31434E+00	0 10910E+02	0 40167E+02
39	770	0 28000E+01	0 23406E+02	0 24468E+05	0 62580E+02	0 78332E+00	0 10890E+02	0 40950E+02
40	790	0 28000E+01	0 27091E+02	0 28321E+05	0 70447E+02	0 18535E+00	0 10870E+02	0 41869E+02
41	810	0 19000E+01	0 16264E+02	0 17002E+05	0 57229E+02	0 55845E+00	0 10850E+02	0 42427E+02
42	830	0 28000E+01	0 33037E+02	0 34536E+05	0 82807E+02	0 11489E+01	0 10830E+02	0 43576E+02
43	850	0 10000E+01	0 77903E+01	0 81438E+04	0 40825E+02	0 27411E+00	0 10810E+02	0 43850E+02
44	870	0 10000E+01	0 84219E+01	0 88041E+04	0 43117E+02	0 29985E+00	0 10790E+02	0 44149E+02
45	890	0 10000E+01	0 88310E+01	0 92317E+04	0 44822E+02	0 31806E+00	0 10760E+02	0 44468E+02
46	910	0 10000E+01	0 80994E+01	0 84670E+04	0 43644E+02	0 29502E+00	0 10730E+02	0 44763E+02
47	930	0 28000E+01	0 36234E+02	0 37878E+05	0 88780E+02	0 13344E+01	0 10700E+02	0 46097E+02
48	950	0 28000E+01	0 37162E+02	0 38848E+05	0 86578E+02	0 13834E+01	0 10670E+02	0 47480E+02
49	970	0 19000E+01	0 25069E+02	0 26207E+05	0 68578E+02	0 94318E+00	0 10640E+02	0 48424E+02
50	990	0 10000E+01	0 13224E+02	0 00000E+00	0 00000E+00	0 00000E+00	0 10610E+02	0 48424E+02

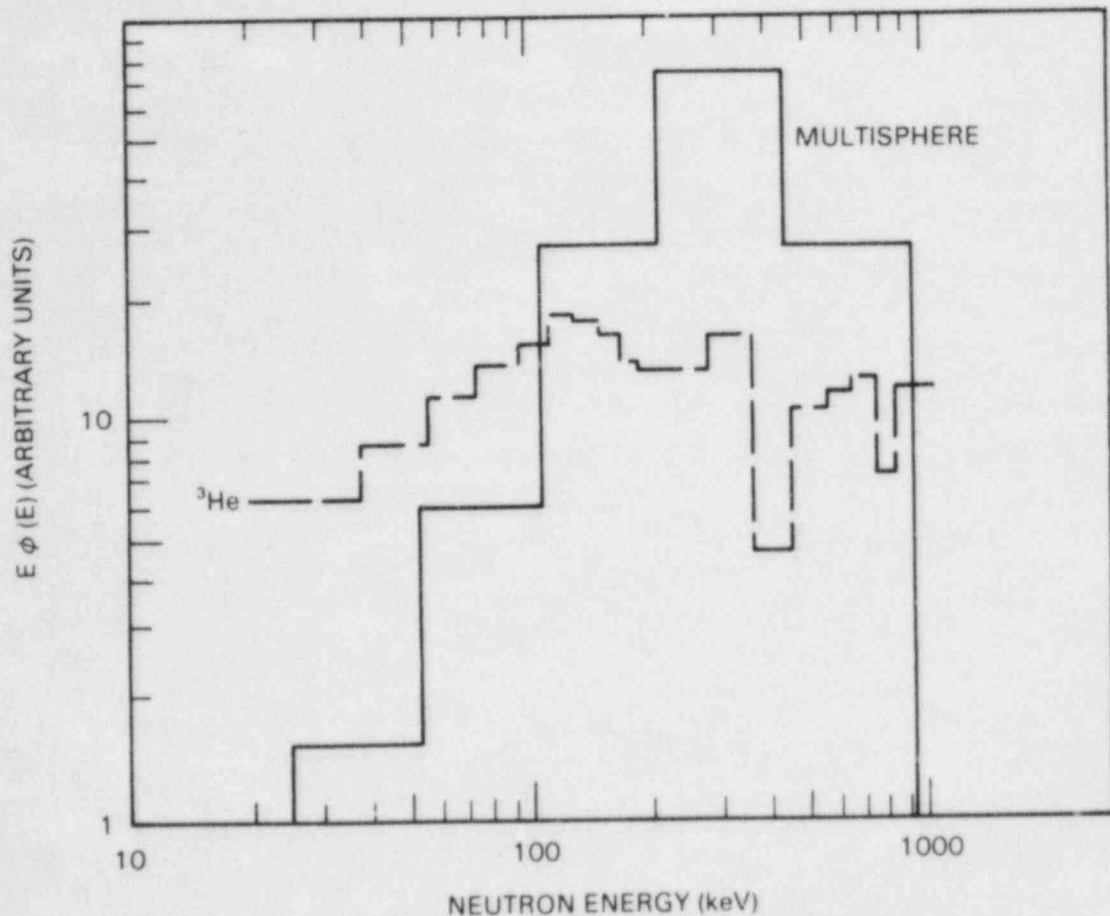


FIGURE 7.5. Fluence Per Unit Lethargy Measured by the  $^3\text{He}$  Spectrometer and Multisphere Spectrometer

### 7.2.2 Reactor Site 6

Measurements were made on the charging floor near the reactor cavity at Site 6. The PNL Snoopy indicated the dose equivalent rate was 50 mrem/hr at locations where the spectrum measurements were made; a PNR-4 supplied by the reactor health physics group indicated a dose equivalent rate of 110 mrem/hr at the same location.

The multisphere spectrometer results are shown in Table 7.3 and displayed graphically in Figure 7.6, which shows the differential neutron flux density ( $\text{n}/\text{cm}^2\text{-sec}$  per energy bin) plotted against the neutron energy. Figure 7.7 displays the fractional dose equivalent rate (mrem/hr per energy bin) as a function of neutron energy. In Figure 7.7 only 72% of the dose equivalent is in Region 3 above 10 keV; this is a "softer" (lower average energy) spectrum than that measured at Site 5.



TABLE 7.3. Results of Multisphere Spectrometer Measurements at Reactor Site 6 Analyzed by the Computer Code SPUNIT

BIN NO	ENERGY (MEV)	FLUX N/CM2-S	* DIFFERENTIAL *		* CUMULATIVE *	
			DOSE (RAD/HR)	DOSE EQUIV. (REM/HR)	DOSE DIST. (RAD/HR)	DOSE EQUIV. (REM/HR)
1	2.57E-07	1.13E+03	2.15E-03	4.58E-03	8.75E-03	4.29E-02
2	5.48E-07	1.96E+02	4.29E-04	8.97E-04	6.60E-03	3.83E-02
3	1.06E-06	1.41E+02	3.13E-04	6.57E-04	6.17E-03	3.74E-02
4	2.25E-06	1.06E+02	2.34E-04	4.96E-04	5.86E-03	3.68E-02
5	4.77E-06	8.01E+01	1.75E-04	3.75E-04	5.63E-03	3.63E-02
6	1.01E-05	6.53E+01	1.41E-04	3.05E-04	5.45E-03	3.59E-02
7	2.14E-05	5.45E+01	1.17E-04	2.49E-04	5.31E-03	3.56E-02
8	4.52E-05	4.90E+01	1.05E-04	2.18E-04	5.19E-03	3.54E-02
9	9.58E-05	4.47E+01	9.48E-05	1.94E-04	5.09E-03	3.51E-02
10	2.03E-04	4.51E+01	9.26E-05	1.88E-04	4.99E-03	3.50E-02
11	4.34E-04	4.89E+01	9.63E-05	1.95E-04	4.90E-03	3.48E-02
12	9.13E-04	5.58E+01	1.05E-04	2.13E-04	4.80E-03	3.46E-02
13	1.92E-03	6.66E+01	1.23E-04	2.49E-04	4.70E-03	3.44E-02
14	4.07E-03	8.28E+01	1.51E-04	3.04E-04	4.57E-03	3.41E-02
15	8.62E-03	1.07E+02	1.93E-04	3.91E-04	4.42E-03	3.38E-02
16	1.82E-02	1.40E+02	2.85E-04	7.85E-04	4.23E-03	3.34E-02
17	3.86E-02	1.92E+02	4.59E-04	1.96E-03	3.95E-03	3.26E-02
18	8.18E-02	2.69E+02	7.61E-04	5.00E-03	3.49E-03	3.07E-02
19	1.67E-01	3.35E+02	1.25E-03	1.07E-02	2.72E-03	2.57E-02
20	3.37E-01	2.19E+02	1.15E-03	1.15E-02	1.47E-03	1.50E-02
21	6.79E-01	3.71E+01	3.00E-04	3.26E-03	3.24E-04	3.50E-03
22	1.39E+00	1.79E+00	2.20E-05	2.16E-04	2.41E-05	2.33E-04
23	2.78E+00	1.35E-01	2.05E-06	1.67E-05	2.13E-06	1.72E-05
24	5.54E+00	3.48E-03	7.25E-08	5.07E-07	7.76E-08	5.45E-07
25	1.12E+01	1.71E-04	4.07E-09	2.81E-08	5.09E-09	3.83E-08
26	2.04E+01	3.41E-09	1.12E-13	7.74E-13	1.03E-09	1.02E-08
TOTAL		3.47E+03	8.75E-03	4.29E-02		

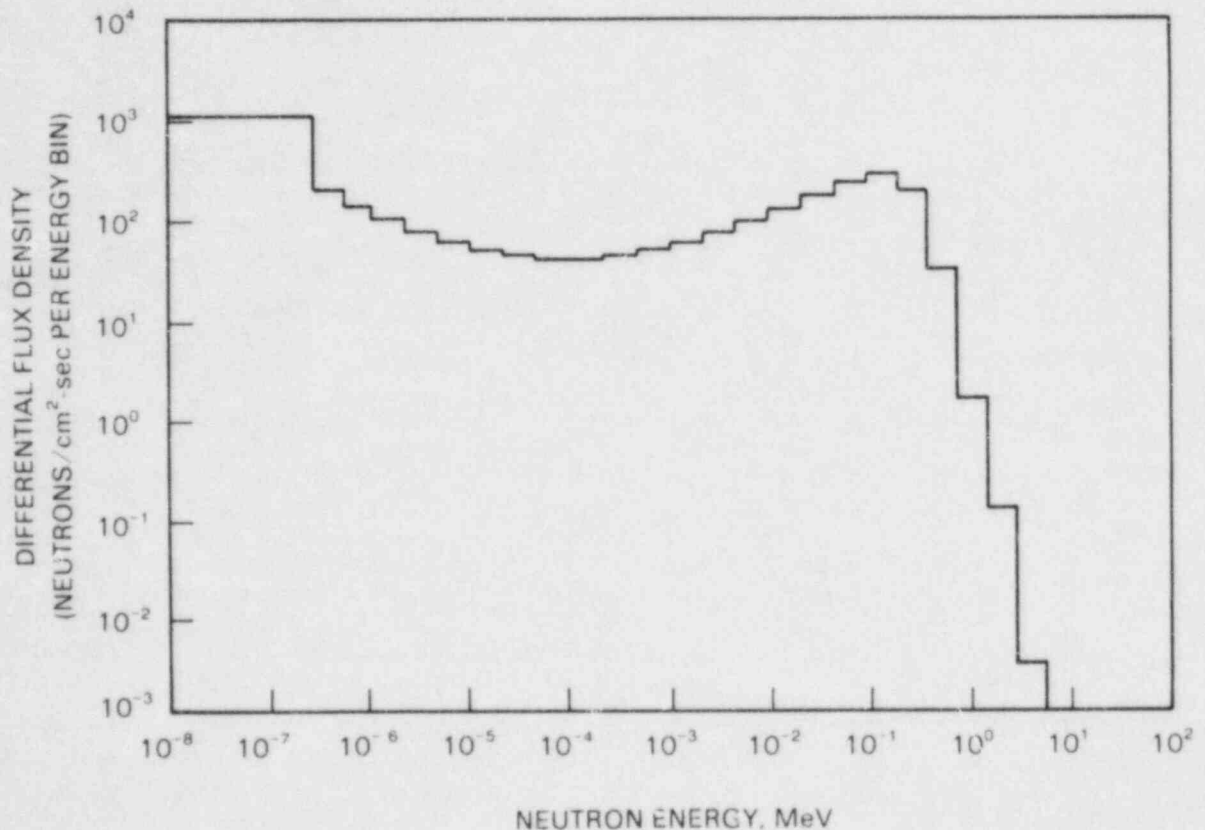


FIGURE 7.6. Differential Neutron Flux Density Calculated from the Multisphere Spectrometer Measurement at Reactor Site 6

The  $^3\text{He}$  spectrometer results calculated by the HESTRIP code are given in Table 7.4. In the energy range between 10 keV and 1 MeV the HESTRIP code calculates that about half of the dose equivalent is produced by neutrons with energies below 300 keV; the SPUNIT code for unfolding multisphere data indicates that about half of the dose equivalent is produced by neutrons with energies below about 200 keV. A plot of the flux per unit lethargy is presented in Figure 7.8. The counting statistics are so poor at higher energies that a plot of flux per unit lethargy may not be correct above about 300 keV. However, the  $^3\text{He}$  results indicate more lower energy neutrons are present than were in the measurements at Site 5, which is consistent with the multisphere spectrometer results. The generic TLD-albedo dosimeter response is calculated to overestimate the dose equivalent by a factor of 20 if exposed in the reactor spectrum and calibrated using a bare  $^{252}\text{Cf}$  source or by a factor of 2.7 if calibrated using a  $^{252}\text{Cf}$  source moderated by 15 cm of deuterium oxide.

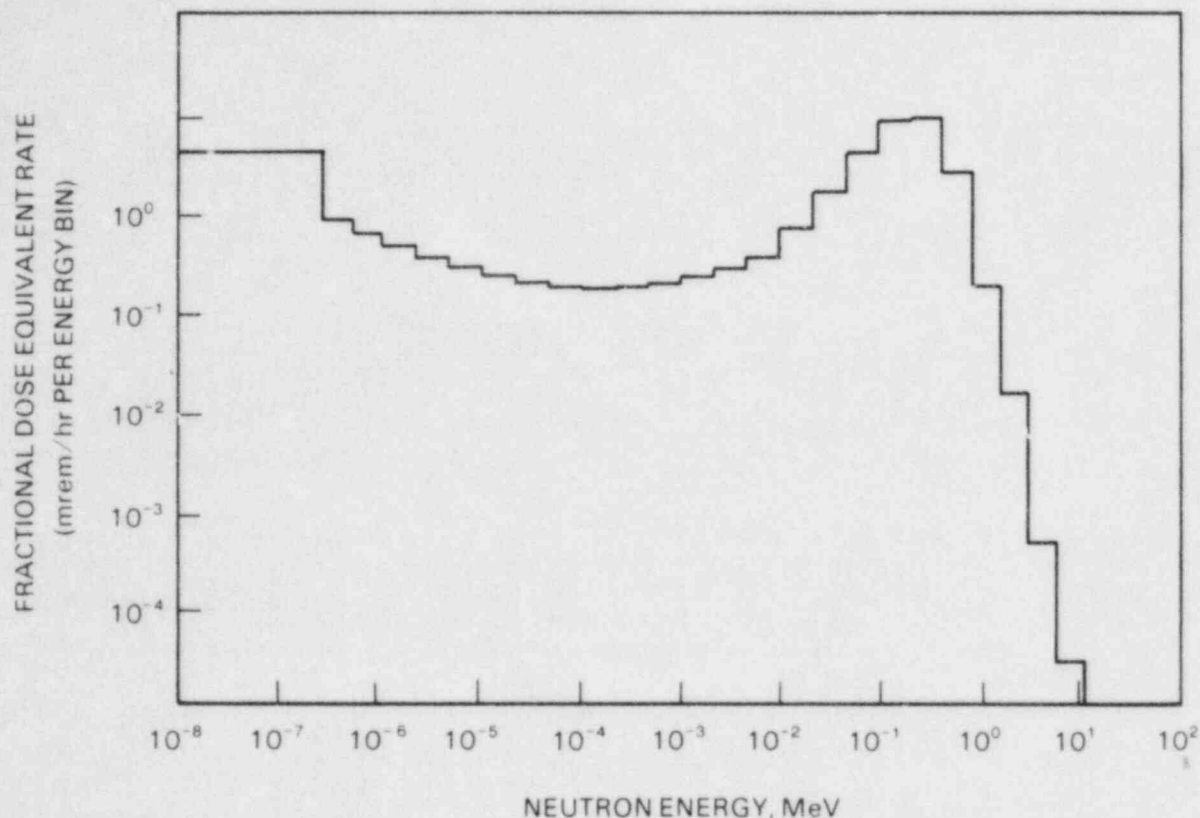


FIGURE 7.7. Fractional Dose Equivalent Rate Calculated from the Multisphere Spectrometer Measurement at Reactor Site 6

Measurements were also made with the cadmium cover over the <sup>3</sup>He proportional counter. Using the formulas from Section 3.2, the dose equivalent rate from thermal neutrons was calculated to be 3.6 mrem/hr by the <sup>3</sup>He proportional counter and 5.5 mrem/hr by the multisphere spectrometer. For neutron energies between 1 eV to 10 keV, the dose equivalent rate was calculated to be 4.0 mrem/hr by the multisphere spectrometer and 7.1 mrem/hr by the <sup>3</sup>He counter, assuming a 1/E energy spectrum.

### 7.2.3 Reactor Site 4

A more complete set of measurements was made at reactor Site 4 at a location near a stairwell on the equipment hatch deck. Measurements were made with the <sup>3</sup>He and multisphere spectrometers, survey meters, and a tissue equivalent proportional counter.

The dose equivalent rate was measured to be 15 mrem/hr using a PNR-4 supplied by the utility. The PNR-4 survey instrument was calibrated using a plutonium-beryllium neutron source. The dose equivalent rate was determined to be 14.9 mrem/hr from tissue equivalent proportional counter (TEPC) measurements using the Rossi algorithm to determine quality factors and linear energy transfer (LET) distributions (Rossi 1968, pp. 70-71). This close agreement is unusual; typically the portable survey instruments overestimate dose equivalent. Unfortunately, the calibrated Snoopy survey meter was not available for measurements.

TABLE 7.4. Results of the <sup>3</sup>He Spectrometer Measurements at Reactor Site 6

ENERGY BIN	AVERAGE ENERGY KEV	UNCORRECTED COUNTS	CORRECTED COUNTS	ABSOLUTE FLUENCE N/CM2	COUNTING UNCERTAINTY N/CM2	DOSE EQUIVALENT (MREM)	QUALITY FACTOR	RUNNING SUM OF DOSE EQUIV (MREM)
1	10	0 50209E+04	0 10747E+05	0 27986E+07	0 22913E+03	0 27765E+01	0 20000E+01	0 27765E+01
2	30	0 82226E+03	0 17054E+04	0 82859E+06	0 94141E+02	0 19461E+01	0 35400E+01	0 47226E+01
3	50	0 32860E+03	0 66638E+03	0 44119E+06	0 60767E+02	0 15469E+01	0 49400E+01	0 62695E+01
4	70	0 18064E+03	0 36262E+03	0 30267E+06	0 46348E+02	0 13817E+01	0 60900E+01	0 76512E+01
5	90	0 11747E+03	0 23887E+03	0 21801E+06	0 38953E+02	0 12121E+01	0 70100E+01	0 88633E+01
6	110	0 83399E+02	0 17005E+03	0 17666E+06	0 34063E+02	0 11624E+01	0 76200E+01	0 10026E+02
7	130	0 54901E+02	0 10872E+03	0 12947E+06	0 28256E+02	0 99020E+00	0 80600E+01	0 11016E+02
8	150	0 38901E+02	0 73362E+02	0 10235E+06	0 24111E+02	0 89037E+00	0 85000E+01	0 11904E+02
9	170	0 34739E+02	0 69886E+02	0 98911E+05	0 24500E+02	0 96312E+00	0 89400E+01	0 12869E+02
10	190	0 29265E+02	0 61864E+02	0 88844E+05	0 24038E+02	0 95622E+00	0 93800E+01	0 13826E+02
11	210	0 19805E+02	0 36318E+02	0 53133E+05	0 19217E+02	0 62579E+00	0 97200E+01	0 14451E+02
12	230	0 20951E+02	0 45607E+02	0 69320E+05	0 22485E+02	0 88612E+00	0 98900E+01	0 15338E+02
13	250	0 17262E+02	0 38427E+02	0 60772E+05	0 21573E+02	0 83742E+00	0 10060E+02	0 16175E+02
14	270	0 12119E+02	0 22867E+02	0 37689E+05	0 17413E+02	0 55660E+00	0 10230E+02	0 16732E+02
15	290	0 13268E+02	0 31481E+02	0 54174E+05	0 21465E+02	0 85323E+00	0 10400E+02	0 17585E+02
16	310	0 10999E+02	0 27286E+02	0 48892E+05	0 21033E+02	0 81771E+00	0 10540E+02	0 18403E+02
17	330	0 63665E+01	0 97198E+01	0 17742E+05	0 13105E+02	0 31391E+00	0 10610E+02	0 18716E+02
18	350	0 83451E+01	0 21749E+02	0 40457E+05	0 20594E+02	0 75474E+00	0 10680E+02	0 19471E+02
19	370	0 43100E+01	0 46150E+01	0 87511E+04	0 99302E+01	0 17163E+00	0 10750E+02	0 19643E+02
20	390	0 59168E+01	0 14813E+02	0 28645E+05	0 18810E+02	0 58909E+00	0 10820E+02	0 20232E+02
21	410	0 40298E+01	0 76087E+01	0 15072E+05	0 14234E+02	0 32422E+00	0 10870E+02	0 20556E+02
22	430	0 19000E+01	0 00000E+00	0 00000E+00	0 86479E+00	0 00000E+00	0 10900E+02	0 20556E+02
23	450	0 19000E+01	0 00000E+00	0 00000E+00	0 93081E+00	0 00000E+00	0 10930E+02	0 20556E+02
24	470	0 44303E+01	0 13820E+02	0 28413E+05	0 22190E+02	0 69119E+00	0 10960E+02	0 21247E+02
25	490	0 28157E+01	0 57533E+01	0 11980E+05	0 11980E+02	0 30257E+00	0 10990E+02	0 21550E+02
26	510	0 10000E+01	0 00000E+00	0 00000E+00	0 81833E+00	0 00000E+00	0 11000E+02	0 21550E+02
27	530	0 19000E+01	0 12607E+01	0 26763E+04	0 77913E+01	0 70899E-01	0 11000E+02	0 21621E+02
28	550	0 19000E+01	0 17800E+01	0 38120E+04	0 97318E+01	0 10290E+00	0 11000E+02	0 21724E+02
29	570	0 19000E+01	0 14856E+01	0 32096E+04	0 93377E+01	0 88222E-01	0 11000E+02	0 21812E+02
30	590	0 46000E+01	0 27299E+02	0 59508E+05	0 42424E+02	0 16645E+01	0 11000E+02	0 23476E+02
31	610	0 10000E+01	0 00000E+00	0 00000E+00	0 76885E+00	0 00000E+00	0 11020E+02	0 23476E+02
32	630	0 19000E+01	0 77497E+01	0 17026E+05	0 25023E+02	0 49235E+00	0 11010E+02	0 23969E+02
33	650	0 10000E+01	0 57515E-01	0 12665E+03	0 21526E+01	0 37207E-02	0 11000E+02	0 23973E+02
34	670	0 10000E+01	0 40530E-01	0 89447E+02	0 18447E+01	0 26686E-02	0 10990E+02	0 23975E+02
35	690	0 19000E+01	0 11068E+02	0 24481E+05	0 34789E+02	0 74133E+00	0 10980E+02	0 24717E+02
36	710	0 10000E+01	0 21903E+01	0 48558E+04	0 16355E+02	0 14919E+00	0 10950E+02	0 24866E+02
37	730	0 10000E+01	0 20627E+01	0 45832E+04	0 16521E+02	0 14281E+00	0 10900E+02	0 25009E+02
38	750	0 19000E+01	0 14177E+02	0 31572E+05	0 45211E+02	0 99736E+00	0 10910E+02	0 26006E+02
39	770	0 19000E+01	0 16720E+02	0 37279E+05	0 51307E+02	0 11934E+01	0 10890E+02	0 27199E+02
40	790	0 10000E+01	0 60953E+01	0 13590E+05	0 13590E+02	0 32428E+02	0 10870E+02	0 27640E+02
41	810	0 10000E+01	0 62904E+01	0 14025E+05	0 34563E+02	0 46068E+00	0 10850E+02	0 28101E+02
42	830	0 19000E+01	0 20993E+02	0 46806E+05	0 64151E+02	0 15566E+01	0 10830E+02	0 29657E+02
43	850	0 10000E+01	0 89454E+01	0 19945E+05	0 42547E+02	0 67132E+00	0 10810E+02	0 30329E+02
44	870	0 10000E+01	0 90831E+01	0 20252E+05	0 43567E+02	0 68974E+00	0 10790E+02	0 31018E+02
45	890	0 19000E+01	0 24486E+02	0 54594E+05	0 72725E+02	0 18809E+01	0 10760E+02	0 32899E+02
46	910	0 10000E+01	0 11961E+02	0 26668E+05	0 51687E+02	0 92922E+00	0 10730E+02	0 33829E+02
47	930	0 10000E+01	0 12117E+02	0 27016E+05	0 50098E+02	0 95175E+00	0 10700E+02	0 34780E+02
48	950	0 10000E+01	0 12259E+02	0 27333E+05	0 48594E+02	0 97336E+00	0 10670E+02	0 35754E+02
49	970	0 10000E+01	0 12459E+02	0 27777E+05	0 47301E+02	0 99970E+00	0 10640E+02	0 36753E+02
50	990	0 10000E+01	0 12955E+02	0 00000E+00	0 00000E+00	0 00000E+00	0 10610E+02	0 36753E+02

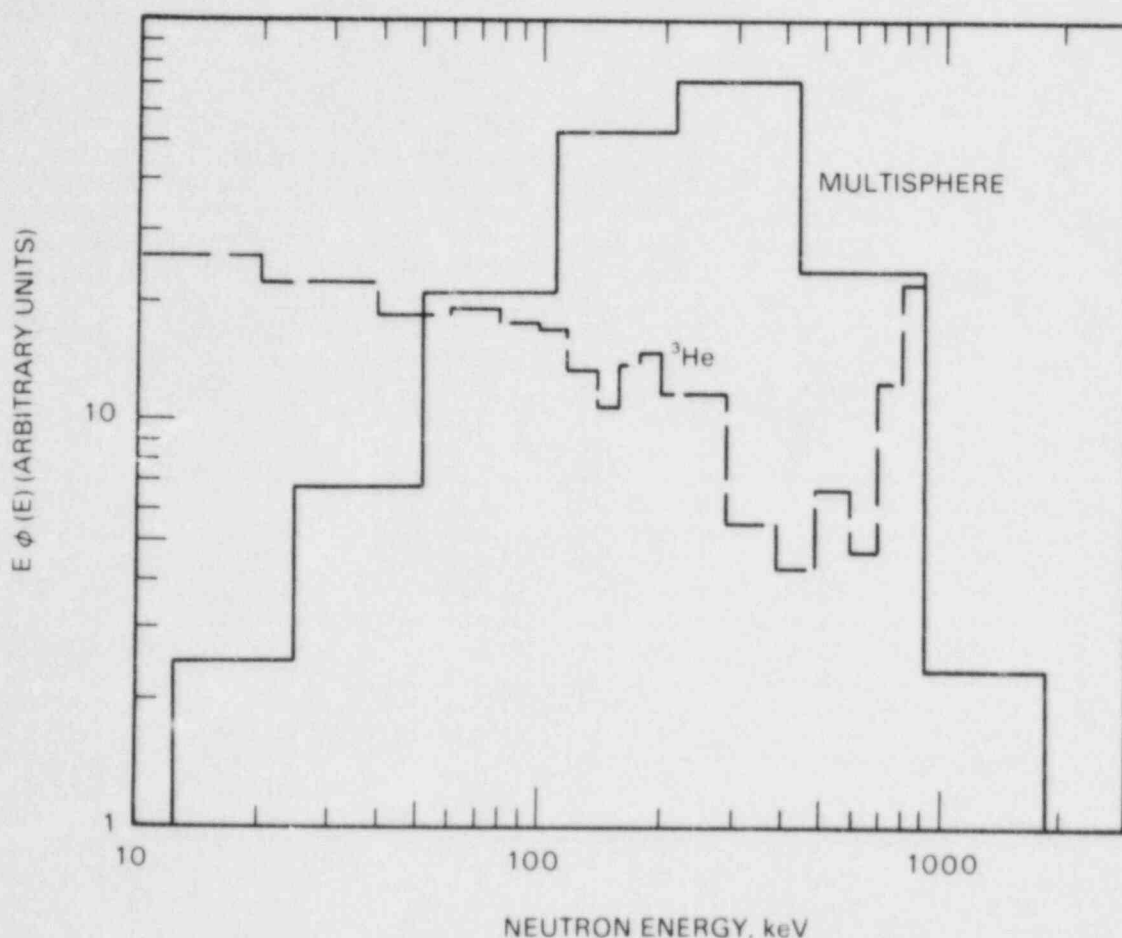


FIGURE 7.8. Flux Per Unit lethargy as a Function of Neutron Energy for the  $^3\text{He}$  Measurements at Reactor Site 6

The results of the multisphere measurements are shown in Table 7.5 for data analyzed with the computer code SPUNIT (Brackenbush and Scherpelz 1983). These same data were also analyzed by the computer code YOGI (Johnson and Gorbics 1981); the results are shown in Table 7.6. The total dose equivalent rate calculated by these two codes agrees closely (12.2 and 11.5 mrem/hr), but the differential quantities vary considerably. Using the SPUNIT results, the differential neutron flux density is plotted in Figure 7.9 and the fraction dose equivalent rate distribution is plotted in Figure 7.10. These spectra have more low-energy neutrons than the previous measurements.

Measurements were also made with the  $^3\text{He}$  spectrometer using a proportional counter that originally contained  $^3\text{He}$  at a partial pressure of 4 psia (0.27 atmosphere) and argon at a partial pressure of 26 psia (1.8 atmospheres). Using the response function for this gas filling, the computer code HESTRIP calculated the dose equivalent rate to differ from the other measured values by a factor of two. By comparing the count rate from this tube

TABLE 7.5. Results of Multisphere Spectrometer Measurements at Reactor Site 4  
Analyzed by the Computer Code SPUNIT

BIN NO.	ENERGY (MEV)	FLUX N/CM2-S	* DIFFERENTIAL *		* CUMULATIVE *	
			DOSE (RAD/HR)	DOSE EQUIV. (REM/HR)	DOSE DIST. (RAD/HR)	DOSE EQUIV. (REM/HR)
1	2.57E-07	7.22E+02	1.37E-03	2.91E-03	3.90E-03	1.22E-02
2	5.48E-07	8.23E+01	1.80E-04	3.77E-04	2.54E-03	9.32E-03
3	1.04E-06	6.21E+01	1.38E-04	2.90E-04	2.36E-03	8.95E-03
4	2.25E-06	5.20E+01	1.15E-04	2.43E-04	2.22E-03	8.66E-03
5	4.77E-06	4.09E+01	8.93E-05	1.91E-04	2.10E-03	8.41E-03
6	1.01E-05	3.62E+01	7.82E-05	1.69E-04	2.01E-03	8.22E-03
7	2.14E-05	3.32E+01	7.13E-05	1.52E-04	1.93E-03	8.05E-03
8	4.52E-05	3.03E+01	6.48E-05	1.35E-04	1.86E-03	7.90E-03
9	9.58E-05	3.31E+01	7.03E-05	1.43E-04	1.80E-03	7.77E-03
10	2.03E-04	3.63E+01	7.45E-05	1.51E-04	1.73E-03	7.62E-03
11	4.34E-04	4.19E+01	8.24E-05	1.67E-04	1.65E-03	7.47E-03
12	9.13E-04	4.93E+01	9.33E-05	1.88E-04	1.57E-03	7.30E-03
13	1.92E-03	5.92E+01	1.10E-04	2.21E-04	1.48E-03	7.12E-03
14	4.07E-03	7.14E+01	1.31E-04	2.62E-04	1.37E-03	6.89E-03
15	8.62E-03	8.62E+01	1.56E-04	3.16E-04	1.24E-03	6.63E-03
16	1.82E-02	1.02E+02	2.06E-04	5.69E-04	1.08E-03	6.32E-03
17	3.86E-02	1.15E+02	2.74E-04	1.17E-03	8.75E-04	5.75E-03
18	8.18E-02	1.11E+02	3.12E-04	2.05E-03	6.01E-04	4.58E-03
19	1.67E-01	6.42E+01	2.40E-04	2.04E-03	2.88E-04	2.53E-03
20	3.37E-01	9.05E+00	4.74E-05	4.76E-04	4.84E-05	4.86E-04
21	6.79E-01	1.21E-01	9.77E-07	1.06E-05	9.81E-07	1.07E-05
22	1.39E+00	2.91E-04	3.57E-09	3.52E-08	4.19E-09	3.67E-08
23	2.78E+00	2.52E-06	3.83E-11	3.12E-10	6.13E-10	1.54E-09
24	5.54E+00	1.30E-08	2.70E-13	1.89E-12	5.75E-10	1.23E-09
25	1.12E+01	2.32E-10	5.53E-15	3.82E-14	5.75E-10	1.23E-09
26	2.04E+01	3.67E-15	1.20E-19	8.32E-19	5.75E-10	1.23E-09
TOTAL		1.84E+03	3.90E-03	1.22E-02		

TABLE 7.6. Results of Multisphere Spectrometer Measurements at Reactor Site 4  
Analyzed by the Computer Code YOGI

BIN NO.	ENERGY (MEV)	FLUX N/CM <sup>2</sup> -S	* DIFFERENTIAL *		* CUMULATIVE *	
			DOSE (RAD/HR)	DOSE EQUIV. (REM/HR)	DOSE DIST. (RAD/HR)	DOSE EQUIV. (REM/HR)
1	2.57E-07	7.52E+02	1.42E-03	3.04E-03	3.94E-03	1.15E-02
2	5.48E-07	2.38E+01	5.22E-05	1.09E-04	2.52E-03	8.42E-03
3	1.06E-06	3.61E+01	8.01E-05	1.68E-04	2.46E-03	8.31E-03
4	2.25E-06	3.98E+01	8.80E-05	1.86E-04	2.38E-03	8.15E-03
5	4.77E-06	4.77E+01	1.04E-04	2.23E-04	2.30E-03	7.96E-03
6	1.01E-05	6.13E+01	1.33E-04	2.86E-04	2.19E-03	7.74E-03
7	2.14E-05	7.26E+01	1.56E-04	3.32E-04	2.06E-03	7.45E-03
8	4.52E-05	7.63E+01	1.63E-04	3.40E-04	1.90E-03	7.12E-03
9	9.58E-05	8.19E+01	1.74E-04	3.55E-04	1.74E-03	6.78E-03
10	2.03E-04	8.18E+01	1.68E-04	3.41E-04	1.57E-03	6.42E-03
11	4.34E-04	8.37E+01	1.65E-04	3.33E-04	1.40E-03	6.08E-03
12	9.13E-04	8.00E+01	1.51E-04	3.06E-04	1.23E-03	5.75E-03
13	1.92E-03	8.19E+01	1.52E-04	3.06E-04	1.08E-03	5.44E-03
14	4.07E-03	8.18E+01	1.50E-04	3.01E-04	9.31E-04	5.14E-03
15	8.62E-03	8.19E+01	1.48E-04	3.00E-04	7.81E-04	4.84E-03
16	1.82E-02	5.71E+01	1.16E-04	3.19E-04	6.33E-04	4.54E-03
17	3.86E-02	3.26E+01	7.79E-05	3.32E-04	5.17E-04	4.22E-03
18	8.18E-02	1.74E+01	4.91E-05	3.22E-04	4.39E-04	3.86E-03
19	1.67E-01	1.05E+01	3.94E-05	3.35E-04	3.90E-04	3.56E-03
20	3.37E-01	8.82E+00	4.62E-05	4.63E-04	3.51E-04	3.23E-03
21	6.79E-01	7.50E+00	6.06E-05	6.60E-04	3.05E-04	2.76E-03
22	1.39E+00	7.77E+00	9.52E-05	9.38E-04	2.44E-04	2.10E-03
23	2.78E+00	7.25E+00	1.10E-04	8.97E-04	1.49E-04	1.17E-03
24	5.54E+00	1.50E+00	3.12E-05	2.18E-04	3.87E-05	2.70E-04
25	1.12E+01	3.00E-01	7.16E-06	4.94E-05	7.44E-06	5.14E-05
26	2.04E+01	8.51E-03	2.79E-07	1.93E-06	2.80E-07	1.93E-06
TOTAL		1.83E+03	3.94E-03	1.15E-02		

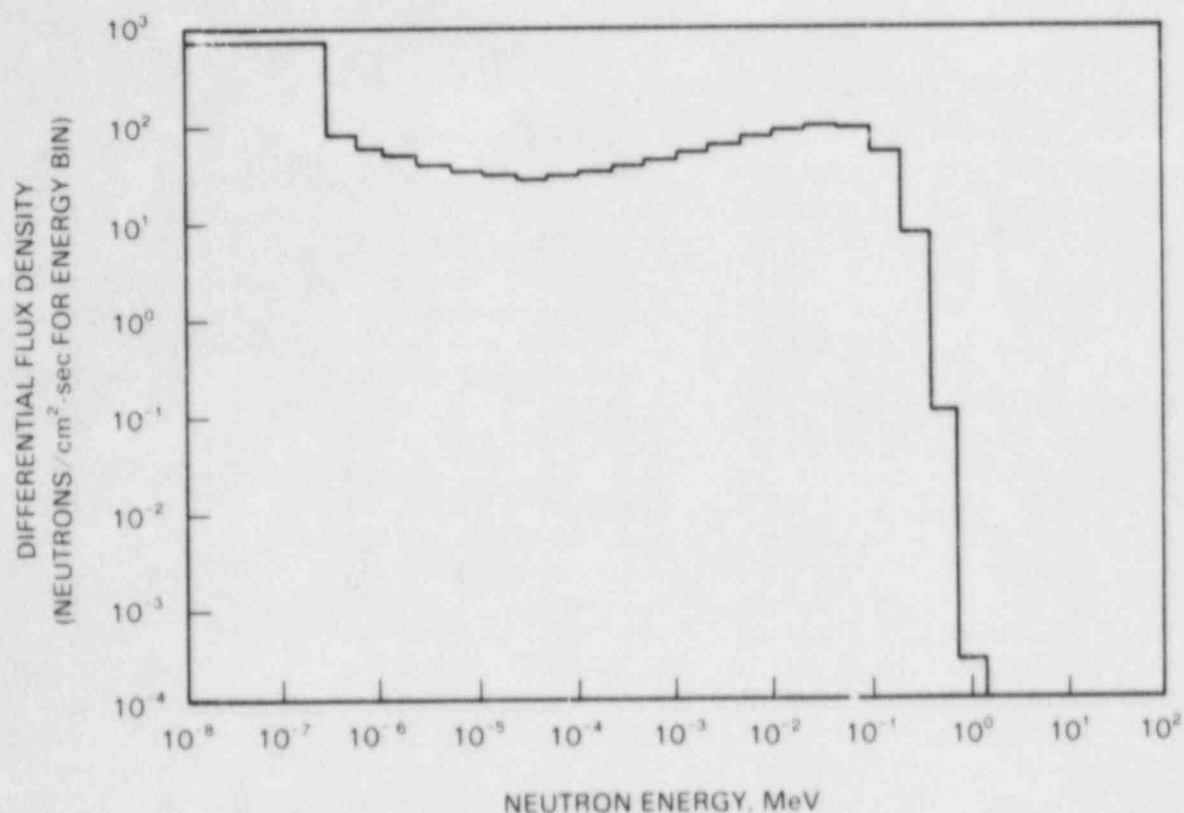


FIGURE 7.9. Differential Neutron Flux Density Calculated from the Multisphere Spectrometer Measurement at Reactor Site 4

with another  $^3\text{He}$  tube in the same neutron flux, the authors discovered that the  $^3\text{He}$  proportional counter had developed a slow leak. Over a 2-year period, half of the  $^3\text{He}$  had leaked away. Using a partial pressure of 2 psia instead of 4 psi gives the dose equivalent rates shown in Table 7.7 for Site 4. The response of a generic Hanford TLD-albedo dosimeter was calculated to overestimate dose equivalent by a factor of 18 when exposed in the reactor spectrum and calibrated using a  $^{252}\text{Cf}$  source in a low scatter room or by a factor of 2.5 if calibrated using a  $^{252}\text{Cf}$  source moderated by 15 cm of deuterium oxide.

The flux per unit lethargy calculated from the  $^3\text{He}$  spectrometer measurements is shown in Figure 7.11. The spectrum at Site 4 contains more low-energy neutrons than the other two sites; this finding is consistent with the multisphere spectrometer results. Measurements with and without a cadmium cover over the  $^3\text{He}$  proportional counter were made to estimate the number of thermal and intermediate energy neutrons. Using the formulas from Section 3.2, the dose equivalent rate from thermal neutrons was calculated to be 2.7 mrem/hr. Assuming a  $1/E$  spectrum, the dose equivalent rate was calculated to be 7 mrem/hr in the energy range from 1 eV to 10 keV. The dose equivalent from intermediate energy neutrons calculated from the assumed  $1/E$  spectrum is considerably higher than that calculated by the multisphere spectrometer, as shown in Table 7.7.



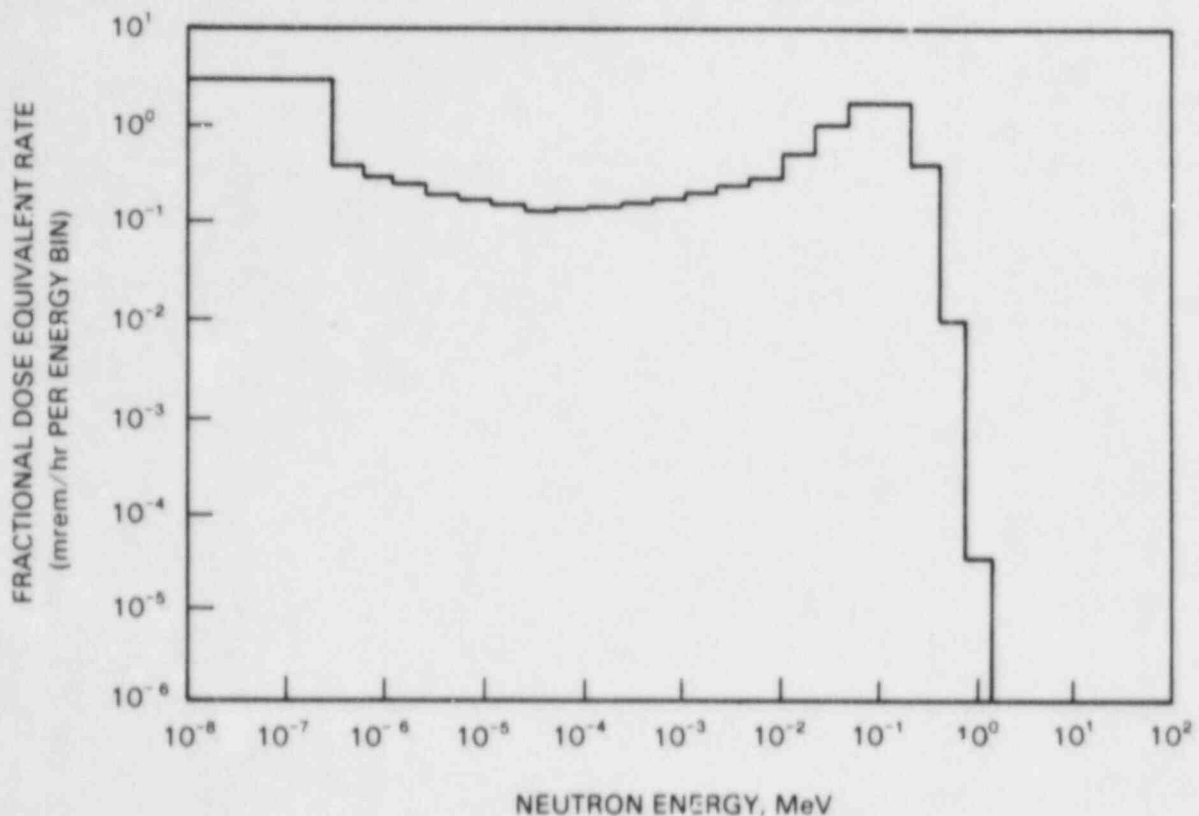


FIGURE 7.10. Fractional Dose Equivalent Rate Calculated from the Multisphere Spectrometer Measurement at Reactor Site 4

### 7.3 REACTOR MEASUREMENT SUMMARY

The dose equivalent rates from the reactor site measured data are summarized in Table 7.7. The data include the results of the <sup>3</sup>He spectrometer analyzed by the HESTRIP computer code and the multisphere spectrometer analyzed by two different codes, YOGI and SPUNIT. The first three columns indicate the dose equivalent rate contribution from each of the energy regions described in Appendix A; the fourth column gives the total dose equivalent rate over all neutron energies. The numbers in parentheses are the percentage of the dose equivalent for each energy region, so one can determine the relative important of neutrons in each energy range. The largest contribution to dose equivalent is from neutrons with energies greater than 10 keV; in this range of energies the <sup>3</sup>He and multisphere spectrometers agree within about 35% for the three examples shown in Table 7.7. The largest differences occur in the energy range of 1 eV to 10 keV, where the <sup>3</sup>He spectrometer indicates a much larger contribution to dose equivalent than calculated by the multisphere spectrometer. For the <sup>3</sup>He spectrometer, dose equivalent rates are calculated from measured count rates with and without a cadmium cover over the <sup>3</sup>He proportional counter. The assumption that the intermediate energy neutrons have a 1/E dependence is apparently not always valid over the energy range of 1 eV to 10 keV.

TABLE 7.7. Summary of Dose Equivalent Rate Measurements Inside Containment of Commercial Nuclear Power Plants

	Dose Equivalent Rate (mrem/hr)				Energy Correction Factor for Hanford Multipurpose Dosimeter Calibrated Using:	
	Thermal	1 eV-10 keV	>10 keV	Total	Unmoderated Cf	D <sub>2</sub> O Moderated Cf
Reactor Site 5						
HESTRIP ( <sup>3</sup> He)	2.4 (6%) (a)	4.4 (12%)	30.8 (82%)	37.5	9.8	1.3
SPUNIT (multisphere)	2.1 (8%)	1.3 (5%)	23.0 (87%)	26.3		
Snoopy Survey Meter				55		
Reactor Site 6						
HESTRIP ( <sup>3</sup> He)	3.6 (8%)	7.1 (15%)	36.1 (77%)	46.8	20	2.7
SPUNIT (multisphere)	5.5 (13%)	4.03 (9%)	33.4 (78%)	42.9		
Snoopy Survey Meter				50		
PNR-4 Survey Meter				110		
Reactor Site 4						
HESTRIP ( <sup>3</sup> He)	2.7 (17%)	7 (44%)	6.3 (40%)	16	18	2.5
SPUNIT (multisphere)	3.3 (27%)	2.6 (21%)	6.3 (52%)	12.2		
YOGI (multisphere)	3.1 (27%)	3.8 (33%)	4.5 (39%)	11.5		
TEPC (Rossi algorithm)				14.9		
PNR-4 Survey Meter				15		

(a) Number in parentheses is the percentage of the total dose equivalent.

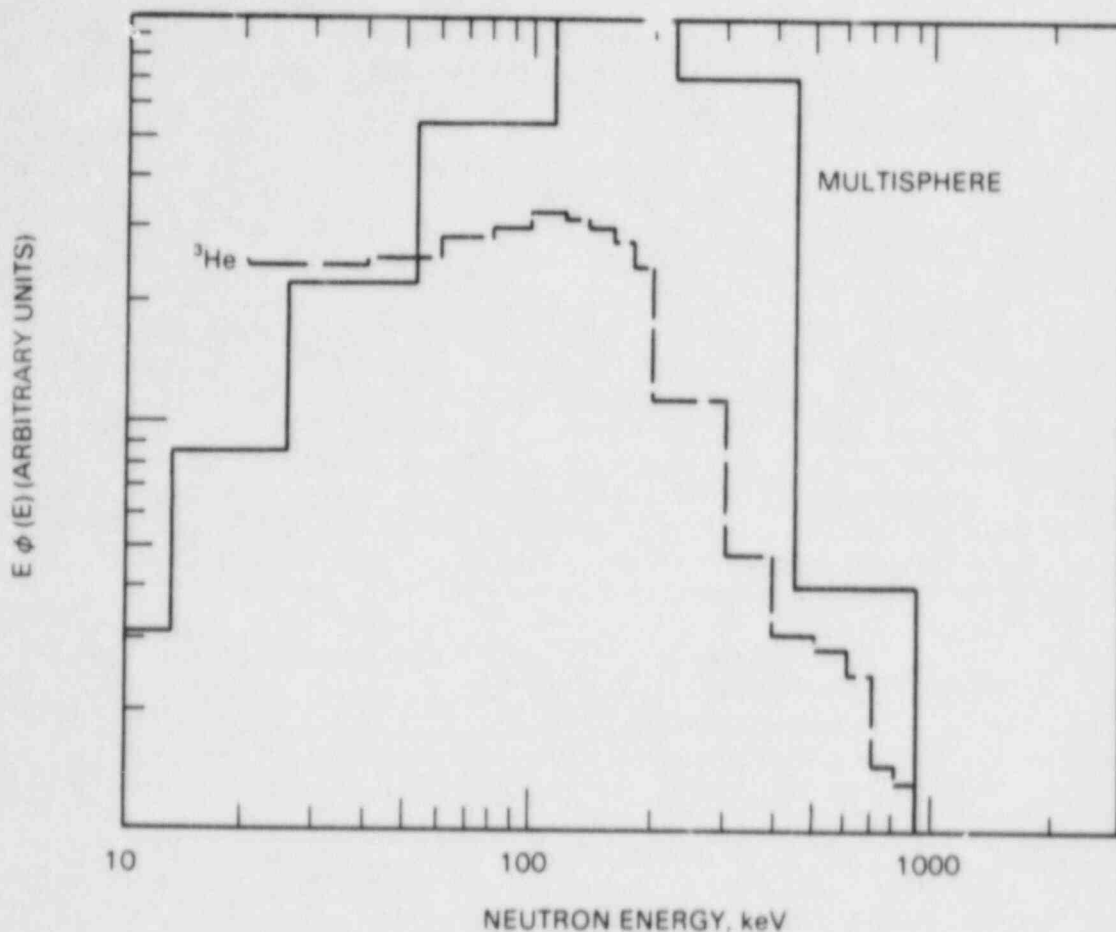


FIGURE 7.11. Flux Per Unit lethargy as a Function of Neutron Energy for the  $^3\text{He}$  Spectrometer Measurement at Reactor Site 4

The fourth column in Table 7.7 lists the total dose equivalent determined by the  $^3\text{He}$  and multisphere spectrometers and by Snoopy and PNR-4 portable survey instruments and by a tissue equivalent proportional counter (TEPC). There is reasonably good agreement between the dose equivalent rates calculated from the  $^3\text{He}$  spectrometer compared to those obtained with the multisphere spectrometer and the tissue equivalent proportional counter. The  $^3\text{He}$  spectrometer results average about 28% higher than the multisphere results. As one might expect, the portable survey instrument results average about 50% higher than those calculated by the  $^3\text{He}$  spectrometer. Moderator based instruments usually overestimate dose equivalent when exposed to low energy neutrons well below 1 MeV (Cosack and Lesiecki 1981). The large variation between the PNL Snoopy and the PNR-4 supplied by the utility at reactor Site 6 is probably due to calibration differences.

The last two columns give an energy correction factor for a "generic" TLD-albedo dosimeter (the Hanford multipurpose dosimeter) calibrated using a bare  $^{252}\text{Cf}$  source and a  $^{252}\text{Cf}$  source moderated with 15 cm of deuterium oxide.

The indicated response should be divided by this factor to obtain the true dose equivalent. The values are calculated specifically for the Hanford TLD-albedo dosimeter and may be only generally indicative of the correction factors for other types of TLD-albedo dosimeters used in commercial nuclear power plants. Reactor Sites 6 and 4 have a lower energy spectrum and thus have larger correction factors than reactor Site 5.

#### 7.4 DISCUSSION

There is reasonable agreement between dose equivalents measured by the  $^3\text{He}$  and multisphere spectrometers at the three PWR sites. These measurements were made with the more complex electronic equipment using pulse shape discrimination in conjunction with a boron carbide shield to absorb neutrons below about 10 keV to reduce pulse pile-up. Although the dose equivalent rates appear to be correct, the differential neutron energy spectrum is of questionable accuracy, especially in the region of 10 keV to 50 keV where there is considerable scattering introduced by the boron carbide and the possibility of pulse pile-up from gamma rays.

Better accuracy could have been achieved using the less complex electronics associated with the pulser technique to estimate pulse pile-up. If pulse pile-up does occur, the technique described in Section 5.2.1 may be used. However, it is much better to eliminate the pulse pile-up problem altogether. In the boron carbide absorber slow neutrons are efficiently absorbed by  $^{10}\text{B}$ , but additional slow neutrons are generated by downscatter from higher energies. The samarium oxide absorber is more effective, because neutrons can lose very little energy from scattering reactions. Pulse pile-up problems can be almost eliminated by:

- using a samarium oxide filter
- using a less sensitive  $^3\text{He}$  proportional counter
- making longer measurements (several hours or overnight) at lower dose equivalent rates.

## 8.0 RECOMMENDATIONS

Personnel at commercial nuclear power plants enter containment to perform inspections and maintenance while the reactor is operating and are thus exposed to neutrons. The TLD-albedo neutron dosimeters used to monitor dose equivalent are energy sensitive as demonstrated in NUREG/CR-2956. The interpretation of dosimeter results may overestimate dose equivalent by as much as a factor of 20 (NUREG/CR-1769) unless precautions are taken to correct for this energy dependence. Also, commercially available portable survey instruments based upon moderator principles overestimate dose equivalent (Cosack and Lesiecki 1981) when exposed to low energy neutrons (below 1 MeV) in reactor containment. Typically, the moderator-based instruments overestimate dose equivalent by factors of 2 when compared with multisphere spectrometer and tissue equivalent proportional counter measurements in containment (NUREG/CR-1769). For these reasons the following general recommendations are made:

1. Neutron energy spectrum measurements should be made at least once at representative locations where workers are exposed to neutrons. This will allow corrections to be made for the energy dependence of TLD-albedo dosimeters as well as portable survey instruments. The energy dependence of available TLD-albedo neutron dosimeters is given in the Final Report of Subtask B: Dosimeter Response (NUREG/CR-2956); some information on the energy response of commercially available neutron survey instruments is given by Cosack and Lesiecki (1981).
2. Because neutron energy spectrum measurements are complex and errors are possible, several independent measurements should be made. As a minimum, it is suggested that the dose equivalents calculated by spectrum measurements be compared to dose equivalents measured by calibrated portable survey instruments such as a PNR-4 or Snoopy. Survey instruments calibrated with unmoderated californium, plutonium-beryllium or americium-beryllium sources should indicate higher dose equivalents than those measured by spectrometers. Comparison between the results obtained by two different types of neutron energy spectrometers is desirable.
3. Several neutron dosimeters should be exposed on water phantoms at locations where the neutron flux and dose equivalent rates have been measured using a neutron energy spectrometer. Also, measurements should be made with the portable neutron survey instruments used at the site. This will help verify the accuracy of the calibration factors used to evaluate the TLD-albedo neutron dosimeters and portable survey instruments.
4. As discussed in Section 2.0, four types of neutron energy spectrometers may be useful for energy spectrum measurements inside commercial nuclear power plants:

- multisphere or Bonner sphere spectrometers
- activation foils
- hydrogen and/or methane filled proton-recoil proportional counters
- $^3\text{He}$  proportional counters.

No single type of spectrometer offers the ideal combination of accuracy, ease of use and simplicity of data analysis. The multisphere spectrometer is the easiest to use, but lacks resolution and accuracy, especially at higher neutron energies. The other spectrometers are considerably more complex and difficult to use, but have better resolution and accuracy. The  $^3\text{He}$  spectrometer offers a compromise between the level of operational difficulty and accuracy of the measured spectra.

With regard to the  $^3\text{He}$  spectrometer system described in this report, eight specific recommendations are offered.

1. Several months may be required to procure, assemble, test, make measurements, and analyze the data from a  $^3\text{He}$  spectrometer. Use of the  $^3\text{He}$  spectrometer should be attempted only by someone skilled in assembling nuclear counting equipment who has the time to commit to making the spectral measurements. Operational health physics staff at many reactors are often too busy with day-to-day problems to devote enough time to the project; corporate health physics staff or outside contractors may be better prepared to commit the necessary time.
2. In using the  $^3\text{He}$  spectrometer to measure reactor spectra, a great deal of care must be taken in setting up the spectrometer, collecting data, and interpreting the results. Pulse pile-up problems can easily lead to errors in determining the spectrum between 20 keV and 700 keV.
3. Because the  $^3\text{He}(n,p)\text{T}$  cross section is inversely proportional to the neutron velocity for neutron energies below about 10 keV, the  $^3\text{He}$  spectrometer is very sensitive to low-energy neutrons, which produce a large "epithermal" peak in the raw data from the  $^3\text{He}$  proportional counter. A neutron absorber must be used to suppress the number of neutrons with energies below 10 keV. It is recommended that 1 to 3 mm of samarium (or an equivalent thickness of samarium oxide) be used. A 1-cm thick boron carbide shield could also be used, but neutrons will be scattered by the low atom number material. These shields are necessary to prevent pulse pile-up from obscuring data in the 20- to 700-keV energy range.
4. A 0.3-cm (1/8-in.) lead shield should cover the  $^3\text{He}$  proportional counter to help prevent pulse pile-up from gamma rays. The gamma

ray pile-up problem was not fully appreciated when the first reactor measurements were taken during this study.

5. One-inch diameter cylindrical  $^3\text{He}$  proportional counters filled with 2 to 5% of  $^3\text{He}$  in argon at 2 to 4 atmospheres total pressure have better resolution than other commercially available proportional counters with different gas fillings or sizes. Measurements should be made for long periods (preferably overnight) in low-level neutron fields below about 50 mrem/hr (0.5 millisievert/hr). Higher  $^3\text{He}$  fillings and higher dose equivalent rates give more pulse pile-up and reduced accuracy.
6. If measurements are made with the  $^3\text{He}$  spectrometer in neutron fields of tens to hundreds of millirem/hr (0.1 to 1 millisievert/hr), there will undoubtedly be some pulse pile-up. The technique of using a precision pulser is recommended to estimate the amount of pulse pile-up. It is much simpler to use a less sensitive tube and make measurements in lower dose rate areas than it is to attempt to subtract out erroneous data for pulse pile-up.
7. Only an approximate estimate of the neutron energy spectrum can be obtained by covering the  $^3\text{He}$  proportional counter with cadmium and assuming the differential neutron flux density varies as  $1/\sqrt{E}$  from 1 eV to 10 keV. A technique to improve accuracy by making measurements with additional neutron absorbers to selectively absorb neutrons in various portions of this energy range was suggested in this report. More work is necessary to refine this technique.
8. Of the two  $^3\text{He}$  spectrometer systems described in this report, the one employing a pulser technique to estimate pulse pile-up is recommended because of its greater simplicity. The system using a pulse shape analysis technique requires more skill to operate.

## REFERENCES

- Anderson, H. H., and J. F. Ziegler. 1977. The Stopping and Ranges of Ions in Matter, Vol. 3. Pergamon Press, New York.
- Alsmiller, R. G., Jr., and J. Barish. 1974. "The Calculated Response of  $^6\text{LiF}$  Albedo Dosimeters to Neutrons With Energies  $\leq 400$  MeV." Health Phys. 26, 13-28.
- ANSI/ANS-6.1.1. 1977. "American National Standard Neutron and Gamma-Ray Flux-to-Dose-Rate Factors." American Nuclear Society, La Grange Park, Illinois.
- Bennett, E. F., and T. J. Yule. 1971. Techniques and Analyses of Fast-Reactor Neutron Spectroscopy with Proton-Recoil Proportional Counters. ANL-7703, Argonne National Laboratory, Argonne, Illinois.
- Brackenbush, L. W., and R. I. Scherpelz. 1983. "SPUNIT, A Computer Code for Multisphere Unfolding." PNL-SA-11645, Pacific Northwest Laboratory, Richland, Washington.
- Brackenbush, L. W., D. E. Hadlock, M. A. Parkhurst and L. G. Faust. 1983. "A Method to Improve the Evaluation of a Combination Track Etch Dosimeter/Spectrometer." PNL-SA-11213, Pacific Northwest Laboratory, Richland, Washington.
- Brackenbush, L. W., W. D. Reece and J. E. Tanner. 1983. A Simple Way to Determine the Response of  $^3\text{He}$  Neutron Detectors. PNL-SA-11076, Pacific Northwest Laboratory, Richland, Washington.
- Bramblett, R. L., R. I. Ewing and T. W. Bonner. 1974. "A New Type of Neutron Spectrometer." Nuclear Instrumentation and Methods, 9, 1.
- Cosack, M., and H. Lesiecki. 1981. "Dependence of the Response of Eight Neutron Dose Equivalent Survey Meters with Regard to the Energy and Direction of Incident Neutrons." G. Burger and H. G. Ebert, eds. Proceedings of Fourth Symposium on Neutron Dosimetry. Office for Official Publication of the European Communities, Luxembourg.
- Doroshenko, J. J., S. N. Kraitov, T. V. Kuznetsova, K. K. Kushnereva and E. S. Leonov. 1977. "New Methods for Measuring Neutron Spectra with Energy from 0.4 eV to 10 MeV by Track and Activation Detectors." Nuclear Technology, 33, 296-304.
- Evans, A. E., Jr. 1981. Response of a  $^3\text{He}$  Neutron Spectrometer to 2- and 3-MeV Neutrons. LA-UR-81-160, Los Alamos Scientific Laboratory, Los Alamos, New Mexico.
- Glasstone, S., and A. Sesonske. 1963. Nuclear Reactor Engineering, 1st ed., D. Van Nostrand Co., Princeton, New Jersey.



- Hankins, D. E. 1972. Factors Affecting the Design of Albedo-Neutron Dosimeters Containing Lithium Fluoride Thermoluminescent Dosimeters. LA-4832, Los Alamos Scientific Laboratory, Los Alamos, New Mexico.
- Ing, H., and S. Makra. 1978. "Compendium on Neutron Spectra in Criticality Accident Dosimeter," Technical Report Series 180, International Atomic Energy Agency, Vienna.
- Johnson, T. L., and S. G. Gorbics. 1981. "An Iterative Perturbation Method for Unfolding Neutron Spectra from Bonner Sphere Data." Presented at the Health Physics Society Annual Meeting, Louisville, Kentucky, June 1981.
- NUREG/CR-1769. 1981. Neutron Dosimetry at Commercial Nuclear Plants, Final Report of Subtask A: Reactor Containment Measurements. U.S. Nuclear Regulatory Commission, Washington, D.C.
- NUREG/CR-2956. 1983. Neutron Dosimetry at Commercial Nuclear Plants. Final Report of Subtask B: Dosimeter Response. U.S. Nuclear Regulatory Commission, Washington, D.C.
- Rossi, H. H. 1968. "Microscopic Energy Distribution in Irradiated Matter." In Radiation Dosimetry, Vol. 1 (2nd ed.). F. H. Attix and W. C. Roesch, eds. Academic Press, New York.
- Routti, J. T., and J. V. Sandberg. 1978. General Purpose Unfolding Program LOUHI 78 with Linear and Non-Linear Regularization. Report TKK-A359, Helsinki University of Technology, Department of Technical Physics, Otaniemi, Finland.
- Schlapper, G. A., R. D. Neff, D. R. Davis and P. S. Sandel. 1983. "Measurement of Routinely Encountered Neutron Doses in Research Facilities." Radiation Protection Management, October, 77-83.
- Schwartz, R. B. 1977. "Calibration and Use of Filtered Beams." In Proceedings of the International Specialists Symposium on Neutron Standards and Applications, held at the National Bureau of Standards, Gaithersburg, Maryland, March 28-31, 1977. National Bureau of Standards Special Publication 493.
- Stewart, L. 1974. "The  ${}^3\text{He}(n,p)\text{T}$ ,  ${}^6\text{Li}(n,\alpha)\text{T}$  and  ${}^{10}\text{B}(n,\alpha)$  Standard Cross-Sections," in Neutron Standard Reference Data, International Atomic Energy Agency, Vienna.

## APPENDIX A

### ENERGY SENSITIVITY OF THE TLD-ALBEDO NEUTRON DOSIMETER

An idea of why the TLD-albedo dosimeter can overestimate the neutron dose equivalent can be obtained by examining Figures A.1 and A.2. Figure A.1 shows the response of a typical TLD-albedo dosimeter compared with the neutron energy spectrum from a nuclear power plant and with the energy spectrum from a "bare"  $^{252}\text{Cf}$  neutron source used to calibrate TLD-albedo dosimeters (NUREG/CR-2233). In Figure A.1 the neutron flux density per unit lethargy has been plotted against the logarithm of the neutron energy; in this type of plot, equal areas represent equal neutron flux densities, so it is easy to see which neutron energies are important. The integral or measured response of the TLD-albedo dosimeter is the integral of the product of the dosimeter response per unit of flux density multiplied by the neutron flux density integrated over the neutron energy. The TLD-albedo dosimeter response for a bare  $^{252}\text{Cf}$  source is quite low, since the  $^{252}\text{Cf}$  source emits fast neutrons with energies generally above 100 keV. The TLD-albedo dosimeter response is much higher for a reactor spectrum, because it consists of mostly low energy (below 1 MeV) neutrons where the dosimeter response per unit of flux is large. For this reason, a TLD-albedo dosimeter calibrated with a bare  $^{252}\text{Cf}$  source can overestimate the dose equivalent when exposed in a reactor.

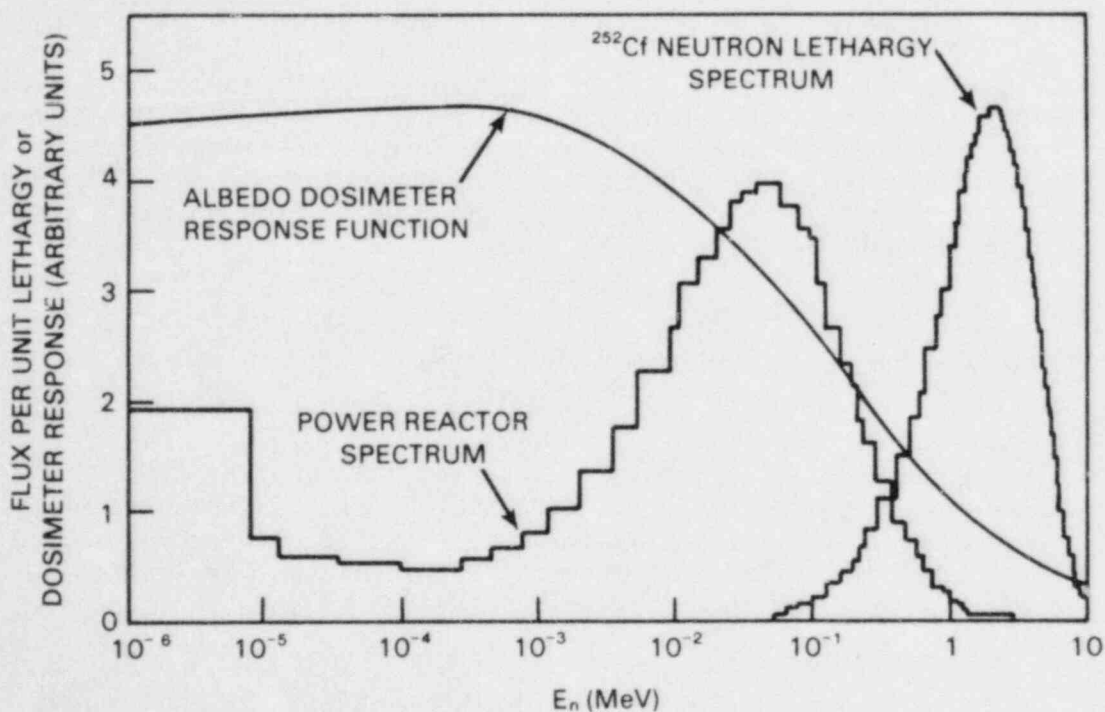


FIGURE A.1. Flux Density per Unit Lethargy for Bare  $^{252}\text{Cf}$  Source, and for a Typical Nuclear Power Plant and Albedo Dosimeter Response Function as a Function of Neutron Energy

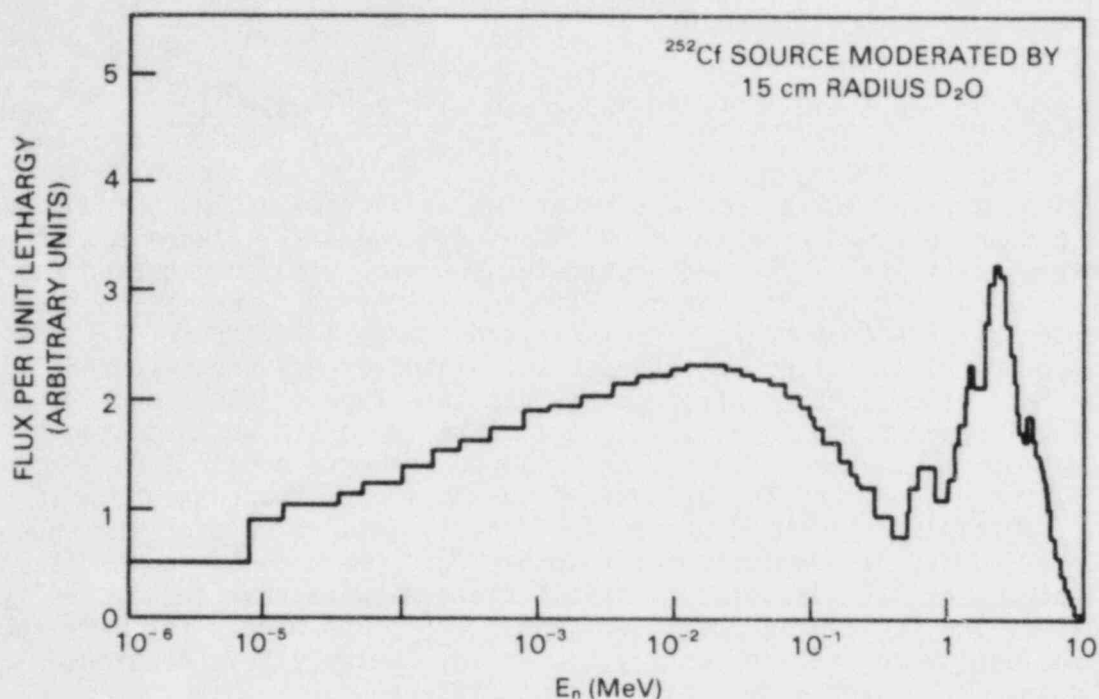


FIGURE A.2. Flux Density per Unit Lethargy for <sup>252</sup>Cf Source Moderated by 15-cm Radius D<sub>2</sub>O

Figure A.2 shows a plot of the neutron flux density per unit lethargy versus the log of the neutron energy for a <sup>252</sup>Cf source moderated by 15 cm of deuterium oxide (heavy water). Although the neutron energy spectrum for the D<sub>2</sub>O moderated source does not resemble the power reactor spectrum shown in Figure A.1, the measured or integrated response of the TLD-albedo dosimeter for the two spectra match closely. The measured dosimeter response, R, is the integral of the response per unit fluence, at a given neutron energy r(E), integrated over all neutron energies, E:

$$R = \int_{E_1}^{E_2} \phi(E) r(E) dE$$

The 15-cm D<sub>2</sub>O moderated californium source is useful for calibrating TLD-albedo dosimeters for reactor exposures because the integral response of a TLD-albedo dosimeter is about the same for the moderated californium source as for the reactor spectrum. This is not true for portable survey instruments, so the moderated californium source is not useful for calibrating survey instruments.

Since we are ultimately interested in dose equivalent, it may be more meaningful to consider the dosimeter response per unit of dose equivalent rather than the dosimeter response per unit of flux density. Alsmiller and Barish have used Monte Carlo computer codes to calculate the response per unit dose equivalent of typical TLD-albedo dosimeters as a function of neutron

energy, as shown in Figure A.3 (Alsmiller and Barish 1974). It is possible to simplify the neutron energy spectrum measurements by considering the neutron flux density (neutrons/cm<sup>2</sup>-sec) or dose equivalent rate (mrem/hr) in the three energy regions shown in Figure A.3. To determine the response of a TLD-albedo dosimeter, it is not necessary to know the exact differential neutron flux density as a function of energy over the entire energy range from thermal to 1 MeV. Only the differential flux density above about 10 keV and the total flux density integrated over the energies of Regions 1 and 2 shown in Figure A.3 need be known.

- Region 1 - the thermal neutron region - Some dosimeter designs have the thermoluminescent (TL) material completely surrounded by cadmium and have a low sensitivity to thermal neutrons. Others have cadmium covering only one side or no cadmium at all and are quite sensitive to thermal neutrons. Therefore, it is necessary to measure the total thermal neutron flux density or dose equivalent rate integrated over all energies below cadmium cut-off, which is about 1 eV.
- Region 2 (neutron energies from 1 eV to 10 keV) - The response per unit dose equivalent is almost constant over this region, and again it is not necessary to determine the differential neutron flux density as a function of energy. One needs only to determine the total neutron flux density or dose equivalent rate integrated over energies from 1 eV to about 10 keV.
- Region 3 (neutron energies above 10 keV) - The TLD-albedo dosimeter response per unit dose equivalent decreases rapidly with increasing neutron energy in this region. Therefore, one needs to accurately measure the differential neutron flux density or fractional dose equivalent rate as a function of neutron energy.

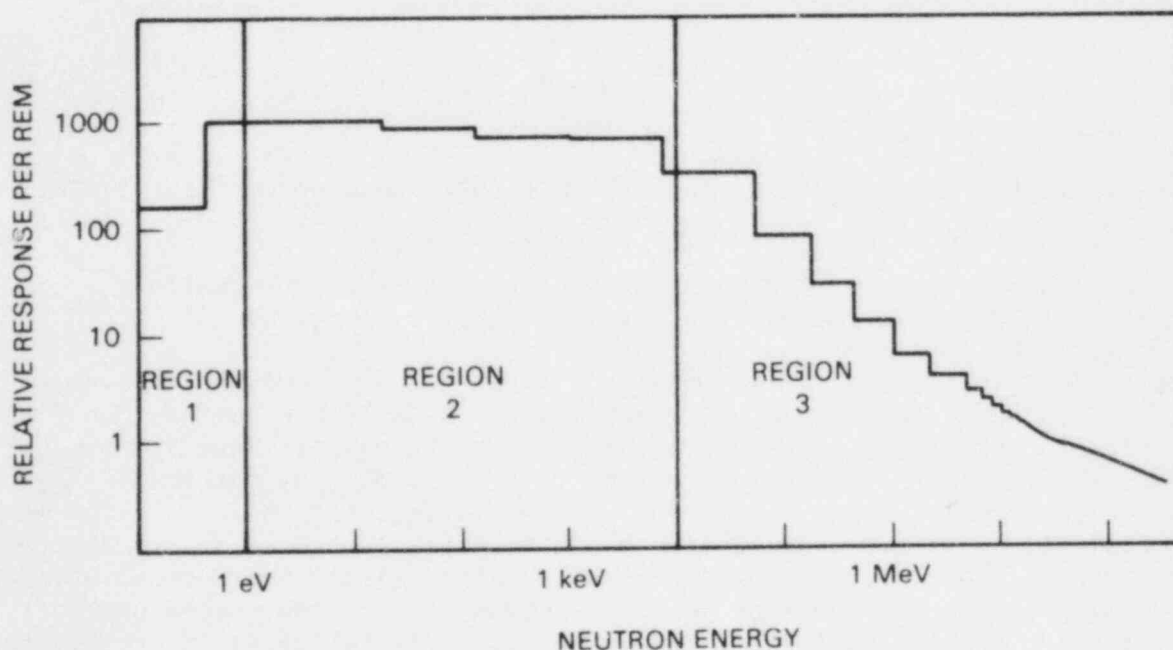


FIGURE A.3. Response of TLD-Albedo Neutron Dosimeter per Unit of Dose Equivalent (Source: Alsmiller and Barish 1974)

## APPENDIX B

### MULTISPHERE SPECTROMETER

#### B.1 INTRODUCTION

Multisphere or Bonner sphere spectrometers are widely used for determining approximate neutron energy spectra and dose equivalent rates. The PNL multisphere spectrometer system consists of a  ${}^6\text{LiI}$  scintillation detector coupled to a photomultiplier, a cadmium cover for the detector, and a set of five polyethylene spheres with holes drilled to position the detector at the center. The signal output from the  ${}^6\text{LiI}$  detector is input to a portable multichannel analyzer with built-in amplifier and power supply. A region of interest is positioned around the neutron peak, to provide the integral count rate. A set of seven measurements are made with different detector/moderator configurations, including a bare and cadmium covered detector and the detector covered with 3-, 5-, 8-, 10-, and 12-in. diameter polyethylene spheres. The count rates from the seven different detector/moderator configurations are used as input to a computer code that "unfolds" the neutron energy spectrum and calculates dose and dose equivalent rates.

#### B.2 THEORY FOR UNFOLDING MULTISPHERE DATA USING THE SPUNIT CODE

One of the primary drawbacks of the multisphere spectrometer system is the mathematical problem of unfolding the neutron energy spectrum. For the PNL system seven count rates are used to determine the neutron energy flux in 26 energy bins in equally spaced logarithmic energy intervals from thermal energies to 20 MeV. The basic equation for this unfolding problem is:

$$C_k = \sum_{i=1}^n \phi_i R_{ik} \quad (B.1)$$

where  $C_k$  is the count rate for the  $k$ th detector/moderator configuration,  
 $\phi_i$  is the neutron flux in the  $i$ th energy bin, and  
 $R_{ik}$  is the response function relating the count rate from the  $k$ th detector/moderator to flux in the  $i$ th energy bin.

Equation B.1 is a set of seven equations known as a discretized version of the Fredholm integral equation of the first kind. With 26 unknown neutron fluxes and 7 known count rates, we have an underdefined problem; there is no single mathematically correct solution, but an infinite number of mathematically correct solutions are possible. Our problem is to determine a solution which is physically possible: one with non-negative fluxes and no abrupt discontinuities in the flux. There is no single mathematically correct solution to uniquely determine the neutron energy spectrum; all of the unfolding codes approach the problem differently and give different solutions. For this reason, only approximate differential neutron flux densities can be determined by multisphere spectrometers.

As explained in Section 2.1, there are a number of different unfolding codes available employing different mathematical techniques. Several codes employ an iterative least-squares method for unfolding; a typical example is the code LOUHI (Routti 1978). The code YOGI (Johnson and Gorbics 1981) uses an iterative perturbation technique. Recently a more efficient method for unfolding spectra using a microprocessor was discovered; this code is called SPUNIT (Brackenbush and Scherpelz 1983).

The computer code SPUNIT uses a new mathematical method for solving the Fredholm integral equation suggested in a paper by members of the USSR Institute of Biophysics in Moscow (Doroshenko et al. 1977). They state their algorithm is based on the principles of statistics and information theory and gives the most probable physically correct solution. The algorithm is an iterative technique using the basic equation:

$$\phi_{i,l+1} = \frac{\phi_{i,l}}{\sum_{j=1}^m R_{ij}} \sum_{k=1}^m R_{ik} \frac{C_k}{N_{k,l}} \quad (\text{B.2})$$

where  $\phi_{i,l}$  = flux for energy bin  $i$  calculated during the  $l$ th iteration

$m$  = number of detector/moderator configurations

$C_k$  = the measured count rates

$N_{k,l}$  = the recalculated count rates, found by

$$N_{k,l} = \sum_{i=1}^n \phi_{i,l} R_{ik} \quad (\text{B.3})$$

$n$  = number of energy bins.

The computer code SPUNIT uses an initial guess at the neutron flux per energy bin then applies the algorithm of Doroshenko et al. (1977) to arrive at a more nearly correct solution. This iterative process is repeated until the recalculated detector counts in Equation B.3 are sufficiently close to the input detector counts.

The SPUNIT code is very simple to program on microprocessors and runs quickly; it is simpler to run than the least-squares or matrix inversion type codes. The solutions calculated by SPUNIT are similar to those calculated by YOGI (Johnson and Gorbics 1981). The integral quantities calculated by SPUNIT, e.g., total flux and dose equivalent, are close to those calculated by other methods for unmoderated  $^{252}\text{Cf}$  sources and  $^{252}\text{Cf}$  sources moderated by 15-cm  $\text{D}_2\text{O}$ . For example, SPUNIT was used to unfold the spectrum at 1 meter from a  $^{252}\text{Cf}$  source moderated by 15-cm  $\text{D}_2\text{O}$ . After 1000 iterations, SPUNIT found an average energy of 0.65 MeV and calculated a dose equivalent rate 18% higher than than calculated from data provided by the National Bureau of

Standards. However, the differential energy spectra may deviate significantly using different types of codes. A great deal of reliance should not be placed upon the differential fluxes, because there is no exact unique solution possible mathematically. There is some evidence that the intermediate energy fluxes can vary considerably between the different codes.

## APPENDIX C

### RESPONSE FUNCTIONS USED IN HESTRIP

#### C.1 INTRODUCTION

As explained in Section 3.2.3, it is necessary to correct the data from the  $^3\text{He}$  proportional counter for wall events - interactions near the walls or ends of the counter where the charged particles produced by neutron interactions strike the walls and do not deposit all of their energy in the sensitive volume of the proportional counter. Unless properly accounted for, these wall events can seriously distort the measured neutron energy spectra. The methodology for correcting for wall events is presented in Equation 3.27, where  $N(E_{ji})$  is the response function for neutron energy  $E_j$  at deposited energy bin  $i$ . Basically, the response function is the fraction of events per energy bin for all energy bins with energies lower than the incident neutron energy plus 764 keV, the energy released by the  $^3\text{He}(n,p)\text{T}$  reaction. The fractions depend upon  $E_j$ , the energy of the incident neutron, and the stopping power of the gas filling and the dimensions of the proportional counter.

#### C.2 WALL - A MONTE CARLO COMPUTER CODE

Perhaps the simplest method to derive the response function is to calculate it using the Monte Carlo computer code WALL (Brackenbush, Reece and Tanner 1983). The FORTRAN code was written for a VAX 750 computer. A simplified flow chart of how the Monte Carlo code generates a response function for a particular cylindrical  $^3\text{He}$  proportional counter tube is shown in Figure C.1.

First, the physical size and gas filling for the proportional counter is inserted in the code. The code calculates stopping powers and particle ranges for the fill gas using empirical formulas (Anderson and Ziegler 1977). Next, the operator specifies the irradiation geometry (point source, beam or isotropic flux). Using a random number generator, the code selects a point of interaction in the tube and the direction of travel for the particles [the proton and triton from the  $^3\text{He}(n,p)\text{T}$  reaction]. The code converts from a center of mass coordinate system to a laboratory coordinate system to account for forward scatter. If the range of the particles is less than the distance to the walls of the proportional counter, the code tallies a full energy event. If the range exceeds the distance to the wall, the code calculates the energy deposited in the proportional counter and tallies this. The process is repeated until a statistically significant "response function" is generated for a single initial neutron energy. Then the code chooses another neutron energy in 100 keV increments, and the process is repeated until a response function matrix is generated. A typical calculation requires 1 to 10 million iterations and requires several hours running time on a VAX 750 computer.



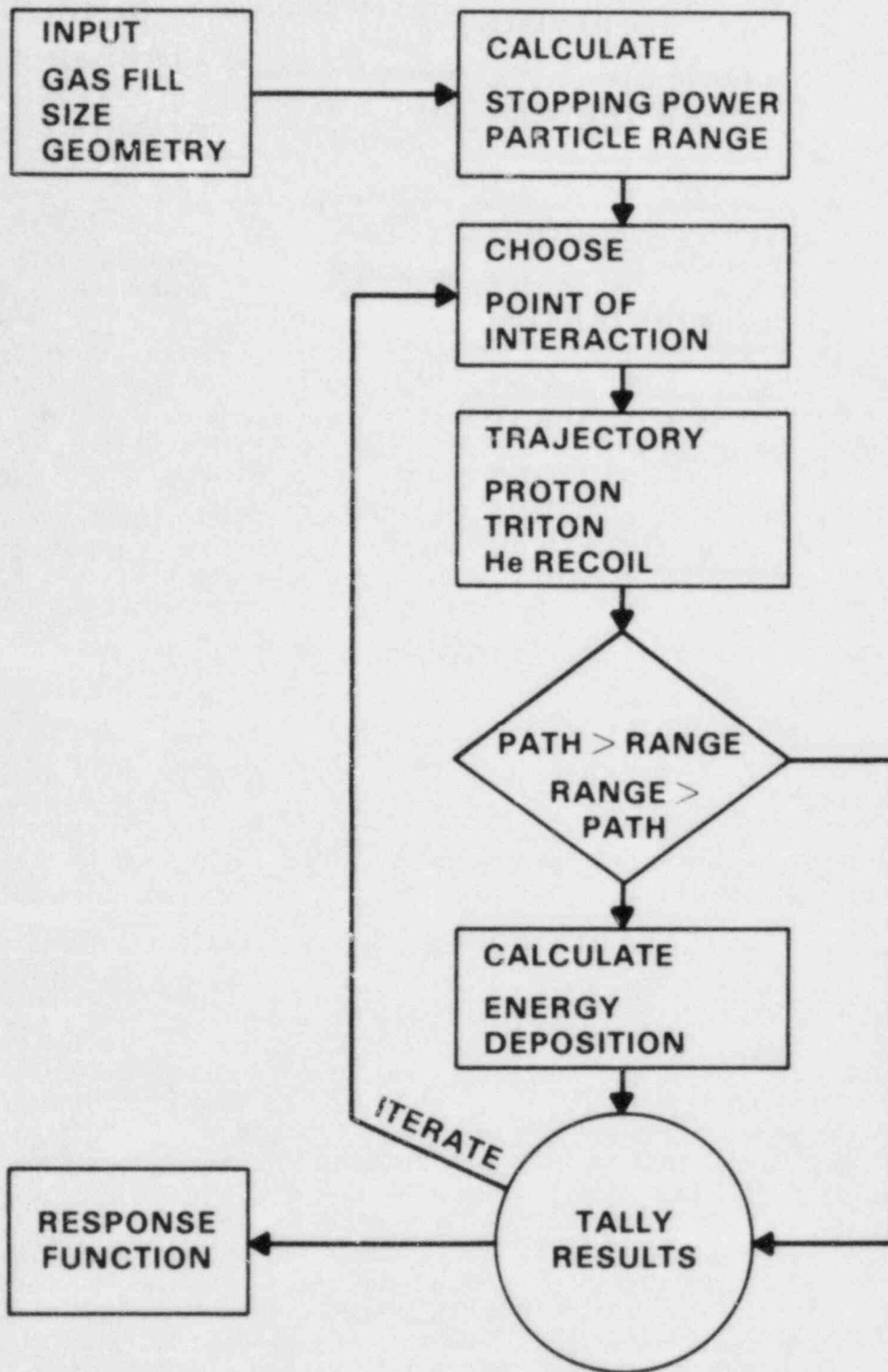


FIGURE C.1. A Simplified Flow Chart for the Monte Carlo Computer Code WALL Used to Calculate a Response Function Matrix for Cylindrical  $^3\text{He}$  Proportional Counters

### C.3 RESPONSE FUNCTION MATRICES

This section presents the response function matrices calculated by the Monte Carlo computer code WALL. The present version of the code calculates a response function matrix for 100 keV increments of the incident neutron energy and 20 keV increments for energy deposited in the sensitive volume of the proportional counter. Using the filling gas compositions specified in Table C.1, the response functions were calculated for 2.54-cm (1-in.) diameter proportional counters with an active length of 30.5 cm (12 in.). These results are given in Tables C.2 through C.6 for the five  $^3\text{He}$  proportional counter fillings listed in Table C.1.

The diagonal elements of these matrices correspond to the efficiency of the tube, i.e., the fraction of the events in which all of the neutron energy is deposited in the tube. Note that the most efficient tube listed has only a 59% efficiency for 1 MeV neutrons and 85% efficiency for slow (thermal and intermediate energy) neutrons. The numbers to the right of the diagonal are the fraction of the neutron interactions which deposit energy in a particular 20 keV wide energy bin. The shape of the response function changes dramatically with increasing neutron energy as a greater fraction of particles strike the wall.

TABLE C.1. Gas Fillings for 1-Inch Diameter  $^3\text{He}$  Proportional Counters Used at PNL

<u>Tube Number</u>	<u>Gas Pressure (psia)</u>		
	<u>Helium-3</u>	<u>Argon</u>	<u>Total</u>
1	4	10.7	15
2	25.4	25.4	51
3	4	26	30
4	2	29.6	32
5	2	12.7	15











## APPENDIX D

### HESTRIP, A COMPUTER CODE FOR UNFOLDING SPECTRA FROM $^3\text{He}$ PROPORTIONAL COUNTER DATA

#### D.1 INTRODUCTION

The code HESTRIP was written in FORTRAN for the Digital Equipment Corporation VAX-750 computer; as such it contains library files and graphing routines which may not be available on other computers. However, the code should be easy to modify, and the library files for the response function matrices for correcting for wall effects are presented in Appendix C. Linear interpolation of the values can provide a finer energy interval if desired. A number of comment statements are included to aid debugging.

#### D.2 SAMPLE INPUT

HESTRIP is designed to be an interactive code; the code asks questions on a video terminal (unit 6 in the code) and the user replies (unit 5 in the code). The input is almost self-explanatory, but a sample case is provided. The sample case, shown in Tables D.1 and D.2, is for a  $^3\text{He}$  proportional counter exposed to a 144 keV neutron beam at the National Bureau of Standards. Table D.1 lists the interactive computer session; Table D.2 lists the data file for the counts per channel from the multichannel analyzer. This case is easier to analyze than the complex reactor spectra. There are two input data items which need to be calculated beforehand. The slow neutron fluence is calculated using Equation 3.9 in Section 3.2.1, and the intermediate neutron fluence is calculated using Equation 3.24 in Section 3.2.2. To obtain estimates of the thermal and intermediate neutron fluences, it is necessary to make additional measurements with a bare  $^3\text{He}$  proportional counter and with the counter covered with a cadmium shield as explained in Section 3.2.

#### D.3 SAMPLE OUTPUT

Table D.3 gives a sample of the printed output from the computer code HESTRIP. Column 1 gives the energy bin number; column 2 gives the average energy of the 20 keV wide energy bins. Column 3 gives the raw data, the number of counts in each energy bin. Note that the code rebins the data into 20 keV wide energy bins based upon the energy calibration provided by the slow neutron peak at 764 keV. Column 4 gives the number of counts per bin which have been corrected for wall effects according to Equation 3.27 in Section 3.2.3. Column 5 gives the neutron fluence (neutrons/cm<sup>2</sup> per 20 keV energy bin), which is found by applying Equation 3.28. Column 6 gives a one standard deviation uncertainty based upon counting statistics, including the effects introduced by subtracting out wall events from higher energy bins. However, no attempt is made to estimate the uncertainty introduced by the calculated response function. The last three columns are calculated from the neutron fluence using the American National Standard neutron conversion factors (ANSI/ANS-G.1.1, 1977). The fractional dose equivalent per 20 keV energy bin is given in Column 7, the quality factor for each neutron energy is given in Column 8, and the cumulative dose equivalent is given in Column 9.



TABLE D.1. Sample Input for Computer Code HESTRIP

Computer: ENTER NAME OF INPUT DATA FILE FOR THIS RUN

User: NBS144.DAT  
[This is the name assigned to the data file from the multichannel analyzer.]

Computer: RFLIB1.DAT = LIBRARY FOR TUBE #1 (4 PSI HE3, 10.7 PSI ARGON)  
RFLIB2.DAT = LIBRARY FOR TUBE #2 (2 ATM HE3, 2 ATM ARGON)  
RFLIB3.DAT = LIBRARY FOR TUBE #3 (4 PSI HE3, 26 PSI ARGON)  
RFLIB4.DAT = LIBRARY FOR TUBE #4 (2 PSI HE3, 29.6 PSI ARGON)  
RFLIB5.DAT = LIBRARY FOR TUBE #5 (2 PSI HE3, 12.7 PSI ARGON)  
ENTER NAME OR RESPONSE FUNCTION LIBRARY FILE

User: RFLIB3.DAT

Computer: ENTER THE NUMBER OF CHANNELS IN THE INPUT SPECTRUM  
1024 for thermal peak in channel 382  
2048 for thermal peak in channel 764

User: 1024.

Computer: ENTER THE SLOW NEUTRON FLUENCE

User: 0.

Computer: ENTER THE INTERMEDIATE (1 eV-10 keV) NEUTRON FLUENCE

User: 0.

Computer: Work! Work! Work!

TABLE D.2. Listing of Counts per Channel From a Multichannel Analyzer for a <sup>3</sup>He Proportional Counter Exposed to the 144 keV Filtered Neutron Beam at the National Bureau of Standards (Data File NBS144.DAT in Table D.1)

TUBE AL6672 EXPOSED TO 144 KEV NEUTS AT NBS 12/5/83								
335484	0	0	0	0	0	0	0	0
0	0	0	0	0	0	0	0	0
0	0	0	0	0	0	0	0	0
0	0	0	0	0	0	0	4033	21791
208407	315065	396677	463465	480727	455682	418689	390618	
368233	339590	315229	294219	271193	252235	234392	218815	
202731	188072	174049	162925	150423	139506	129690	120770	
112271	104295	96841	90779	83870	78115	73142	68919	
63828	60428	56376	53497	50328	49232	47773	47913	
47321	47079	45796	44365	42733	41087	39828	38593	
37364	36383	34634	34186	33117	32429	31472	31069	
30126	29580	28981	28741	28435	28020	27295	27077	
26947	26358	25785	25820	25511	25547	24934	25184	
24942	24495	24309	24392	24192	24255	23821	24114	
23608	23514	23521	23862	23479	23738	23608	23387	
23235	23681	23581	23701	23640	23311	23263	23556	
23666	23588	23534	23617	23353	23551	23360	23697	
23721	23601	24032	23640	23888	23895	23850	24198	
23922	23927	24129	24520	24102	23968	24161	24489	
24129	24466	24732	24724	24252	24884	24637	24823	
25072	25204	24946	24957	25083	25224	25261	24894	
25397	25635	25183	25293	25244	25398	25549	25229	
25152	25479	25006	25298	25059	24926	24974	25305	
24765	25136	24779	24976	24692	24938	24488	24689	
24494	24347	24078	24641	24166	24420	24306	24488	
24417	24198	24003	24055	23831	24132	23566	23978	
24110	23739	23628	23606	23720	23648	23404	23387	
23215	23267	23083	23542	23354	22932	22775	23264	
22736	23131	22791	23054	22397	22607	22692	23050	
22825	22692	22590	22694	22683	23036	22759	22894	
23079	22761	22730	22775	22569	22703	22963	22964	
22570	22836	22676	22827	22678	22836	22613	22957	
23013	23225	23226	23865	24003	24193	24645	25245	
25998	26049	26897	27216	27106	27580	27585	27724	
27848	27592	27597	27717	27553	27432	27573	27553	
27653	27578	27459	27740	27521	27632	27383	27497	
27563	27077	27805	27635	27130	27724	27420	27676	
27622	27913	27742	27453	27316	27496	27968	27983	
28300	28211	28124	28297	27918	28186	28455	28523	
28623	29033	29010	29310	29203	29653	29537	29862	
29946	30777	30564	30744	30925	30804	30884	31175	
31587	31970	32064	32236	32404	33148	33560	34548	
35446	37291	39062	42041	46144	51905	59149	69293	
82299	98456	118588	142973	170901	205116	243858	292803	
347455	407060	473331	542248	600662	652626	677995	680665	
643728	578826	486890	391702	295735	216773	154453	109711	
79276	58670	44619	36295	31012	27919	26626	26450	
26736	27955	29179	31041	32680	34207	35553	36864	
36658	35894	33668	31159	27973	25490	22451	20716	
19894	19259	18690	19140	19162	20147	20856	22066	
23297	25621	27607	31390	34816	39624	44754	52074	
60462	70452	8028	93599	107573	124006	141460	163477	
187384	213975	242367	277302	307288	345067	379269	414040	
442685	466612	479498	489408	480378	467433	441603	409933	
368750	322075	270827	220379	172118	129291	92516	64033	
42198	27438	17258	11081	7148	4979	3680	2964	

TABLE D.2. (continued)

2666	2383	2283	2144	2107	2140	1987	1982
1978	1931	1920	1903	1852	1918	1866	1861
1769	1784	1792	1653	1699	1596	1536	1423
1413	1350	1274	1121	1051	938	914	798
681	569	509	423	309	271	230	167
147	124	96	77	81	72	75	75
59	72	58	59	72	44	50	57
56	46	54	42	36	51	58	47
47	32	52	43	43	55	30	53
43	46	51	39	41	38	49	40
43	45	43	48	37	49	41	36
33	44	40	47	46	29	47	35
35	37	45	38	29	35	34	37
43	36	29	36	36	27	32	34
28	40	35	32	31	33	29	32
35	31	22	34	27	32	35	10
30	20	33	27	20	30	25	17
31	26	26	33	34	30	35	26
37	38	25	33	26	18	21	24
29	33	29	34	25	32	15	27
22	28	13	28	24	29	26	24
27	39	23	19	33	22	27	26
30	29	18	35	25	25	23	17
26	27	24	34	28	23	34	10
23	23	22	29	37	31	28	19
22	24	25	36	24	31	26	21
18	26	25	25	24	18	23	21
20	21	31	16	15	27	20	21
22	21	28	31	19	27	26	19
28	25	24	16	18	26	27	22
24	25	18	17	16	16	13	20
28	28	15	25	26	31	25	30
22	20	26	25	24	35	31	20
21	21	26	16	21	24	26	34
26	20	32	19	25	25	23	24
31	24	17	24	36	39	30	28
28	21	29	23	32	22	20	25
15	24	20	23	18	14	20	17
11	23	17	21	14	20	12	10
10	21	14	10	18	21	16	20
20	20	25	17	15	12	12	18
14	21	23	18	14	12	16	10
20	26	15	25	24	15	23	16
21	17	28	26	14	27	27	22
19	25	20	19	22	21	26	18
16	22	15	20	22	11	13	10
5	17	9	9	7	7	6	2
6	10	5	4	8	8	9	11
4	16	9	8	6	6	7	6
9	10	5	4	8	3	8	7
7	10	8	6	14	9	8	16
9	8	7	8	10	10	13	6
7	11	6	9	12	5	5	3
7	7	6	10	8	8	10	8
4	7	6	5	2	5	1	3
3	3	3	8	6	3	2	3
2	8	2	3	10	2	0	0
5	3	2	6	3	8	5	0
1	1	2	0	2	5	3	0
0	0	0	0	0	0	0	0
0	0	0	0	0	0	0	0
0	0	0	0	0	0	0	0
0	0	0	0	0	0	0	0
0	0	0	0	0	0	0	0
0	0	0	0	0	0	0	0
0	0	0	0	0	0	0	0



TABLE D.3. (continued)

\*\*\* H E S T R I P \*\*\*

TUBE AL6672 EXPOSED TO 144 KEV NEUTS AT NBS 12/5/83

INPUT VALUES--

INPUT DATA FILE            NBS144 DAT.3  
 HE-3 TUBE NUMBER    3 (4 PSI HE3, 26.0 PSI AR)  
 LIVE TIME (SECONDS)    335484

CALCULATED VALUES--

	INTEGRAL FLUENCE (N/CM2)	INTEGRAL FLUX (N/CM2-S)	DOSE EQUIVALENT (MREM)	DOSE EQUIV RATE (MREM/HR)
SLOW (<1EV)	0.00E+00	0.00E+00	0.00E+00	0.00E+00
INTERMEDIATE (1EV-10KEV)	0.00E+00	0.00E+00	0.00E+00	0.00E+00
FAST (10KEV-1MEV)	7.99E+09	2.38E+04	6.68E+04	7.17E+02
TOTAL	7.99E+09	2.38E+04	6.68E+04	7.17E+02

AVERAGE VALUES--

FLUENCE TO DOSE EQUIV FACTOR =  $8.36 \times 10^{-6}$  MREM PER N/CM2  
 AVERAGE QUALITY FACTOR = 8.3  
 AVERAGE NEUTRON ENERGY (KEV) = 144  
 ENERGY CORRECTION FOR HANFORD TLD-ALBEDO  
 DOSIMETER FOR BARE CF-252 CALIBRATION = 6.0

CALCULATIONS CORRECT \_\_\_\_\_ DATE: \_\_\_\_\_

VERIFIED BY \_\_\_\_\_ DATE: \_\_\_\_\_

There may be some error in the first three energy bins because of gamma-ray pile-up. The computer code fits a Gaussian to the slow neutron peak and subtracts out a "background" based upon the assumed Gaussian shape. This procedure may not be adequate if there is significant gamma-ray pile-up, and the spectrum calculated from 10 keV to 50 keV may be in error. A good way to check for this is to use the pulser technique described in Section 3.2.1 or plot the flux per unit lethargy [ $E \phi(E)$ ] versus the neutron energy on a logarithmic scale. Gamma pile-up will be evident as a sharp increase in the value for the flux per unit lethargy. Obviously, there is no gamma-ray pile-up in the data for the 144 keV neutron beam.

The second page of the output contains a summary of the calculations. A title is listed to identify the run. Next the input values are listed: the name of the input data file from the multichannel analyzer, the identification for the  $^3\text{He}$  proportional counter used and the live time for data collection. A summary of the calculated values is presented next. Using the values input to the code for the thermal (<1 eV) and intermediate energy values (1 eV to 10 keV) of the neutron fluence, the code calculates the fluence, flux, dose equivalent and dose equivalent rate in each energy range and the values for the total energy range. The last section calculates average values for the fluence-to-dose equivalent conversion factor (mrem per n/cm<sup>2</sup>), the quality factor and the average neutron energy averaged over an energy range from thermal to 1 MeV. The code also calculates the energy correction factor for the Hanford multipurpose TLD-albedo neutron dosimeter. If the dosimeter is calibrated with a bare  $^{252}\text{Cf}$  source in a low-scatter facility, the observed dosimeter response should be divided by this number to obtain the actual dose equivalent. If the Hanford multipurpose dosimeter is calibrated using a californium source moderated by 15 cm of deuterium oxide, this correction factor should be divided by 7.4. This correction factor can be used only as a guide; the energy responses of TLD-albedo dosimeters may vary depending upon their design. For instance, the Hanford TLD-albedo dosimeter has a separate element for thermal neutrons and does not overestimate thermal neutron exposures. The only way to be certain of accurate calibration of a particular type of dosimeter is to determine its response on a phantom placed in a neutron field where the dose equivalent has been determined by spectral measurements with the  $^3\text{He}$  spectrometer or by other accurate methods.

Provisions are included for quality assurance procedures. Each page of the output is numbered, and two signoffs and dates are provided so that the code results can be checked and verified if necessary.

#### D.4 LISTING OF HESTRIP

A complete listing of the computer code HESTRIP is given in Table D.4 for the PNL version written in FORTRAN and operating on a Digital Equipment Corporation VAX-750 computer. Several data files are necessary for proper operation of the code. First, the data from the  $^3\text{He}$  spectrometer must be placed into a data file on the computer disk for access by HESTRIP; in the sample case in Table D.1, the input data file, listed as Table D.2, was called NBS144.DAT. A response function library for the specific tube used must be read in. In the code these are referred to by RFLIB1.DAT to RFLIB5.DAT. The name of the proper file is entered as input data, and the response function

$W(k,j)$  is read in by the DO-loop terminated by statement numbers 1 and 2 in the listing. For the PNL version of the code, the response function matrix is given in 20 keV increments. The 50 x 50 matrix is too large to list here; the response matrix is obtained by linear interpolation of the matrices listed in Appendix C for the gas fillings listed for 2.54-cm (1-in.) diameter tubes. The PNL version includes a screen graphics subroutine, GRAF, which is machine specific and should be replaced or eliminated. In the code written for the VAX-750, Unit 5 is input from the terminal, Unit 6 is the video screen, Unit 12 is the disk the response function is read from, Unit 13 is the disk the  $^3\text{He}$  spectrometer data is stored on, and Unit 14 is defaulted to the printer for a hardcopy of the results of the calculations. These units can be changed as appropriate for other computers.

TABLE D.4. Listing of HESTRIP Code

```

PROGRAM HESTRIP
C
C VERSION 2 0 FEBRUARY 1984
C
C CORRECTIONS BY WD REECE - 16 AUGUST 1982
C
C CORRECTIONS BY JE TANNER - 19 OCTOBER 1983
C
C CORRECTIONS BY LW BRACKENBUSH - FEB 1984
C
C HE-3 SPECTROMETER ANALYSIS PROGRAM
C THIS PROGRAM CORRECTS HE-3 DATA FOR WALL EFFECTS
C C IS THE RAW DATA - COUNTS/BIN
C CC IS THE COUNTS/BIN CORRECTED FOR WALL EFFECTS FROM HIGHER E'S
C SUM IS THE CORRECTION SUBTRACTED FROM C TO OBTAIN CC
C VAR IS THE VARIATION - THE SQUARE OF THE UNCERTAINTY
C RMS IS THE ROOT MEAN SQUARE ERROR FOR COUNT ERRORS
C PHI IS THE ABSOLUTE FLUENCE IN NEUTRONS/CM2
C PHITH IS THE SLOW NEUTRON FLUENCE
C PHINT IS THE INTERMEDIATE NEUTRON FLUENCE
C ERR IS THE UNCERTAINTY IN THE SPECTRUM DUE ONLY TO COUNTING
C W(J,K) IS THE RESPONSE FUNCTION FOR THE HE-3 TUBE - IT IS
C THE FUNCTION OF THE COUNTS IN BIN K FROM NEUTRONS WITH ENERGY
C E(J) IN BIN J. NOTE THAT THE RESPONSE FUNCTION HAS UNITS
C OF COUNTS/BIN PER INCIDENT NEUTRON/CM2
C ND IS THE NUMBER OF ATOMS OF HE-3 IN THE TUBE
C
C DIMENSION W(51,51),C(51),CC(51),PHI(51),ERR(51),CA(2048)
C DIMENSION CB(2048),QF(50),DOSE(51),XSEC(50),MR(8),XX(50)
C DIMENSION HPND(50),GAUS(50),ITITLE(30)
C CHARACTER*45 ENTER,TITLE,RFLIB
C CHARACTER*28 HESPECIN,TXLINE,RESFUNCT
C DIMENSION IDATE(3),ITIME(3)
C CALL DATE(IDATE)
C CALL TIME(ITIME)
C
C XSEC = THE MICROSCOPIC ABSORPTION CROSS SECTION FOR HELIUM
C DATA XSEC/7.50,4.02,2.95,2.34,2.14,1.88,1.64,1.40,1.38,1.36,
1 1.335,1.285,1.235,1.185,1.135,1.09,1.07,1.05,1.03,1.01,0.986,
2 0.974,0.962,0.950,0.938,0.928,0.920,0.912,0.904,0.896,0.891,
3 0.889,0.887,0.885,0.883,0.881,0.879,0.877,12*0.876/
C
C DATA ENTER/'ENTER NAME OF INPUT DATA FILE FOR THIS RUN'/
C DATA RFLIB/'ENTER NAME OF RESPONSE FUNCTION LIBRARY FILE'/
C OPEN(UNIT=14,FILE='HESTRIP.DAT',STATUS='NEW')
C CALL LIB$GET_SCREEN(HESPECIN,ENTER,LEN2)
C OPEN(UNIT=13,FILE=HESPECIN,READONLY,STATUS='OLD')
C WRITE(6,*)'RFLIB1.DAT=LIBRARY FOR TUBE #1 (4PSI HE3, 10.7PSI ARGON)
C WRITE(6,*)'RFLIB2.DAT=LIBRARY FOR TUBE #2 (2ATM HE3, 2 ATM ARGON)
C WRITE(6,*)'RFLIB3.DAT=LIBRARY FOR TUBE #3 (4PSI HE3, 26 PSI ARGON)
C WRITE(6,*)'RFLIB4.DAT=LIBRARY FOR TUBE #4 (2PSI HE3, 29.6PSI ARGON)
C WRITE(6,*)'RFLIB5.DAT=LIBRARY FOR TUBE #5 (2PSI HE3, 12.7PSI ARGON)
C CALL LIB$GET_SCREEN(RESFUNCT,RFLIB,LEN3)
C OPEN(UNIT=12,FILE=RESFUNCT,READONLY,STATUS='OLD')
C WRITE(6,*)'ENTER THE NUMBER OF CHANNELS IN INPUT SPECTRUM'
C WRITE(6,*)'1024 FOR THERMAL PEAK IN CHANNEL 382'
C WRITE(6,*)'2048 FOR THERMAL PEAK IN CHANNEL 764'
C READ(5,*)NOC
C WRITE(6,*)'ENTER THE SLOW NEUTRON FLUENCE'
C READ(5,*)PHITH
C WRITE(6,*)'ENTER THE INTERMEDIATE NEUTRON FLUENCE (1EV-10KEV)'
C READ(5,*)PHINT
C WRITE(6,*)'WORK! WORK! WORK!'

```



```

C
C READ IN RESPONSE FUNCTION
DO 1 K=1, 50
DO 2 J=1, 50
READ(12, *) W(K, J)
2 CONTINUE
1 CONTINUE
IF(W(1, 1).EQ.0.44709)NTUBE=1
IF(W(1, 1).EQ.0.71620)NTUBE=3
IF(W(1, 1).EQ.0.71752)NTUBE=4
IF(W(1, 1).EQ.0.45227)NTUBE=5

C
C READ IN HE-3 SPECTROMETER DATA (COUNTS PER CHANNEL)
READ(13, 250)(ITITLE(I), I=1, 30)
250 FORMAT(30A2)
DO 51 N=1, 127
NU=(N-1)*8
READ(13, *) (MR(M), M=1, 8)
C99 FORMAT(5X, 5I9)
DO 52 MM=1, 8
CA(NU+MM)=MR(MM)
52 CONTINUE
51 CONTINUE
C
C LOCATE THERMAL PEAK
TOP=CA(NOC/4)
ITOP=NOC/4
DO 9 J=NOC/4+1, NOC*2/5
IF(CA(J).LE.TOP)GO TO 9
TOP=CA(J)
ITOP=J
9 CONTINUE
C
C REBINNING ROUTINE THAT DOES NOT ADD PATTERNS
C
C WIDTH=FLOAT(ITOP)/382.
DO 15 I=2, 1020
CB(I)=0.
AI=I
FINISH=WIDTH*AI
IEND=FINISH
IF(IEND.GT.1020)GO TO 15
STRT=FINISH-WIDTH
ISTART=STRT
DO 16 J=ISTART, IEND
CB(I)=CB(I)+CA(J)
16 CONTINUE
CB(I)=CB(I)+(FLOAT(ISTART)-STRT)*CA(ISTART)-(FLOAT(IEND+1)
& -FINISH)*CA(IEND)
IF(CB(I).LE.0.5)CB(I)=0.1
IF(CB(I).GT.0.5.AND.CB(I).LE.1.0)CB(I)=1.0
15 CONTINUE
END OF REBINNING
C
C FIT A GAUSSIAN TO THE THERMAL PEAK AND SUBTRACT THERMAL
C COMPONENT FROM 20 CHANNELS PAST THE THERMAL PEAK.
C
SUMQ=0.0
FWHM=11.9
ALPHA=(-2.7726)/(FWHM**2)
YCB=CB(382)
DO 40 I=360, 402
DIFF=FLOAT(I-382)

```

```

        GAUS(I-359)=YCB*EXP(ALPHA*(DIFF*DIFF))
        SUMG=SUMG+GAUS(I-359)
        CB(I)=CB(I)-GAUS(I-359)
40)    CONTINUE
C
C      COMBINE CHANNELS INTO ENERGY BINS OF 20 KEV INTERVALS
C
        IF(NDC.EQ.1024) NIC=10
        IF(NDC.EQ.2048) NIC=20
        DO 5 M=1,50
        C(M)=0.0
        MM=(M-1)*10
        DO 6 N=1,NIC
        C(M)=C(M)+CB(382+N+MM)
6      CONTINUE
5      CONTINUE

C      UNFOLDING ROUTINE (EVANS AND BRACKENBUSH AND REECE)
C      AD = THE NUMBER OF HE-3 ATOMS IN THE DETECTOR , ATOMS-
C      CM2/BARNS (MULTIPLIED BY 10E-24 TO CONVERT BARNS TO CM2)
C      THE NUMBER OF ATOMS IS CALCULATED FROM AVAGADRO'S NUMBER,
C      THE IDEAL GAS LAW, THE PRESSURE OF HE-3 AND THE TUBE VOLUME
C
        IF(NTUBE.EQ.1.OR.NTUBE.EQ.3)AD=1.092E-03
        IF(NTUBE.EQ.4.OR.NTUBE.EQ.5)AD=0.546E-03
        CC(50) = C(50)/W(50,50)
C
        TPHI=0.
        HMDR=0
        DO 3 K = 49,1,-1
        VAR = 0.
        SUM = 0.
C
        DO 4 J = K+1,50
        IF(W(J,J).EQ.0.)GO TO 999
        SUM = SUM + CC(J)*W(J,K)
        VAR = VAR + CC(J)*W(J,K)*W(J,K)
4      CONTINUE
C
        CC(K)=(C(K)-SUM)/W(K,K)
        IF(CC(K).LT.0.0)CC(K)=0.0
        RMS = SQRT(ABS(CC(K) - VAR))
        PHI(K) = CC(K)/(XSEC(K)*AD)
        TPHI=TPHI+PHI(K)
        ERR(K) = RMS/W(K,K)
3      CONTINUE
        DANF=130.0*TPHI
C
C      TITLE FOR OUTPUT TABLES
C
        WRITE(14,100) IDATE,ITIME
        WRITE(14,101)
100    FORMAT(1H1,T90,'HESTRIP VERSION 2.0, PAGE 1 OF 2',/,
&      T90,'RUN ON ',3A4,' AT ',3A4,/)
101    FORMAT(2X,'ENERGY',1X,'AVERAGE',3X,'UNCORRECTED',5X,'CORRECTED',
&      5X,'ABSOLUTE',6X,'COUNTING',10X,'DOSE',10X,'QUALITY',5X,
&      'RUNNING SUM OF'/3X,'BIN',
&      4X,'ENERGY',5X,'COUNTS',9X,'COUNTS',5X,' FLUENCE ',3X,
&      'UNCERTAINTY',5X,'EQUIVALENT',7X,'FACTOR',5X,'DOSE EQUIV.
&      /12X,'KEV',35X,
&      'N/CM2 - ',3X,' N/CM2 ',6X,' (MREM) ',20X,
&      '(MREM)')
C      READ IN FLUX TO DOSE EQUIVALENT RATE CONVERSION FACTORS

```

```

C      IN (MREM/HR)/(N/CM2-SEC) AND QUALITY FACTORS FROM ICRU-20 DATA
C      N = NEUTRON ENERGY (KEV)
C      DF = FLUX TO DOSE CONVERSION FACTOR (ANSI/ANS-6.1.1)
C      HDR = HANFORD DOSIMETER RESPONSE/REM * REM IN BIN
C      GF = QUALITY FACTOR (FROM ICRU-20 DATA)
C
C      DATA GF/2 00,3 54,4 94,6 09,7 01,7 62,8 06,8 50,8 94,9 38,
1     9 72,9 89,10 06,10 23,10 40,10 54,10 61,10 68,10 75,10 82,
2     10 87,10 90,10 93,10 96,10 99,5*11 00,11 02,11 01,11 00,10
3     99,10 98,10 95,10 93,10 91,10 89,10 87,10 85,10 83,10 81,
4     10 79,10 76,10 73,10 70,10 67,10 64,10 61/
C
C HDR IS THE HANFORD DOSIMETER RESPONSE GIVEN BY THE
C FORMULA HDR=403*(KEV)**-.846 FROM A FIT OF THE DATA GIVEN
C IN FIGURE 3 & OF PNL-3536 THE RESPONSE IS RELATIVE TO
C CALIBRATION IN A LOW SCATTER ROOM AT NBS OR PNL WITH A BARE
C CF-252 SOURCE HAVING A VALUE OF 1.00
      RUN=0.0
      AVGE=0.0
      HDR=0.0
      AVGG=0.0
      DOBK = 1.50
      NE = 20*K - NIC
      XX(K)=FLOAT(NE)
      E = .001*FLOAT(NE)
      IF(E.LT.0.1) EDF = -8.9302+ 78440*ALOG(E)
      IF(E.GT.0.1.AND.E.LT.0.5) EDF=-8.6632+ 90037*ALOG(E)
      IF(E.GT.0.5.AND.E.LT.1.0) EDF=-8.9359+ 50696*ALOG(E)
      IF(E.GT.1.0) EDF = -8.9359- 055979*ALOG(E)
      DF = EXP(EDF)
      DOSE(K) = DF*PHI(K)/3.6
      RUN=RUN+DOSE(K)
      AVGE=AVGE+PHI(K)*XX(K)
      AVGG=AVGG+PHI(K)*GF(K)
      HDR=HDR+DOSE(K)*403*(XX(K))**(-.846)
      WRITE(14,200) K,NE,C(K),CC(K),PHI(K),ERR(K),DOSE(K),GF(K),
&      RUN
200  FORMAT(I6,I8,7E15,5)
      CONTINUE
C
C
C      CALCULATE DOSE EQUIV FROM SLOW NEUTRONS
      DETH=(1.02E-6)*PH1H
C      CALCULATE DOSE EQUIV FROM INTERMEDIATES
      DEINT=(1.1E-6)*PH1H
C      CALCULATE TOTAL FLUENCE AND DOSE EQUIV
      PHITOT=TPHI+PHINT+PH1H
      DETOT=RUN+DEINT+DETH
C      CALCULATE AVERAGE QUALITY FACTOR, ENERGY & DOSIMETER RESPONSE
      QBAR=(PH1H*2.3+PHINT*2. +AVGG)/PHITOT
      EBAR=(PH1H*0.5+PHINT*5. +AVGE)/PHITOT
      HDRBAR=(HDR+DEINT*57.)/DETOT
C
C
C      GRAPHING ROUTINE
      CALL GRAF(50,XX,PHI)
C
C      WRITE OUTPUT TO HESTRIP OUT
C
      WRITE(14,201) IDATE,ITIME
      WRITE(14,202) (ITITLE(I),I=1,30)
      WRITE(14,203)
      WRITE(14,204)HESPECIN

```

```

IF(NTUBE EQ 1)WRITE(14,205) NTUBE
IF(NTUBE EQ 3)WRITE(14,206) NTUBE
IF(NTUBE EQ 4)WRITE(14,207) NTUBE
IF(NTUBE EQ 5)WRITE(14,208) NTUBE
WRITE(14,209) CA(1)
WRITE(14,210)
WRITE(14,211) PHITH, PHITH/CA(1), DETH, DETH/CA(1)
WRITE(14,212) PHINT, PHINT/CA(1), DEINT, DEINT/CA(1)
WRITE(14,213) TPHI, TPHI/CA(1), RUN, RUN/CA(1)
WRITE(14,214) PHITOT, PHITOT/CA(1), DETOT, DETOT/CA(1)
WRITE(14,215)
WRITE(14,216) DETOT/PHITOT
WRITE(14,217) QBAR
WRITE(14,218) EBAR
WRITE(14,219) HDRBAR
WRITE(14,299)
201 FORMAT(1H1,5X,'* * * H E S T R I P * * *',T97,
1 'VERSION 2 0, PAGE 2 OF 2',/,T97,'RUN ON ',3A4,' AT ',3A4 )
202 FORMAT(///,30A2)
203 FORMAT(///' INPUT VALUES--',/)
204 FORMAT(5X,'INPUT DATA FILE ',T30,A20,/)
205 FORMAT(5X,'HE-3 TUBE NUMBER ',I2,' (4 PSI HE3, 10.7 PSI AR)')
206 FORMAT(5X,'HE-3 TUBE NUMBER ',I2,' (4 PSI HE3, 26.0 PSI AR)')
207 FORMAT(5X,'HE-3 TUBE NUMBER ',I2,' (2 PSI HE3, 29.6 PSI AR)')
208 FORMAT(5X,'HE-3 TUBE NUMBER ',I2,' (2 PSI HE3, 12.7 PSI AR)')
209 FORMAT(/,5X,'LIVE TIME (SECONDS): ',1P1F8.0)
210 FORMAT(/' CALCULATED VALUES--',/,T23,'INTEGRAL',T37,'INTEGRAL'
1 ,T51,'DOSE',T66,'DOSE EQUIV ',/,T23,'FLUENCE',T37,'FLUX',T51,
2 'EQUIVALENT',T66,'RATE',/,T23,'(N/CM2)',T37,'(N/CM2-S)',T51,
3 '(MREM)',T66,'(MREM/HR)',/)
211 FORMAT(5X,'SLOW',T21,1PE10.2,T36,E10.2,T51,E10.2,T66,
1 E10.2,/,7X,'(<1EV)')
213 FORMAT(5X,'FAST',T21,1PE10.2,T36,E10.2,T51,E10.2,T66,E10.2,/,
1 7X,'(10KEV-1MEV)',/)
212 FORMAT(5X,'INTERMEDIATE',T21,1PE10.2,T36,E10.2,T51,E10.2,
1 T66,E10.2,/,7X,'(1EV-10KEV)')
214 FORMAT(5X,'TOTAL',T21,1PE10.2,T36,E10.2,T51,E10.2,
1 T66,E10.2//)
215 FORMAT(' AVERAGE VALUES--',/)
216 FORMAT(5X,'FLUENCE TO DOSE EQUIV. FACTOR =',1PE10.2,
1 ' MREM PER N/CM2' )
217 FORMAT(/,5X,'AVERAGE QUALITY FACTOR =',F5.1 )
218 FORMAT(/,5X,'AVERAGE NEUTRON ENERGY (KEV) = ',F5.0 )
219 FORMAT(/,5X,'ENERGY CORRECTION FOR HANFORD TLD-ALBEDO',/,
1 8X,'DOSIMETER FOR BARE CF-252 CALIBRATION = ',F5.1 )
299 FORMAT(/////,' CALCULATIONS CORRECT: ',18(' '), ' DATE: ',10(' '),
1 ///, ' VERIFIED BY ',27(' '), ' DATE: ',10(' ') )
C
C
CLOSE(UNIT=12)
CLOSE(UNIT=13)
CLOSE(UNIT=14,DISPOSE='PRINT/DELETE')
STOP
999 WRITE(6,*)'ERROR!!! W(J,J)=0 -- J=',J
STOP
END

```

DISTRIBUTION

<u>No. of Copies</u>		<u>No. of Copies</u>	
	<u>OFFSITE</u>	2	N. A. Dennis U.S. Nuclear Regulatory Commission Region 1 631 Park Avenue King of Prussia, PA 19406
20	U.S. Nuclear Regulatory Commission Division of Technical Information and Document Control 7920 Norfolk Avenue Bethesda, MD 20014	2	E. Geiger Eberline Company P.O. Box 2108 Santa Fe, NM 87501
	Margaret Federline Office of Radiation Protection 1130SS U.S. Nuclear Regulatory Commission Washington, DC 20555	2	Richard Griffith Hazards Control Department Lawrence Livermore National Laboratory P.O. Box 5505 Livermore, CA 94550
	R. E. Alexander Occupational Radiation Protection Branch 1130SS U.S. Nuclear Regulatory Commission Washington, DC 20555	2	R. B. Schwartz U.S. National Bureau of Standards Quince Orchard Rd. Gaithersburg, MD 20760
	S. Block Radiological Assessment Branch P-712 U.S. Nuclear Regulatory Commission Washington, DC 20555		D. Sly Safeguards & Materials Programs Branch EW 359 U.S. Nuclear Regulatory Commission Washington, DC 20555
	J. D. Buchanan Occupational Radiation Protection Branch 1130SS U.S. Nuclear Regulatory Commission Washington, DC 20555	2	R. V. Wheeler R. S. Landauer, Jr. and Co. Glenwood Science Park Glenwood, IL 60425
2	F. M. Costello U.S. Nuclear Regulatory Commission Region 1 631 Park Avenue King of Prussia, PA 19406		J. E. Wigginton Engineering & Generic Communications Branch EWS 312 U.S. Nuclear Regulatory Commission Washington, DC 20555

No. of  
Copies

No. of  
Copies

ONSITE

Pacific Northwest Laboratory  
(continued)

50 Pacific Northwest Laboratory

F. M. Cummings (2)  
L. W. Brackenbush (20)  
G. W. R. Endres  
L. G. Faust  
J. J. Fix  
R. T. Hadley  
D. E. Hadlock  
D. L. Haggard

G. R. Hoenes  
J. J. Jech  
M. A. Parkhurst  
W. D. Reece (5)  
R. I. Scherpelz  
K. L. Soldat  
J. E. Tanner (5)  
Technical Information (5)  
Publishing Coordination (2)

**BIBLIOGRAPHIC DATA SHEET**

NUREG/CR-3610  
PNL-4943

SEE INSTRUCTIONS ON THE REVERSE

2 TITLE AND SUBTITLE

Neutron Dosimetry at Commercial Nuclear Plants  
Final Report of Subtask C: <sup>3</sup>He Neutron Spectrometer

3 LEAVE BLANK

4 DATE REPORT COMPLETED

MONTH

YEAR

July

1984

6 DATE REPORT ISSUED

MONTH

YEAR

September

1984

5 AUTHOR(S)

L.W. Brackenbush, W.D. Reece, J.E. Tanner

7 PERFORMING ORGANIZATION NAME AND MAILING ADDRESS (Include Zip Code)

Pacific Northwest Laboratory  
Richland, WA 99352

8 PROJECT/TASK/WORK UNIT NUMBER

9 FIN OR GRANT NUMBER

B2282

10 SPONSORING ORGANIZATION NAME AND MAILING ADDRESS (Include Zip Code)

Division of Radiation Programs & Earth Sciences  
Office of Nuclear Regulatory Research  
U.S. Nuclear Regulatory Commission  
Washington, D.C. 20555

11a TYPE OF REPORT

Technical

b PERIOD COVERED (Inclusive dates)

12 SUPPLEMENTARY NOTES

13 ABSTRACT (200 words or less)

In commercial nuclear power plants, personnel routinely enter containment for maintenance and inspections while the reactor is operating and can be exposed to intense neutron fields. The low-energy neutron fields found in reactor containment cause problems in proper interpretation of TLD-albedo dosimeters and survey instrument readings. Described is a technique that can aid plant health physicists to improve the accuracy of personnel neutron dosimetry programs. A <sup>3</sup>He neutron spectrometer can be used to measure neutron energy spectra and determine dose equivalent rates at work locations inside containment. Energy correction factors for TLD-albedo dosimeters can be determined from the measured spectra if the dosimeter energy response is known, or from direct measurements with dosimeters placed on phantoms at locations where the dose equivalent rate has been measured. This report describes how to assemble a spectrometer system using only commercially available components, how to use it for reactor energy spectrum measurements, and how to analyze the data and interpret the results. Both <sup>3</sup>He and multisphere spectrometers were used to measure neutron energy spectra and dose equivalent at three PWRs and one BWR. In general, the <sup>3</sup>He spectrometer measures higher dose equivalent rates than the multisphere spectrometer. In the energy range from 10 keV to 1 MeV, the dose equivalents measured by the <sup>3</sup>He spectrometer and multisphere spectrometer agree within about 35% for the spectra measured.

14 DOCUMENT ANALYSIS - a KEYWORDS/DESCRIPTORS

neutron dosimetry  
neutron spectrometry  
<sup>3</sup>He neutron spectrometer

15 AVAILABILITY STATEMENT

Unlimited

16 SECURITY CLASSIFICATION

(This page)

Unclassified

(This report)

Unclassified

b IDENTIFIERS/OPEN ENDED TERMS

17 NUMBER OF PAGES

18 PRICE

UNITED STATES  
NUCLEAR REGULATORY COMMISSION  
WASHINGTON D.C. 20555

OFFICIAL BUSINESS  
PENALTY FOR PRIVATE USE, \$300

FOURTH-CLASS MAIL  
POSTAGE & FEES PAID  
USNRC  
WASH D.C.  
PERMIT No. 67

120555078877 1 IANIRHRL  
US NRC  
ADM-DIV OF TIDC  
POLICY & PUB MGT BR-PDR NUREG  
W-501  
WASHINGTON DC 20555